EXPERIMENTAL STUDY OF COHERENCE PHENOMENA IN ELECTRIC DIPOLE SYSTEMS AT MILLIMETRE WAVELENGTHS

by

G.S. Uppal, M.Sc.,M.Sc.(Tech.)

Thesis submitted to the
University of Keele for the
Degree of Doctor of Philosophy.

Department of Physics,
University of Keele,
Staffordshire.

March, 1969.

ACKNOWLEDGEMENTS

The author wishes to express his grátitude to

Professor. D.J.E. Ingram for the provision of research facilities and interest in this work.

Dr. D.C. Lainé for his supervision, valuable advice and help throughout this work,

Dr, E.F. Slade for the loan of 4mm and 2mm components.

Mr. G.D.S. Smart for collaboration in experiment on molecular ringing in NH_3 bulk gas.

Dr. A.L.S. Smith, Mr. F. Rowerth, members of the Maser research group and other academic and technical staff of the department for their continued help.

Miss K.B. Davies for the typing and preparation of this thesis.

The University of Keele for the award of a research scholarship.

The staff of the Library for much cooperation and assistance.

Mr. Michael Davies for help in general electronics.

Mr. M.T. Cheney, Mr. N. Banks and Mr. J.D. Sunderland for help in the preparation of photographs and diagrams.

Dr. Darshan for helping in various ways in completing this thesis.

ABSTRACT

The work described in this thesis is concerned with the development of millimetre wave spectrometers and their application to the study of coherence phenomena in a system of electric dipoles. The investigations reported here were aimed at developing measurement techniques at millimetre wavelengths using harmonics of an 8 millimetre klystron. The difficulties of constructing 4mm and 2mm components are considerable because of the small dimensions and tolerances involved and a consideration in the work was to keep the number of these millimetre components to a minimum.

Firstly, an outline of the techniques for generation and detection of millimetre waves is given. A description of the spectrometers along with the fabrication of components is also given in some detail. The various resonant cavities which were fabricated and checked during these investigations are discussed.

Carbonyl sulphide and formaldehyde were used as working substances to test these spectrometers. The results obtained at 4mm and 2mm wavelengths are given.

Experimental results on molecular ringing in OCS using 72.976 GHz transition are given along with calculations for relaxation times and line widths. The results were obtained by using simple crystal video detection. The simplicity of the scheme shows its potential as a technique for measurement of relaxation mechanisms and line widths.

Experimental results on molecular ringing in ammonia both in bulk gas and the beam maser (23.870 GHz) at 12.5mm wavelength are also discussed.

Investigations on the $0_{00} - 1_{01}$ transition in formaldehyde at 72.838 GHz showed that this transition was too weak for the molecular ringing to be observed. The suitability of this transition for beam maser operation was then studied in some detail and experimental work was carried out to solve a number of basic problems involved in the construction of such a device. The discussion is terminated with suggestions of how this work might be extended.

CONTENTS

CHAPTER I

MILLIMETRE WAVE TECHNIQUES

Introduction

The very rapid development of the field of microwave electronics has opened up the region of the electromagnetic spectrum lying between the radio region and the infra red region. The segment of the electromagnetic spectrum which is encompassed by wavelengths of 4 to 0.4 millimetre is a region of opportunity for the present day spectroscopist. The techniques used to generate, propagate and detect millimetre radiation are many and varied. The problem has been approached from the microwave region by scaling down conventional components and from the infra red region of the spectrum by using a range of quasi optical techniques, with equal success. This chapter will review the situation paying particular attention to the harmonic generators and semiconductor detectors which were used during these investigations for the design and construction of millimetre wave spectrometers.

1.1 Generation of Millimetre Radiation

1.1.a Thermionic sources

One method of obtaining millimetre wave tubes is to scale down those types used at centimetre wavelengths. Klystrons, travelling wave tubes, and backward wave oscillators have been built to produce wavelengths near 4mm, while pulsed magnetrons[1] have reached 2.5mm and

carcinotrons[2] down to 0.48mm. Of these, the rather new backward wave oscillator appears most promising as a flexible high frequency source for spectroscopy. The first three types of tubes are in practice inefficient and are necessarily small, so that neither conduction nor radiation is sufficient to dissipate heat for more than very low power operation. Furthermore circuit losses increase approximately as the square of the frequency. Magnetrons, by virtue of their pulsed operation, are able to operate with moderate efficiency and power output in millimetre region.

Fabrication tolerances become exceedingly critical when centimetre wave klystrons are scaled to operate in the millimetre wave range. For these reasons it is desirable to have tube types whose dimensions are all large in comparison with the wavelength. Klystrons, travelling wave or backward wave tubes, and magnetrons are an advance over conventional triodes for the microwave region in that they have sizes not very much less than the wavelength generated. Neither they nor any other type yet invented have critical dimensions which are greater than the output wavelength. Nevertheless, all these types have been successfully scaled down to operate in the millimetre region, and in spite of the difficulties further progress may be expected. Klystrons are commercially available to produce wavelengths as short as 2mm with a power output of a few milliwatts. However, millimetre wave klystrons tend to be noisier and less stable than their centimetre wave counterparts, and the power emitted sometimes varies rapidly over the range of tuning. Pulsed magnetrons have been built to oscillate at wavelengths as short as 2mm, but the shorter

wavelength tubes are not tunable. Because these magnetrons have simpler structures than, for example, klystrons and because of the advantages of pulsed operation, efficiencies of the order of 5 per cent are achieved. This efficiency permits fairly high output powers, and the millimetre wave magnetrons have peak pulse outputs of around 25KW.

Millimetre wave power can now be generated very effectively using extended interaction oscillators, such as backward wave oscillators. The operation of this type of oscillator depends on the interaction of an electron beam with a slow wave structure such as a helix. They have the advantage that their frequency depends only on the accelerator voltage and consequently can be made very stable. They also have a much wider band width than any other type of vacuum tube generator since they do not contain any tuned elements. The principal disadvantage is that they require very large, stable power supplies and the high frequency ones have a rather short cathode life, due to the high beam current density required.

1.1.b Harmonic generation

Harmonic generation is the most widely used technique in the field of millimetre wave spectroscopy and until recently was the only means of producing coherent radiation at shorter millimetre and sub-millimetre wavelengths. Although this range is now also reached by electronic oscillators and far infra red lasers the harmonic generator is as yet unsurpassed as a broad band spectroscopic source of high resolution.

Work on the harmonic generation of longer millimetre wavelengths by means of microwave rectifier diodes started at Massachussets Institute of Technology in 1945, but the credit for the development of this work into a sustained and determined attack on the problems of generating submillimetre wavelengths must go to Gordy[3]. He and his co-workers at Duke University tried many methods of fabricating and mounting these diodes and in 1954 brought out an "open guide" type of mounting that has remained essentially unchanged ever since.

In this section we consider the use of a rectifying point contact between a metal and a semiconductor to generate millimetre wavelength harmonics of the signal from a conventional microwave source of frequency f. This is termed the fundamental, whilst the harmonic at frequency nf is termed the nth harmonic.

The current-voltage characteristics of a microwave diode can be represented by a power series of the form

$$i = ae + be^2 + ce^3 + ...$$

where e is the applied oscillating electric field and it is easily shown that the crystal generates all harmonics. The practical methods of using the properties of this type of crystal have been described by many authors[4-7]. The simplest method is to place the crystal across the guide and then taper the guide to a suitable size for the harmonic required. Matching is then carried out by means of stub tuners in each wave guide region. The most popular alternative is to use the crossed waveguide

method, in which two lengths of wave guide are arranged at right angles to one another with the converting element, in this case a crystal, located across the junction. The waveguide dimensions in one direction are such as to propagate the dominant mode of the fundamental frequency, and in the other direction such as to propagate the dominant mode of the desired harmonic. The harmonic guide can be designed to filter out all frequencies below the harmonic required. Tuning plungers are located in both guides behind the crystal. This type of harmonic generator can be designed either to use a commercially available microwave diode or to enable the rectifying junction to be formed in the generator using replaceable crystals and whiskers.

Although most semiconductors will give some lower harmonics when used in a harmonic generator of the type described, the selection of a suitable semiconductor material for this purpose demands reasonable care.

Crystal materials

The figure of merit for the material of a crystal is given by

$$\frac{a\varepsilon^{\frac{1}{2}}}{N^{\frac{1}{2}}u}$$

where a = radius of contact

ε = permittivity of the semiconductor

N = majority carrier density

u = mobility

It is apparent that, other things being equal, the higher the value of the mobility, the better the material.

Table 1

Type	Semiconductor	Mobility cm^2/vs	Energy gap eV
n	Indium antimonide (InSb)	57,000	0.17
n	Indium arsenide (InAs)	27,000	0.37
n	Mercury Telluride (HgTe)	11,800	0.40
n	Mercury Selenide (HgSe)	10,000	0.65
n	Gallium arsenide (GaAs)	4,000	1.35
n	Gallium antimonide (GaSb)	4,000	0.69
n	Germanium (Ge)	3,600	0.72
n	Indium Phosphide (InP)	3,500	1.25
n	Silicon (Si)	1,400	1.09
p	Silicon (Si)	440	1.09

In terms of mobility alone indium antimonide appears to be the best material, although the energy gap is much too small to be useful at ordinary temperatures (where the material is an intrinsic semiconductor anyway). However, particularly with the attention being paid to the achievement of low noise figures by crystal cooling, indium antimonide

may well find a use for low temperature applications. We see that germanium and silicon are well down the list as regards mobility. Silicon is in some ways a more useful material in that its larger energy gap enables it to be used at higher temperatures. Gallium arsenide, however, possesses an energy gap which is 30 per cent greater than silicon with a better mobility than germanium. In recent years gallium arsenide diodes have been made with cut off frequencies of the order of 200 Gc/s and have found considerable use for many applications in the microwave range. Gallium arsenide crystals are far less temperature dependent, because of their high energy gap, than either germanium or silicon crystals and appear to be still capable of operating at temperatures exceeding 350°C.

Silicon, germanium and gallium arsenide have all been used successfully at millimetre wavelengths; but silicon has so far produced the best results at submillimetre wavelengths. In every case high resistivity (0.01 - 0.02 Ωcm) material is used by contrast to the low resistivity material needed for detectors. The most dramatic results have been obtained from the use of bombarded silicon, first produced by Ohl in 1952 and developed as a harmonic generator by Burrus, Trambarulo and Ohl[8], who succeeded in increasing the available power at 0.78mm wavelength thirtyfold. This material is made by high temperature bombardment of silicon with 40,000 eV positive ions, and its production demands considerable experience in the handling of semiconductors, but

it has unfortunately never been made commercially available. Recently Burrus[9] has described a much simpler process of high temperature phosphorus diffusion that produces material of as good a performance as bombarded silicon.

The effect of these treatments on the characteristics of a point contact diode is to raise the backward breakdown voltage and to increase the abruptness of avalanche breakdown. Both of these features tend to increase the harmonic power output as the theoretical treatment shows. The exact cause of this change in electrical characteristics is not known, but it is believed that a thin n type layer forms on the surface of the p-type semiconductor. At low frequencies this forms a junction diode of large area, but millimetre wavelengths are confined by the skin effect to a transmission line with an area corresponding to that of the extremely small metal point. Thus the size of the contact may be determined by the experimenter without affecting its electrical properties.

Fabrication techniques

The general processes for making high quality rectifiers are now well established. At present, these are (1) purification of the semiconductor, (2) controlled addition of a selected impurity that produces the desired properties, (3) preparation of an ingot from which the wafers used in the cartridge are cut, (4) preparation of the surface of the wafers by a process of polishing, heat treatment and etching,

(5) shaping and pointing the "cat whisker", (6) assembly and adjustment, and (7) performance testing. No attempt will be made in this chapter to describe in detail the procedures that have been used successfully by all the various manufacturers. However, the process of etching and polishing will be given in some detail.

Electrolytic polishing

Specimens may be polished electrolytically by being made the anode in a suitable solution. If the potential is gradually increased, the current rises rapidly to a maximum, and then falls sharply to a constant value. At this point a smooth bright surface develops which is often superior to that produced by mechanical polishing and is free from distortion. The voltage depends on the concentration of the solution (which frequently has a high resistance) and especially on the position of the anode, and is generally approximately that at which evolution of gas occurs. In general, optimum conditions for polishing a given type of material may be determined by plotting curves of current (I) against voltage (v). A level portion parallel to the voltage axis is usually observed; this is associated with the existence of an anodic film, and its higher voltage end corresponds with the best conditions for electro-polishing. Optimum conditions correspond with the maximum of the function $\frac{(v-e)}{I} = fv$, where e is the back e.m.f. of the cell. Thus by plotting this function, optimum conditions may be established in difficult cases for which no well marked level position exists in the normal I-v curve.

The apparatus required is simple and may take a variety of forms. All surfaces of the specimen except that to be polished should be suitably insulated, and the cathode (copper, graphite or stainless steel) should be symmetrically disposed with respect to the anode. Rotation of the sample is advisable and the use of a pulsating current is frequently recommended. The pulses may be arranged by means of a contact operated by the device which rotates the specimen, and assist in avoiding pitting of the sample, or the production of a wrinkled finish. In some cases the potential is critical, and in others not. A supply of 50 to 80 volts dc should be available, owing to the low conductivity of some of the solutions. Gas bubbles must not be allowed to adhere to the surface which is being polished, or solution is prevented underneath them, and 'hillocks' develop. It is essential that the surface to be examined should be thoroughly degreased (carbon tetrachloride, benzene or caustic soda where possible).

In the procedure used by North[10] for antimony-doped germanium, the ingot is cut into wafers 0.020 inch thick and these are ground with 600-mesh alumdum under water on a glass lap. The wafers are then plated with rhodium and cut into squares 0.070 inch on a side.. These are soldered to the cartridge studs which are then mounted, 20 at a time, on a jig for polishing. A wet polishing wheel is used. There are three steps to the polishing process. First the crystals are ground on a fine stone to bring all the surfacesin the same plane; they are then polished

with 600-mesh Alundum on cloth, and finally with fine magnesium oxide on cloth to give a high polish. Heat treatment and etching appear to be unsuited to antimony doped germanium. Experiments by North show that heat treatment in air, followed by an etch to remove the oxide, produces a germanium surface which when probed showed almost short circuit characteristics.

Whiskers

For silicon rectifiers, tungsten has been almost universally used. The British-Thomson-Houston Company prefers molybdenum-tungsten which they have found to be more consistent in quality than pure split-free tungsten. Other manufacturers have found commercial tungsten satisfactory. The mechanical properties of tungsten are well suited to whisker fabrication. Platinum-ruthenium whiskers have been found to give somewhat higher back resistance than tungsten ones in germanium mixer crystals. The platinum is alloyed with 10% ruthenium to increase the hardness. It is a standard practice to solder the whisker to the cartridge component. Both Bell Telephone Laboratories and Westinghouse Research Labs[11] have successfully used a hot dip method in which the tungsten wire is coated with an alloy of 69% gold, 6% platinum and 25% silver. The wires are readily wetted by the alloy which forms a thin adherent coating that can be easily soldered. Nickel plating the tungsten has also been found satisfactory. In the Radiation Lab. coaxial cartridge, the whisker is spot-welded to the centre conductor of the

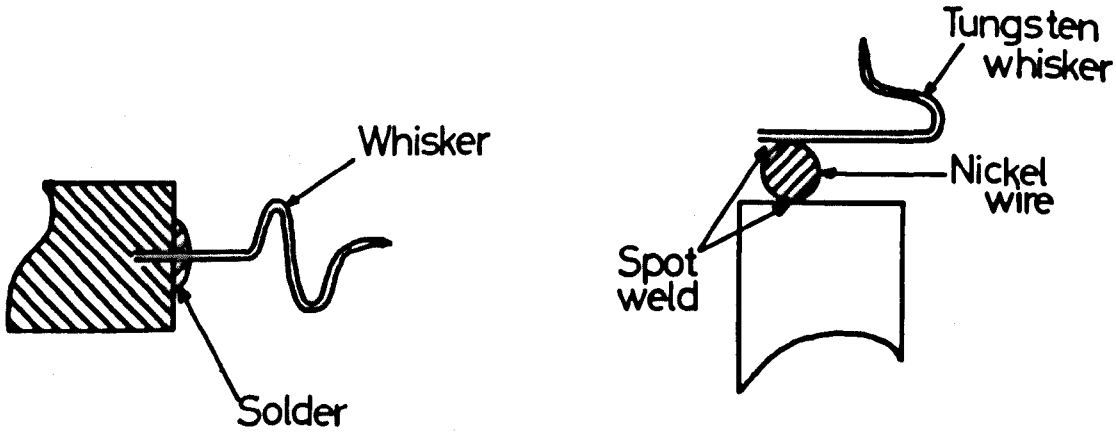

Fig. 1.1. WHISKER ASSEMBLY.

cartridge, a 10 mil nickel wire being used (Fig. 1.1). The nickel wire serves also to separate the whisker from the end of the centre conductor so that space is provided for the deflection of the spring.

In the case of welded contact germanium rectifiers the whisker is a 0.0015 inch diameter platinum-ruthenium alloy (10% ruthenium). The ruthenium is used solely to lend mechanical strength to the whisker. The whisker tip is carefully pointed to a point radius of less than 0.00002 inch. The silver plug holding the germanium is pressed into the cartridge and advanced until electrical contact is just made. It is then further advanced to produce enough spring deflection to give a force on the contact of 150 mg. At this point 250 ma of direct current are passed through the contact in the forward direction for 5 to 10 seconds. This treatment results in a secure weld.

A crystal rectifier, when driven by a local oscillator, in general generates more noise than the Johnson noise produced by an equivalent resistor. The "noisiness" of a crystal rectifier is measured by its noise temperature, defined as the ratio of the noise power available from the rectifier to the noise power available from a resistor, $KT_o\Delta f$, at the reference temperature $T_o = 290^oK$. The large values of noise temperature have been correlated with microscopic irregularities in the geometry of the tungsten point contact. An electrolytic polishing process has been used by the Western Electric Company to remove these irregularities. This process as reported by Pfann[12] gives the point the desired contour and

surface smoothness. The process consists of making the point anodic in a solution containing 25% by weight of potassium hydroxide and applying 0.8 volt for 2 seconds followed by two successive flashes of 0.2 seconds duration at 2 volts. A number of points may be connected in parallel and polished simultaneously. The cathode is a copper gauze. After the polishing process the points are washed in a stream of hot water and dried.

Pfann has also developed a process of eliminating the mechanical forming of the point by electrolytic pointing as well as polishing. The electrolyte used for the pointing operation is an aqueous solution containing 25% potassium hydroxide by weight with about .01% or more of copper in solution. The cathode is a copper gauze that has remained in the electrolyte long enough for a film of oxide to form. The pointing operation is accomplished by placing the whisker wires in a vertical position with their lower ends in the electrolyte and applying 1 volt until the current drops to a value between 0.25 and 0.30 ma; for points having a radius of curvature of 0.0003 inches, the shut off current always falls within this range. The pointing process is then followed by polishing flashes as previously described.

The drop in current at constant voltages arises from the decrease in wetted area as the tungsten is dissolved and from the polarization at the wires. The shaping of the point depends on the formation of a meniscus of a suitable shape about the wire. The potassium hydroxide

solution specified produces a satisfactory meniscus for 5 mil wires, and the addition of the copper to the solution produces the required adhesion of the liquid to the wire. Copper gauze is the only cathode material that has been found satisfactory. The concentration of KOH is not critical, large changes having little effect on the contour of the point; the value of the shut off current increases with increase in concentration.

The efficiency of harmonic generation decreases with increasing fundamental frequency. The power generated by an ideal resistive element in these crystal diodes can be shown to be proportional to n^{-2} where n is the harmonic number, and to be related to the fundamental power by a relation $P_n \propto \frac{a}{n^2} P_1^S$, where $S \geq 1$ and P_1 is the fundamental power. In practice the lowest conversion loss for generating the first harmonic in the 4mm region are of the order of 20 dbs, but figures up to 30 dbs are more usual. This is largely due to instabilities in the microwave structure and a departure from the non linear characteristics of the crystal as the frequency is increased. The conversion ratio for higher harmonics is usually even further from the ideal case because of the narrow bandwidth of the supporting structure.

In contrast to the relatively low theoretical power available from the non linear resistive element of a crystal diode, a purely reactive element should be capable of producing 100% conversion of the fundamental power into harmonic power. In recent years this has become a practical possibility with the advent of varactor diodes capable of

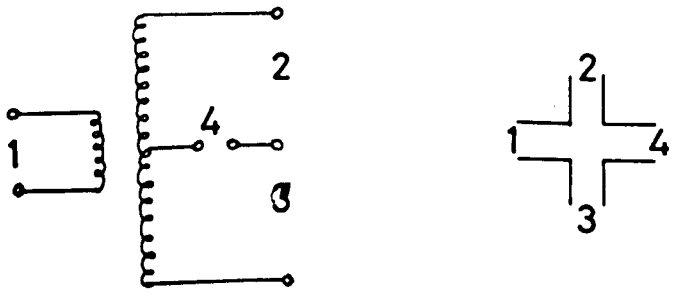

FIG 1.2

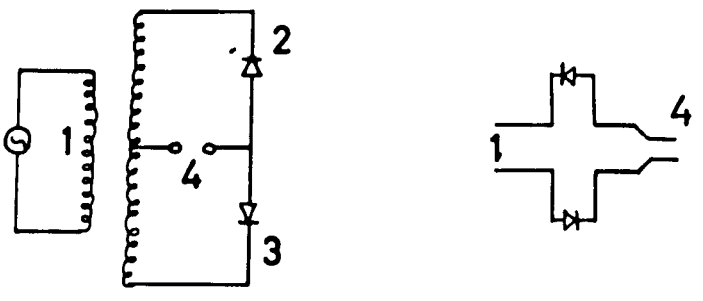

FIG 1.3

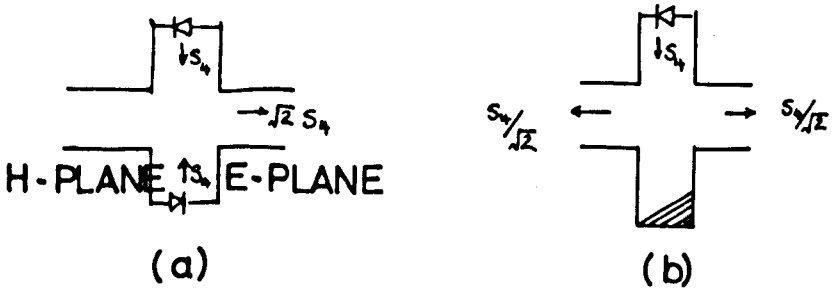

FIG 1.4

operating in the millimetre wavelength region. Here there is little loss of energy in the resistive part of the diode and the non linear reactance enables practical values for the conversion ratio as high as 12 dbs to be obtained.

Full Wave Harmonic Generator

At microwave frequencies a four arm magic tee has equivalent properties to a centre trapped transformer (Fig. 1.2). Crystals placed in the symmetry arms 2 and 3 are in the corresponding positions to a full wave rectifier. In contrast, a filter passing only the second harmonic frequency is in arm 4. The equivalent circuits are as shown in Fig. 1.3. The crystals are in anti-phase with respect to the fundamental voltage. The currents flowing through the crystals, i_1 and i_2 are given by

$$i_1 = f(V) = a_0 + a_1V + a_2V^2 + a_3V^3 + ...$$
$$i_2 = f(-V) = a_0 - a_1V + a_2V^2 - a_3V^3 + ...$$

Output from terminal 4 is

$$i_1 + i_2 = 2a_0 + 2a_2V^2 + 2a_4V^4 + ...$$

Output from terminal 1 is

$$i_1 - i_2 = 2aV + 2a_3V^3 + ...$$

Even harmonics are therefore in anti-phase with respect to odd harmonics (which include the fundamental). In the waveguide (Fig. 1.3b) this corresponds to inverting one crystal mount with respect to the other. As the generated second harmonic signals are now in anti-

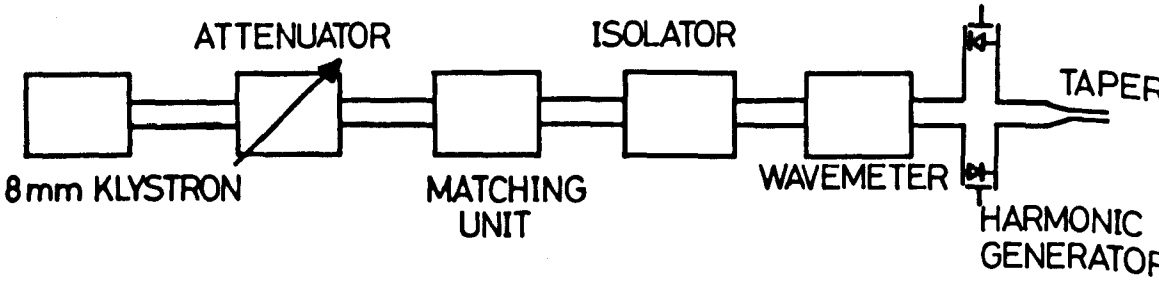

Fig. 1.5. Full Wave Harmonic Generator.

phase, they combine to give an output in arm 4 only, providing arms 2 and 3 are otherwise identical. Consider the T junction at the harmonic frequency only. Two four millimetre signals of equal amplitude S_4 and in antiphase will give a maximum combined signal of $\sqrt{2}S_4$ in the output arm. With one crystal arm replaced by a matched termination (Fig. 1.4b) the signal in the output arm is $S_4/\sqrt{2}$. The voltage gain for the two conditions is a factor of two.

This improvement of full wave generation over the single crystal generator is to be expected from Fourier analysis, for the effective characteristic of two crystals is symmetrical about the origin. In microwave terms, the generator can be perfectly matched to the fundamental. The advantages of this arrangement over a single crystal are:-

1) Easier to set up than the single crystal type.
2) Can handle twice the power of single crystal, or each crystal can be run at a lower level for the same output.
3) Can be matched near to unity, and for properly adjusted crystals the matching device for the fundamental is isolated from the harmonic power.

The experimental arrangement for a full wave multiplier used in these investigations is shown in Fig. 1.5.

1.1.c Other sources

An alternative approach to the problem of generating millimetre radiation is to approach the problem from the infra-red end of the

spectrum. In this region, black body sources are the most common. Unfortunately the power radiated by a black body source falls off very rapidly towards the millimetre region of the spectrum. Other possible millimetre sources[13-18] include quantum generators, Cherenkov radiation, tunnel diode oscillators, Froome generator, spark oscillators and the Josephson superconducting junction. Although, in theory Cherenkov interaction is weak, high current densities should enable appreciable amounts of power to be generated, and in 1960 the first experimental results in a 35 GHz Cherenkov radiator driven by a 0.042 ampere beam gave output powers approaching 1 watt. In practice megavolt power supplies are required and the need for filters poses a considerable problem.

1.2 Propagation of Millimetre Radiation

The problem of propagating millimetre radiation can also be approached from both the optical and the microwave sides. The first approach follows the principles of geometrical optics and requires components such as lenses, whose dimensions are many orders of magnitude larger than the wavelengths concerned. The second approach simply involves the scaling down of standard microwave components, with many associated technological difficulties. Because of the difficulties involved in these two approaches, several alternative methods have been developed which employ combinations of the two. A conventional rectangular wave guide which propagates microwaves only in the dominant (TE_{10}) mode is usable for millimetre waves, although attenuation increases with

frequency and, at the shortest wavelengths, attenuation may be prohibitively large. Oversize waveguide (for example, K-band size) may be used if it is matched to the generator, or to a small guide used to filter out low frequencies, by a suitable gradual taper. However, such a guide will transmit any higher modes generated at discontinuities, and so special care must be taken to avoid irregularities. For instance, flanged joints must be carefully assembled to ensure accurate alignment of the waveguide sections. Many generators of millimetre waves emit the waves into a number of different modes in an oversized waveguide. In such cases a complex of modes is already present, but careful elimination of irregularities at flanges is still important to reduce reflections and losses.

Attenuators used for millimetre waves resemble those for longer wavelengths, although they are reduced in dimensions. Carbon-coated tapered strips of mica inserted through an axial slot in the broad waveguide face is satisfactory.

Sometimes techniques based on those of optical spectroscopy may be used to advantage. For instance, reasonably small horns will produce a fairly narrow beam in free space or through an absorbing gas. This beam may also be reflected by a diffraction grating which permits rough wavelength measurements. For high efficiency, the grating can be of the echelette type, in which the rulings are shaped to throw as much of the diffracted radiation as possible into one order. One typical

echelette grating, designed to operate around 1.6 mm wavelength, had eighty $\frac{1}{8}$ in. grooves milled into a flat metal surface. An echelette grating is most efficient only for one particular wavelength, although the maximum is fairly broad.

1.3 Detection of Millimetre Radiation

Techniques adapted from those used in both the infra-red and the centimetre-wave region can be applied to detect millimetre waves. In the infra-red region, thermal detectors predominate; for centimetre waves thermal detectors are sometimes used, but crystal detectors are usually best and are most widely used.

One of the sensitive thermal detectors is the Golay cell. The Golay detector contains an air space between two films, one of which is an absorber of radiation. The other film is a very light flexible mirror. When radiation falls on the absorber, it heats the film and hence the air in the cell which then expands and slightly deflects the mirror. Motion of the mirror affects the amount of light falling on a photo-cell, and the resultant photo-current is proportional to the radiation intensity.

When the cell is used as a detector of millimetre waves, the end of the waveguide is pointed at the cell[19]. Some resonance effects are observed in this region because of the finite size of the cell aperture, so that it is helpful to optimize the cell response by adjusting its distance from the waveguide. The radiation is chopped at 10 cycles/sec by

a rotating semicircular absorber passing into the waveguide through a slot. When used with a circuit having a time constant of 5 sec., one cell of this type had a sensitivity of about 5×10^{-11} watt. The same sensitivity can be expected for shorter wavelengths, and so the Golay cell may be useful for submillimetre waves.

In the longer millimetre range the packaged cartridge-type crystals designed for 1.25 cm (IN26) or 8 mm (IN53, SIM8) wavelength are convenient as detectors or harmonic generators. Detectors using commercial crystals, are most successful at wavelengths above 4 mm, but their use at short wavelengths is quite difficult due to the very careful selection of the crystals required and because each crystal operates only over a narrow range of frequencies.

For most spectroscopic purposes, it is best to use components which are "broad band" so that they operate satisfactorily over a wide range of frequencies without complicated and critical tuning. Detectors and other circuit components which are simple and broad band are particularly desirable in the highest frequency ranges. This is partly because at the shortest wavelengths any critical dimensions become so difficult to control that they are best avoided. Furthermore, present spectroscopy below a few millimetres is still in a rather primitive state and is limited enough by other difficulties that an additional restriction of detectors to a narrow frequency range is very objectionable. Although detectors using pieces of silicon mounted individually in a waveguide

without a surrounding cartridge are somewhat time consuming to construct and less rugged than the commercial IN26 and IN53 crystals, they give enormously better performance at the shortest wavelengths. Problems of matching the microwave power into the crystal are very much reduced and the detector is usable over a much broader frequency range. Detectors of this type were shown by Klein, Loubser, Nethercot and Townes to be fairly sensitive over a wide range of frequencies and down to wavelengths of 1 mm.

The performance of these detectors is very sensitive to whisker pressure and to moisture present in the system. They are also rather unstable. Despite the disadvantages involved in their operation they remain the most widely used detector in the millimetre region.

1.4 Summary

The various techniques for the generation, detection and propagation of millimetre radiation have been discussed. The obvious source of millimetre power is a 4 mm klystron, but the short lifetime and high cost of the tube and power supply make this an impracticable choice. The next best source is a high power 8 mm reflex klystron from which several harmonics can be generated, and this was the method chosen for the studies reported in this thesis.

Harmonic generators and detectors were designed by using silicon, germanium and gallium arsenide crystal materials. Germanium was found to be more suitable. The whiskers were made from 1.5 mil tungsten wire and

given a sharp electropoint. Other materials could not be made available for evaluation. The whisker pressure could be adjusted by a differential screw mechanism. These are discussed in Chapter IV in some detail. Full wave harmonic generation was used due to advantages already discussed. Biasing of harmonic generators was also investigated. It was found that bias does not always bring about an improvement but its effect appears to be a function of the specific run-in conditions.

Experimental results obtained are discussed in Chapters IV, VI and VII.

CHAPTER II

MILLIMETRE WAVE RESONANT STRUCTURES

Introduction

The Resonant cavity forms an almost indispensable component in the fields of microwave techniques and microwave measurements. In the millimetre region of the spectrum it often becomes difficult to scale down the corresponding centimetre wave resonator. The reasons are primarily the difficulties involved in fabricating small components to any high degree of accuracy. The resonant properties of a cavity are specified by its Q-factor defined by

$$Q = 2\pi \frac{\text{energy stored}}{\text{energy dissipated per cycle}}$$

The energy stored is proportional to the square of the magnetic or electric flux density integrated throughout the volume of the resonator, while the energy lost per cycle in the walls is proportional to the skin depth and to the square of the magnetic or electric flux density integrated over the surface of the cavity. Thus, to obtain high Q, the resonator should have a large ratio of volume to surface area, since it is the volume that stores energy and it is the surface area that dissipates energy. For cavity resonators, a knowledge of the electromagnetic field distribution is of prime importance to the designer. For cavities of the same material, shape and mode of operation, the

Q values are proportional to the square root of the resonant wavelength. This leads to a reduced precision in measurements, and to an increased effect of losses in these resonant structures at short wavelengths. In general, the dimensions of each cavity must be comparable with the wavelength in order to avoid undue trouble from higher order modes, and at shorter wavelengths such cavities would become difficult to make. Providing considerable care is taken in their manufacture, conventional cavities are still useful at wavelengths as short as 4mm, but at 2mm wavelengths they are becoming a little impracticable.

An alternative to this problem is to turn to optical techniques and consider some of the Fabry-Perot type of optical resonators[20-22] which have been extended to the millimetre and infra red region of the spectrum. The advantages of such an interferometer or cavity resonator for ultra-microwaves are that the reflectors and component parts are large compared with the wavelength. In fact the larger they are the less are the effects of diffraction on the measurements, and instead of becoming more difficult, the problem of maintaining a high Q with a single mode of propagation and a structure of adequate size, become easier the smaller the wavelength.

A second type of resonator which has been suggested for use in the millimetre region is the dielectric tube resonator[23]. The resonator consists of a tube of dielectric material with metallic end plates, and power is coupled through one end plate. Its main advantage lies in the

fact that only cylindrically symmetric modes (H_{omn}) can be generated and so fairly high order modes can be used without the problem of generating many unwanted modes. Such cavities have been successfully used as E.S.R. sample cavities at Q band, but at higher frequencies they become rather difficult to fabricate.

The work for the design and construction of the millimetre wave resonators was undertaken with the object of making high Q tunable cavities for millimetre wave spectrometers and for using them in a millimetre wave beam maser using the $0_{00} - 1_{01}$ transition of formaldehyde molecule. The following types of resonant structures were designed and tested.

(a) Cylindrical cavities

(b) Plane parallel Fabry Perot resonators

(c) Confocal resonators

2.1 Cylindrical Cavities

By fundamental and general considerations every cavity resonator, regardless of its shape, has a series of resonant frequencies, infinite in number and more closely spaced as the frequency increases. The total number N of these having a resonant frequency less than f is given approximately by

$$N = \frac{8\pi}{3C^3} Vf^3$$

where V = volume of cavity in cubic metres

C = velocity of electromagnetic waves in the dielectric in metres per second

f = frequency in cycles per second.

With each resonance there is associated a particular standing wave pattern of the electromagnetic fields, which is identified by the term "mode".

In right cylinders (ends perpendicular to axis) the modes fall naturally into two groups, the transverse electric (TE) and the transverse magnetic (TM). In TE modes, the electric lines lie in planes perpendicular to the cylinder axis, and in TM modes, the magnetic lines so lie. Further identification of a specific mode is accomplished by the use of indices.

The Mode Chart

The formula relating the resonant frequency to the mode, shape and dimensions of the cylinder is of prime interest. It may be written as

$$(fD)^2 = A + Bn^2\left(\frac{D}{L}\right)^2 \qquad (1)$$

where f = frequency in megacycles per second

D = diameter of cavity in inches

L = length of cavity in inches

A = a constant depending upon the mode. Values of A are given in Table II for the few lowest modes.

B = a constant depending upon the velocity of electromagnetic waves in the dielectric. For air at 25°C and 60%

relative humidity, B = 0.34799×10^8 inches/second

n = third index defining the mode, i.e. the number of half wavelengths along the cylinder axis.

Table II

Constants for use in accurate computation of the resonant frequencies of circular cylinders.

$$(fD)^2 = \left(\frac{Cr}{\pi}\right)^2 + \left(\frac{Cn}{2}\right)^2\left(\frac{D}{L}\right)^2 = A + Bn^2\left(\frac{D}{L}\right)^2$$

$B = 0.34799 \times 10^8$ $\quad$ $C = 1.17981 \times 10^{10}$ in./sec

Mode	r	A
TM_{01}	2.40483	0.81563×10^8
02	5.52008	4.2975
03	8.65373	10.5617
11	3.83171	2.0707
12	7.01559	6.9415
13	10.17347	14.5970
21	5.13562	3.7197
TE_{01}	3.83171	2.0707
02	7.01559	6.9415
03	10.17347	14.5970
11	1.84118	0.4781
12	5.33144	4.0088
13	8.53632	10.2770
21	3.05424	1.3156

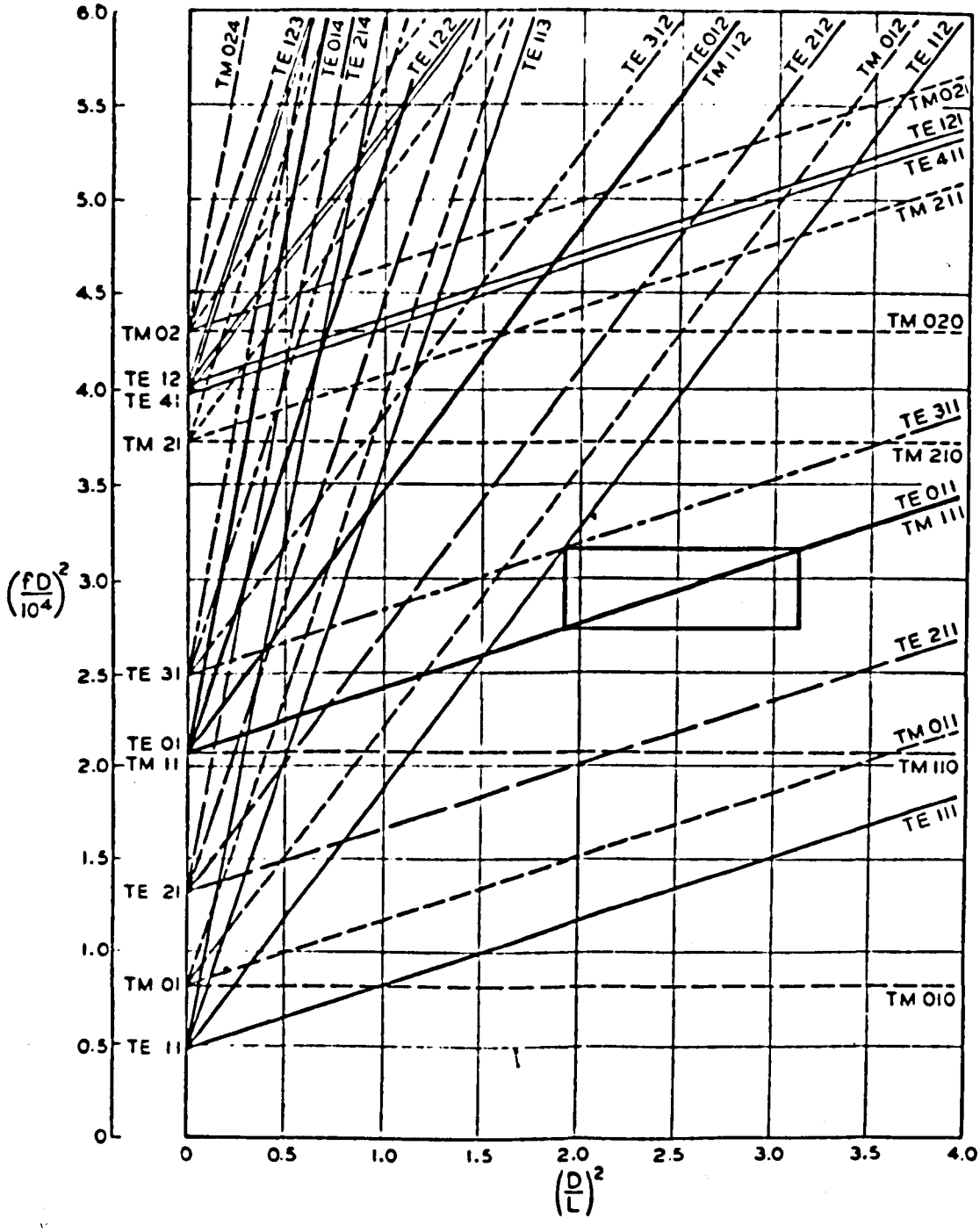

Fig. 2.1 Mode chart for right circular cylinder resonant cavity.

Value of C is for air at 25°C and 60% relative humidity. D and L are in inches, f in megacycles.

Formula (1) represents a family of straight lines, when $(\frac{D}{L})^2$ and $(fD)^2$ are used as coordinates, and leads directly to the easily constructed and highly useful "Mode chart" of Fig. 2.1.

As already mentioned the difficulties involved in fabricating millimetre wave resonators arise due to a decrease in electrical conductivity with increasing frequency and the consequent increase in skin depth. The difficulty can be partially overcome by using higher order modes, but care must be taken to suppress any unwanted modes. Suppression of the undesired modes requires a thorough knowledge of their field configurations and a number of effective techniques which may be applied on a practical engineering basis. Skin depth is a factor which recognizes the dissipation of energy in the walls and ends of the cylinder. With increase of resistivity of these surfaces the currents penetrate deeper and the resulting Q is lower. A comparison of the relative Q's computed from the resistivity of several metals will show the importance of this factor.

Silver	1.03
Copper	1.00
Gold	0.84
Aluminium	0.78
Brass	0.48

Therefore a brass cavity will have about one half of the Q that a similar cavity would have if made of copper. Similarly, the silverplating of a copper cavity will gain about 3 per cent in Q.

The Electroforming of Millimetre Wavelength Cavities

The electroforming process offers a means of fabricating parts where precise inside dimensions are desired. The electroform is made on a suitable mandrel having the inside dimensions of the piece to be made. By plating to the desired thickness on this mandrel, which is subsequently removed, the desired piece is readily made.

Electroforming baths

Of all the metals that can be plated, copper is one of the easiest to use for electroforming. The acid-copper bath is perhaps best and is quite simple to use. It operates at room temperature, and its fumes are not particularly toxic. Fairly smooth electroformed surfaces may be formed using copper. The following is a satisfactory copper bath:

Solution Composition		Operating Conditions
$CuSO_4$	200 gms	Temp. 60° - $120^\circ F$
H_2SO_4(pure) spg. 1.84	56 gms. or 31 millilitres	Current density 10 - 150 amps/sq.ft.
Potassium alum	12 gms	Anodes - Anode grade copper

The current density used depends upon the shape of the piece being electroformed, the condition of the bath, and the type of agitation of the cathode that is used. Agitation of the cathode is essential in electroforming copper. When commercial copper anodes are used, they should be covered with bags, from which all grease or oil has been removed to prevent the anode sludge from getting into the bath. A suitable bag material is spun-glass cloth.

Mandrels for Electroforming

Either re-usable or disposable mandrels may be used. The re-usable type is appropriate when the configuration of the electroformed piece is such that the mandrel can be removed without damage to the mandrel or to the formed piece. Mandrels of this type are usually made of metal or quartz, and a means of separating the mandrel from the formed piece must be provided. With many types of metal mandrels, the plating adheres to the mandrel, and therefore the mandrel has to be coated with a separating film before electroforming. A film having a low melting point such as tin or cadmium makes a good separator. When using a tin or cadmium separator the mandrel is made slightly undersize (0.001 inch) and is then tin or cadmium plated to size. The electroforming material is then plated over the separating film. When the electroforming is finished, the whole piece is heated to the point where the separator melts and the mandrel is withdrawn and wiped clean before the separator has time to cool. Some of the separator will stick to the inside of the formed piece but it can be removed by proper stripping solution. Cold HCl works well in removing cadmium or tin from electroformed copper pieces, since it does not react with the copper.

Mandrel materials such as stainless steel, chromium-plated steel, and quartz are desirable because the plating does not adhere very well to them, and thus no separating film is necessary if the mandrel and electroforming metal have different coefficients of thermal expansion.

In order to separate the mandrel from the formed piece a small amount of heat is applied until the differential expansion of the two metals breaks the poor bond between them; the mandrel can then be removed. The required temperature depends on the temperature at which the electroforming was done and the size of the piece.

2.1.1 Experimental

TM_{010} mode was selected for the design and construction of cylindrical cavities to be used in setting up a formaldehyde gas spectrometer at 72838.14Mc using the $0_{00} - 1_{01}$ transition. This particular mode is independent of the length of cavity, so that a long cavity can be used resulting in an increased sensitivity and resolution over other modes. This increased sensitivity arises due to the increased downward transition probability of an excited molecule on account of longer time spent within the microwave field of the cavity. The cavity has an internal diameter of 0.1239 inches. A number of cavities of lengths from 1.37 ins to 2.75 ins were fabricated. In order to prevent the loss of microwave power from within the cavity, but at the same time allowing the free passage of molecules, hollow concentric brass caps are inserted into the ends of the cavity. These caps have a slot along their length so that they are a push fit into the cavity ends. A coupling hole (dia. .052 ins) is provided in the centre of the cavities used in reflection and two holes of the same diameter separated by 3.2 cms for cavities used in transmission.

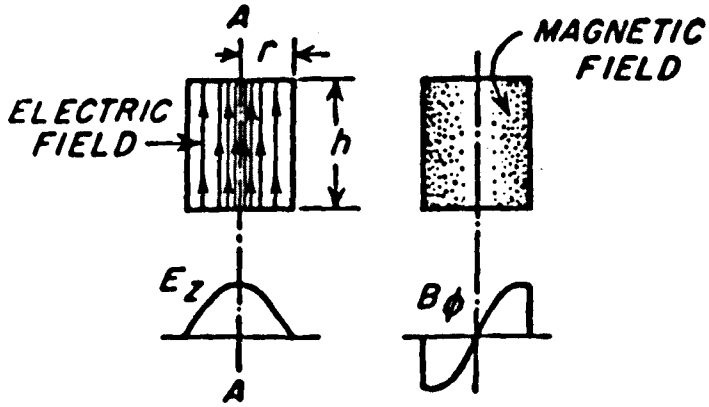

Fig. 2.2 Field configuration TM_{010} mode.

Cavities were formed by electroforming on stainless steel mandrels. Mandrels were ground from S80 stainless steel and copper was electrodeposited on the mandrels from an acid copper bath. The mandrel was rotated slowly during the electroforming process and the current was reversed 15 seconds every 50 seconds to ensure an even deposition. The first layer of copper was deposited slowly with a current of about 50 milliamperes and was gradually increased.

The loaded Q of the cavity was about 2400. The Q was determined by measuring the frequency width at half power points. The cavity is tuned to the appropriate transition frequency by heating it electrically. The cavity expands when heated and reduces the resonant frequency. The heater coil is bifilar wound so that there is no Zeeman splitting effect on the molecular resonance inside the cavity. The cavity temperature is controlled by adjusting the current flowing through the heater coil. The input potential is switched on and off by a relay system ('Airmec' type 299) operated by a copper resistance thermometer (8.9 ohm at $20^{\circ}C$) attached to the cavity.

TM_{010} mode was excited. The electric field vector in such a resonator is directed along the geometrical axis of the cylinder, perpendicularly to the ends. The electric field is a maximum at the resonator axis and is zero at the walls. The magnetic field lines form closed circles in cross sectional planes of the resonator. The field configuration is shown in Fig. 2.2.

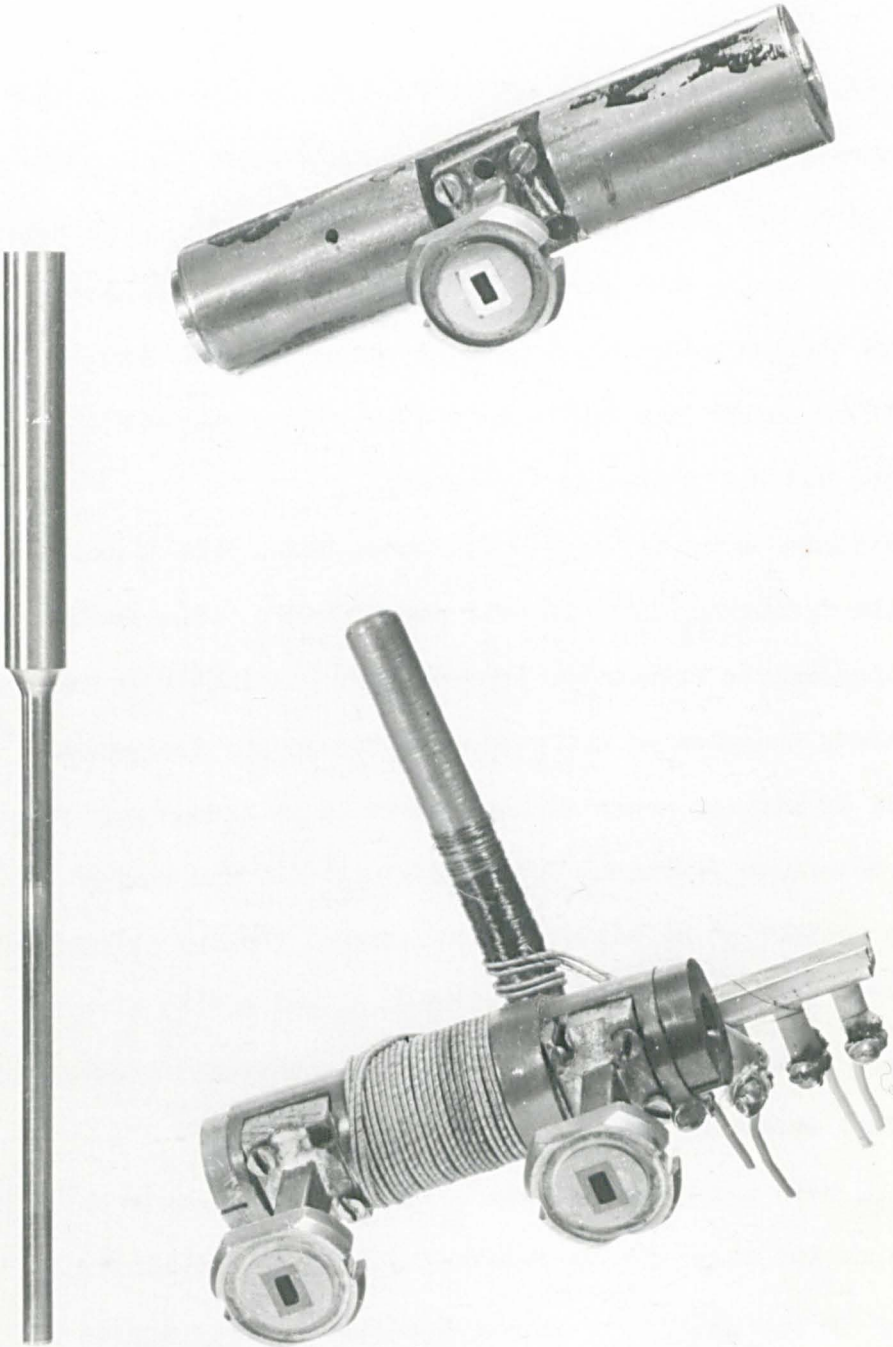

Fig. 2.2a Cylindrical cavities.

One of the advantages of using a cylindrical cavity is that it can be designed for a particular mode. From the mode Chart (Fig. 2.1) it can be seen that at $(\frac{D}{L})^2 > .06$, TM_{010}, TM_{011}, TM_{012}, TE_{112}, TE_{111} and TE_{214} modes are excited. For $(\frac{D}{L})^2 < .06$, TM_{010}, TM_{011} and TM_{012} modes are excited which is applicable in our case: A TM_{010} resonance is always observed at a lower frequency than TM_{011} and TM_{012} modes. Hence it was possible to distinguish between these modes. If many modes rather than a single one are present in the cavity, a rather large background of noise can occur, the noise temperature being proportional to the number of modes which are confused within the resonance width of the molecular system. Isolation of an individual mode avoids this severe difficulty.

There has been considerable difficulty in tuning these cavities to the exact frequency because of the difficulty of machining the mandrels to the required accuracy. A change of 0.0001" in the diameter shifts the frequency by about 60 Mc/sec. Hence the cavities were generally either too small or too large in diameter and had to be polished or squeezed which decreased the Q.

Cavities were also machined and mechanically polished. They were first bored with a drill of diameter 0.120 inch. Standard reamers of diameter 0.125 inch were ground to diameters 0.1230 in and 0.1238 ins. and were used for polishing. The final polishing was done with the help of mandrels. Cavities machined directly in this way were easier to make but were found to be inferior in Q to the electroformed ones. Experimental results are shown in Chapter VII.

2.2 Plane Parallel Fabry Perot Resonators

In the short wavelength region there is a definite need for some replacement of the conventional cavity resonator. Since cavities operate on the principle of multiple reflections and interference, it is natural to consider the use of microwave form of an optical interferometer to replace the cavity in this region. Thus, the use of microwave interferometers based on the optical Fabry-Perot interferometer is indicated.

In the millimetre region the ratio of wavelength to the mirror dimensions, although small compared to unity, is much larger than in the optical region. Therefore diffraction losses in the millimetre region tend to be much larger. At the same time modes are separated more widely, and it is usually possible to work with a single mode. The apertures which can be used in such microwave interferometers are very much smaller in terms of the wavelength than those normally used in optical instruments, and a consideration of the diffraction which inevitably occurs is most important in their design and use. In Fabry-Perot resonators the major factors contributing to the Q (i.e. resolving power) are reflection losses and diffraction losses. Reflection losses result from absorption in the reflectors, and from transmission through them. Diffraction losses result from the finite aperture of the reflectors and from imperfections in the "flatness".

Resonator Quality Factor

Resonator quality factor, or Q, is defined as

$$Q = \omega \cdot \frac{\text{energy stored}}{\text{energy lost per second}} \tag{2}$$

Consider an interferometer consisting of two reflecting surfaces separated by a distance d which is large compared to the wavelength in the medium λ. By considering waves bouncing back and forth between the surfaces, one may derive an approximate Q as

$$Q = \frac{2\pi d}{\alpha \lambda} \tag{3}$$

where α is the fractional power loss per bounce from a reflector and is the sum of the diffraction and reflection losses. This is to be compared to the resolving power derived in optics[24] as

$$R = \frac{2\pi d\sqrt{r}}{\lambda(1-r)} \tag{4}$$

where the power reflection coefficient per bounce is $r = 1 - \alpha$. Resolving power is thus synonymous with Q within the small loss approximation of (3). If diffraction losses are small compared with reflection losses, then resonator Q is proportional to the spacing between the reflecting surfaces. For a given reflector aperture size, the resonator Q will continue to increase with the spacing d between the reflectors until the diffraction losses become roughly comparable with the reflection losses. Further increase in spacing then decreases the Q because of increasing diffraction losses.

The Resonant Frequencies of Parallel Plate Interferometers

In all practical applications of the Fabry-Perot interferometer, observation is made along the central axis perpendicular to the plates. What is considered as a resonance from the microwave point of view corresponds to a maximum in intensity at the centre of the field of view in an optical interference pattern. In elementary texts, the behaviour is explained in terms of the multiple reflection of plane waves between the reflectors. It is assumed that these plane waves have the same wavelength λ_o and phase velocity as in an unbounded medium. If the plates are perfectly reflecting, the condition for resonance is then

$$\lambda_o = \frac{2D}{m} \qquad (5)$$

where D is the separation and m is any positive integer. The frequency is given by dividing λ_o into the phase velocity.

Such a description is inadequate to explain all of the recent observations. Schawlow and Townes[25] in proposing the use of the Fabry-Perot interferometer as a resonator for optical masers, suggested that it should be considered as a rectangular box with four open sides. A transmission line with both ends short circuited resonates at the same frequencies as when both ends are open circuited, except that the positions of the nodes and antinodes are interchanged. Analogously, if the interferometer has rectangular plates, each of dimensions A and B separated by a distance D, it can be expected to resonate at the same frequencies as a closed rectangular box of the same dimensions where the

freespace wavelengths are given very accurately by

$$\lambda_{m,n,p} = 2\left[\frac{m^2}{D^2} + \frac{n^2}{A^2} + \frac{p^2}{B^2}\right]^{-\frac{1}{2}} \qquad (6)$$

where m, n, and p are non-zero integers.

The theoretical work of Fox and Li[26] investigated the field patterns and showed that they do indeed differ from plane waves. Symmetry considerations require that n and p be odd integers for modes which are observed with coupling which is symmetrical about the central axis of the instrument.

In most practical situations, the second and third terms in the brackets of (6) are small compared to the first. In cases where they may be completely neglected, it can be seen that $\lambda_{m,n,p}$ becomes equal to λ_o obtained in the elementary theory. In conventional optical situations these terms are generally so small that modes of the same m and differing n and p lie so close together as not to be resolved, and the elementary theory is adequate. However, with masers, the resolution is such that the frequencies emitted as the result of simultaneous oscillation in several of these modes can be resolved. The modes with the lowest values of n and p, namely unity, have the highest Q and give rise to the strongest absorption or emission lines. The original report on the helium-neon gas maser[27] contains excellent experimental verification of the validity of (6). In that paper the strong signals at 150 Mc intervals are due to beating of modes with different m's but all with n = 1 and p = 1.

The weaker peaks displaced by 1.5 Mc are due to beats between a mode described by n = 1 and p = 1 and a mode with a different m and either n or p equal to 3 while the other of these two quantities remains equal to 1. Quantitatively these values are consistent with (6) and the geometry of the apparatus, in which B = A.

For many purposes it is convenient to employ an approximation for (6) by expressing D in terms of λ_o by (5) and retaining only first-order terms. B is set equal to A, since this condition usually prevails. Then

$$\lambda_{m,n,p} = \lambda_o \left[1 - \frac{(n^2 + p^2)\ \lambda_o^2}{8A^2} \right] \qquad (7)$$

Since n and p are never zero, the second term on the right is not identically zero and it must be considered if the Fabry-Perot resonator is used as a wavemeter of the highest available accuracy. λ_o may be determined by measuring the displacement of one plate between major resonances. Then a correction can be determined by substituting this value into the second term of (7). A can be determined from geometry or by measuring the frequency shift between a main resonance for which n = 1 and p = 1 to a subsidiary one where one or both has a higher value.

The planar type of reflector system, due to the absence of mode degeneracy, possesses some advantages. Diffraction losses, though larger for given dimensions than those of the confocal type resonator, can still be made small at the shorter wavelengths, and their effect on measurements reduced. However, for a given wavelength and reflector size,

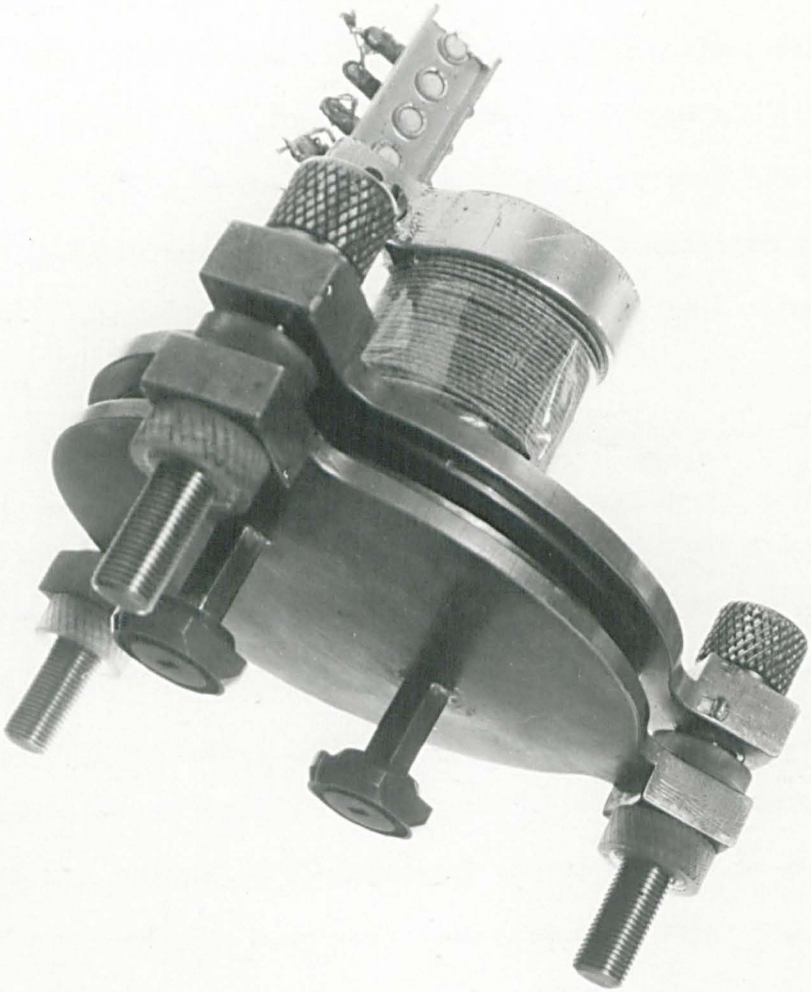

Fig. 2.3 Plane parallel Fabry Perot resonator.

such losses do limit the Q value obtainable, and for some purposes such as filter applications, and threshold conditions in lasers, the confocal type may be preferable. However, the planar geometry, though more critical in adjustment and in the degree of flatness required, readily permits single mode operation, and potentially gives a larger power output than the confocal system.

2.2.1 Experimental

The Fabry-Perot resonators used here were constructed with plane parallel brass plates with a diameter of the order of 15λ. The plates were polished to an accuracy of about 1 micron. Two 4mm wave guides passed through one of the mirrors and were open within the resonator symmetrically relative to the centre of the mirror. The distance between them was 3.2 cms. The mirrors were fastened with three screws with springs between them with which coarse adjustment of the resonator was accomplished. The distance between the plates was first adjusted with the feeler gauge and then with the screws. Precise tuning was achieved by heating. The temperature of the resonator was held constant by means of a thermostat consisting of a sensing element which formed one arm of a Wheatstone bridge; an arrangement similar to the one used for heating the cylindrical cavities mentioned earlier. It was designed to keep the two plates insulated from each other so that it could also be used as a parallel plate Stark cell. It is found that the Q is highly dependent upon the parallelism of the plates and the

Fig. 2.4a Confocal resonator.

cleanness of the surfaces. The electric parallelism does not coincide with the geometric parallelism because of the disturbance introduced by the coupling elements. The positions of the mirrors were adjusted by moving them apart in such a way that a large resonance maximum would appear without any preceding small resonances. This resonance corresponded to the simplest mode with a single maximum of E at the centre between the mirrors and was used for investigations on the $0_{00} \leftrightarrow 1_{01}$ transition of formaldehyde. A thin film of silver was deposited on the plates in an evaporating chamber to increase the Q.

2.3 Confocal Resonators

For some experiments and applications, the planar type of interferometer or resonator is not suitable. Examples of this occur in solid state research, optical maser work and electronic interaction with electric fields. Here, the resonator fields must be concentrated into a smaller volume and it is natural to consider the use of cylindrical or spherical Fabry-Perot plates and focused radiation to produce concentrated fields in the vicinity of a focal point. Such an arrangement resonates in an analogous way to the plane reflector geometry. A resonator formed by two spherical reflectors of equal curvature and separated by their common radius of curvature is considered in detail by Boyd and Gordon[28]. The focal length of a spherical mirror is one-half of its radius of curvature. Therefore the focal points of the reflectors are coincident and the resonator is termed confocal. Fox and Li[29] have suggested confocal resonators.

The use of confocal reflectors as an interferometer has been described by Connes[30]. The adjustment of the spherical Connes interferometer is trivial compared to the plane parallel Fabry-Perot. Parallelism between the reflectors is not a strict requirement, the only fine adjustment therefore being the spacing between the surfaces. Confocal resonator was used by Marcuse[31] in the design of his HCN maser to give a high Q resonant cavity at 88 Gc. Parabolic surfaces may also be used, but they have an axis and thus lose the advantage of ease of adjustment. Mode patterns and diffraction losses of such a resonator have been obtained analytically by Boyd and Gordon. The results show that the diffraction losses are generally considerably lower for the curved surfaces than for the plane surfaces. Diffraction losses and mode volume are a minimum when the reflector spacing equals the common radius of curvature of the reflectors. The modes of the confocal resonator are degenerate. This degeneracy is split if the resonator is non-confocal. The splitting is comparable with that of the plane parallel resonator if the spacing of the reflectors is about 3 per cent different from the common radius. The confocal resonators were first used at infrared - optical wavelengths. However, such resonators may be useful down to the millimetre wave range by virtue of their low loss.

The condition of resonance for the TEM_{mnq} mode is given by[28]:

$$\frac{4b}{\lambda} = 2q + (1 + m + n) \qquad (8)$$

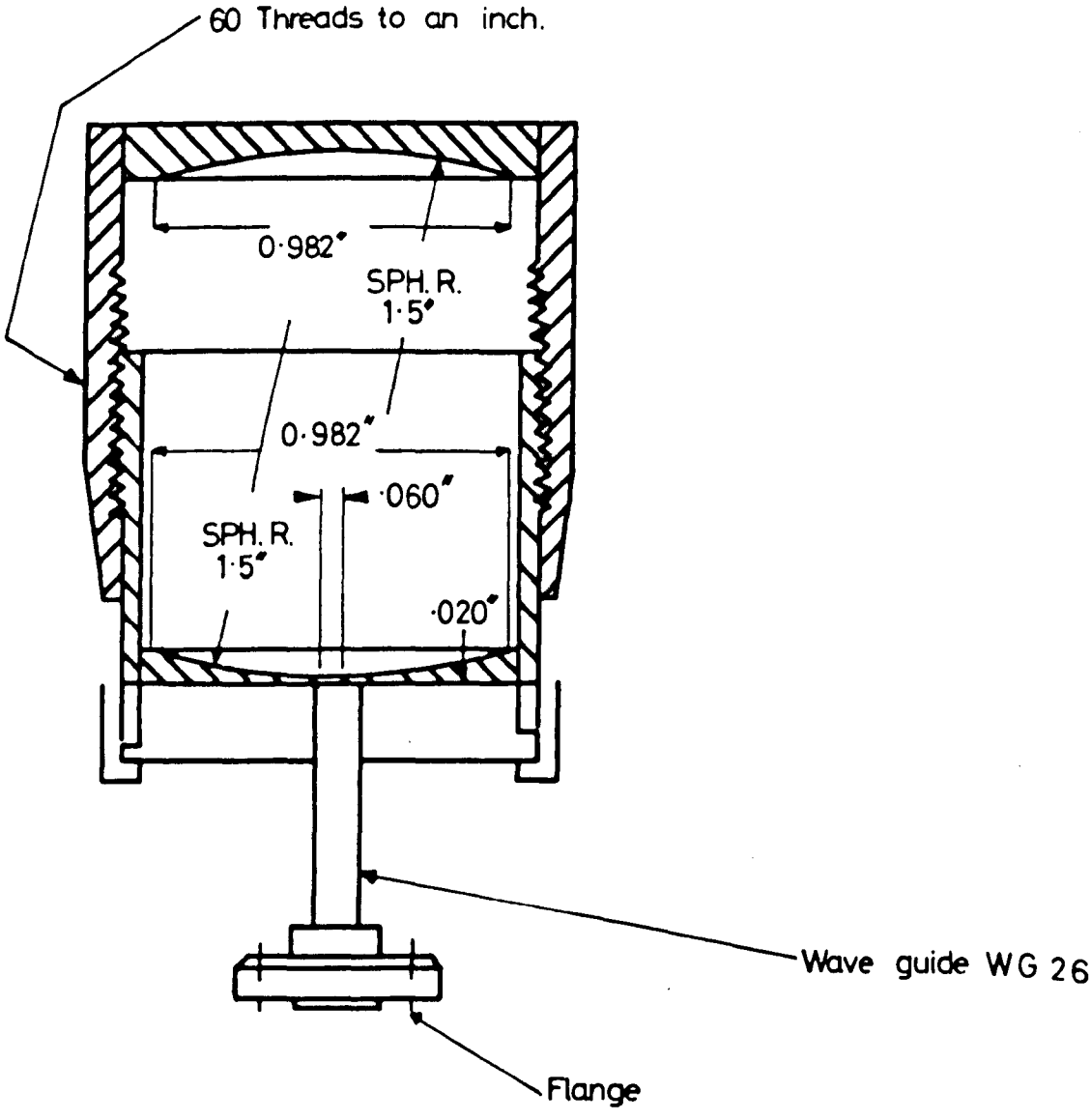

Fig. 2.4. Confocal resonator.

where $b = R$ is the radius of curvature

q = number of half wavelengths between reflectors

$m,n = 0, 1, 2$ represent the mode variations.

The confocal resonator is seen to have resonances only for integral values of the quantity $\frac{4b}{\lambda}$. If $\frac{4b}{\lambda}$ is odd, $(m + n)$ must be even, likewise if $\frac{4b}{\lambda}$ is even, $(m + n)$ must be odd. Note that considerable degeneracy exists in the spectrum; increasing $(m + n)$ by two and decreasing q by unity gives the same frequency. The degenerate modes are orthogonal over the reflector surface. The modes have negligible axial electric and magnetic fields and thus are designated by TEM_{mnq}.

2.3.1 Experimental

In order to achieve high signal to noise ratio in the millimetre region where low power is available a high Q confocal-type Fabry-Perot resonator was designed. In operation one spherical mirror is moved back and forth with respect to the other by screwing the outside cylinder as shown in Fig. 2.4. The mirrors were machined out of brass with a diameter of 1.0 in. and 1.5 in. radius of curvature. The mirrors were polished to an accuracy of a micron. A coupling hole of .06 in. was used. The mirrors were designed such that the parameter $\frac{a^2}{b\lambda} \approx 1$ at 73 Gc, where a is the radius of the mirrors, b is the radius of curvature of the mirrors, and λ is the wavelength in the medium. For large values of $\frac{a^2}{b\lambda}$, the field at the edge of the reflectors decreases, thereby decreasing the diffraction losses. By limiting this parameter to a

value of 1.0 or slightly less, the diffraction losses for the fundamental mode (TEM_{ooq}) are comparable to the reflection losses. Since the Q is also limited by the reflection losses, little is gained by lowering the diffraction losses below the value obtained for a ratio $\frac{a^2}{b\lambda} = 1$. Since the diffraction losses for the next higher mode are an order of magnitude greater than the losses for the fundamental mode, some mode discrimination can be realized by such a limitation of the $\frac{a^2}{b\lambda}$ parameter. Although the ratio given above was calculated for a frequency of 73 Gc, the resonator had sufficient bandwidth to cover the millimetre transitions in carbonyl sulphide and formaldehyde. For the fundamental mode TEM_{ooq}, equation (8) reduces to

$$\frac{4b}{\lambda} = 2q + 1 \qquad (9)$$

The cavity resonances occur at intervals of $\lambda/2$. Hence by noting the distance the cylinder moves between successive absorption dips, the wavelength can be directly measured. The resonator was also used as a high Q wavemeter for off setting the klystron by 30 Mc in superheterodyne spectrometers used for increasing the signal to noise ratio of the OCS and CH_2O millimetre absorption. Experimental results are shown in Chapters IV, VI and VII.

CHAPTER III

WORKING SUBSTANCES

3.1 Carbonyl Sulphide (OCS)

OCS is a linear molecule and the spectrum produced is particularly simple because its more abundant isotopic types show no nuclear quadrupole effects. Nuclei of the most plentiful isotopic species $O^{16}C^{12}S^{32}$ have zero spins, and since the nuclei can, therefore, take no preferred orientation in the molecule, no quadrupole effects are possible. Again because no quadrupole effects are present the Stark effect in this molecule is simple and lends itself to very accurate determination of the OCS dipole moment. Dakin, Good, and Coles[32] obtained a value of 0.72 Debye unit for the OCS moment. Electron diffraction measurements had assigned distances 1.16 ± 0.02A for the O-C bond and 1.56 ± 0.03A for the C-S bond. Computation of the moment of inertia I from these internuclear distances shows that of the expected series of rotational lines, the transitions from J=5 to J=6 and J=11 to J=12 should produce absorptions near 4 millimetre and 2 millimetre wavelengths.

Intensity and shape of microwave absorption lines are given according to Van Vleck and Weisskopf[33,34] by the expression

$$\gamma = \frac{4\pi N f |\mu_{ij}|^2 \nu^2}{3ckT\tau} \left[\frac{1}{(\nu-\nu_o)^2 + (\frac{1}{2\pi\tau})^2} + \frac{1}{(\nu+\nu_o)^2 + (\frac{1}{2\pi\tau})^2} \right] \qquad (1)$$

where γ is the absorption coefficient in cm^{-1}, $\gamma/2$ is the loss in nepers/cm.

N is the number of gas molecules per unit volume.

f is the fraction of molecules in the lower state of the transition $i \rightarrow j$.

ν_o is the molecular resonant frequency.

τ is the time between inter-molecular collisions.

μ_{ij} is the quantum-mechanical matrix element for the absorption transition averaged over all values of the magnetic quantum number m.

c,k,T are the velocity of light, Boltzmann Constant, and absolute temperature of the gas respectively.

At pressures less than $^1/_{10}$ atmosphere the second term in brackets of expression (1) is quite negligible. The first term in brackets appears to agree well with experiment under low pressure conditions down to pressures of about 10^{-2}mm Hg, where various complicating effects may be of importance. For the rotational transition $J = J_o \rightarrow J_o + 1$ of a linear molecule, $|\mu_{ij}|^2 = \mu^2(J_o + 1)/2J_o + 1$, where μ is the molecular dipole moment, and

$$f = f_v \frac{(2J_o + 1)\exp\left[-J_o(J_o + 1)B/kT\right]}{\sum_J (2J + 1)\exp\left[-J(J + 1)B/kT\right]}$$

where B is the molecular rotational constant and related to the moment of inertia I by $B = h^2/8\pi^2 I$. The quantity f_v is the fraction of molecules

in the vibrational and electronic state under consideration - usually close to one for the lowest state. For a line occurring in the microwave region $J_o B << kT$ and the sum may be fairly accurately replaced by an integral so that $f = f_v(2J_o + 1)B/kT$ and, neglecting the second term of (1) at low pressures,

$$\gamma = \frac{2\pi N f_v h\mu^2 \nu^2 \nu_o}{3c(kT)^2\tau\left[(\nu-\nu_o)^2 + (\frac{1}{2\pi\tau})^2\right]} \qquad (2)$$

It should be noted that this formula gives a maximum absorption coefficient (when $\nu = \nu_o$) which increases approximately as the cube of the frequency ν_o. This is one of the reasons why microwave absorption measurements in gases have been mostly made at as high frequencies as can conveniently be used. Even after the molecular dipole moment is known, the peak intensity or value of γ when $\nu = \nu_o$ cannot be predicted because it depends on the value of τ, which usually must be determined empirically, although enough measurements have now been made to allow in some cases a rough guess at τ. The half width or width in frequency of the absorption line at one-half maximum, may be used as a measure of τ, since it equals $1/\pi\tau$.

Although most of the OCS molecules are in the ground vibrational state, an appreciable number are excited to higher vibrational states. Molecular vibrations interact slightly with the molecular rotational levels, producing small changes in the rotational constant B of the order of B^2/ω, where ω is the vibrational frequency. These effects are

generally taken into account by writing the rotational frequencies as

$$\nu = 2J\left[B_e - \alpha_1(v_1 + \tfrac{1}{2}) - \alpha_2(v_2 + 1) - \alpha_3(v_3 + \tfrac{1}{2})\right] \qquad (3)$$

where B_e is the value of the rotational constant B assuming no vibration; α_1, α_2 and α_3 are coefficients representing the change in the effective value of B due to vibration. The quantum numbers v_1, v_2 and v_3 are integers representing the degree of excitation of the three vibrational modes. Mode number two gives a contribution α_2 rather than $\alpha_2/2$ in the ground state ($v_1 = v_2 = v_3 = 0$) because it is the degenerate bending mode. In addition, interaction between rotational and vibrational motions removes the degeneracy of this bending mode. This effect is manifested most prominently in case $v_2 = 1$, when the level which is doubly degenerate in the absence of rotation is split by rotation into what is known as ℓ-type doublets. The rotational frequencies are then[35]

$$\nu = 2J\left[B_e - \alpha_1(v_1 + \tfrac{1}{2}) - 2\alpha_2 \pm \frac{q}{2} - \alpha_3(v_3 + \tfrac{1}{2})\right] \qquad (4)$$

The quantities of α_1, α_2, α_3 have been calculated by Nielson[36]. Unfortunately they are primarily dependent on the generally unknown anharmonic force constants of vibration. A theoretical evaluation of q is given by Nielson and Shaffer[37]. This q must be carefully distinguished from the q sometimes used as a measure of the molecular quadrupole field. The α's and q may be determined experimentally if rotational lines due to molecules in the ground state and various excited states can be

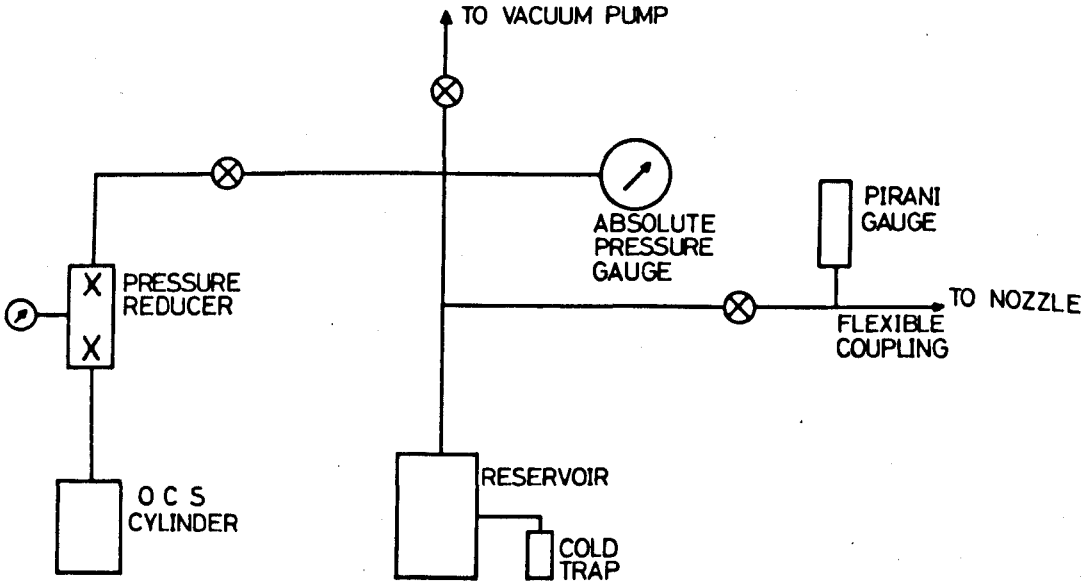

Fig. 3.1. O C S SUPPLY SYSTEM.

observed. For OCS the vibrational frequencies are known so that the fraction of molecules in excited states may be calculated.

3.1.1 Properties

It is a colourless, highly poisonous gas with a mild odour. It forms an explosive mixture with air. It is decomposed by water and bases; with the formation of carbon dioxide and hydrogen sulphide. In itself it is slightly irritating and works principally on the central nervous system. Concentrations of 6,000 parts per million by weight can cause death after exposure of 50 minutes. It should be stored in a cool place away from moist air and in sealed containers. Personnel should be cautioned against careless handling and containers should be plainly labelled. It should be used and placed in a well ventilated place. It has an M.P. = $-138^{\circ}C$, B.P. = $-48^{\circ}C$ and vapour pressure of 210mm at $-75^{\circ}C$.

3.1.2 Experimental

This gas is commercially available as a compressed gas. A pressure reducer unit model 11-330 (Cambrian Chemicals Ltd.) was used. The layout is shown in Fig. 3.1. Respiratory equipment was used for longer operations for safety.

The vacuum connecting pipes are made from $\frac{1}{2}$ inch diameter copper pipe with "Yorkshire" lead solder sealed junctions and "Genevac" or "Edwards" pressure actuated hand valves are used.

3.2 Formaldehyde (CH_2O)

CH_2O is a nearly prolate symmetric top molecule. Molecular rotors can be classified on the basis of their relative principal moments of inertia.

Relative moments of Inertia	Type	Examples
$I_A = I_B = I_C$	Spherical Top	CH_4
$I_A < I_B = I_C$	Symmetric Top (Prolate)	NH_3
$I_A = I_B < I_C$	Symmetric Top (Oblate)	$CHCl_3$
$I_A < I_B < I_C$	Asymmetric Top	H_2O, CH_2O

In the case of CH_2O in the ground state

$$I_A = 2.98 \times 10^{-40} \text{gm cm}^2$$

$$I_B = 21.65 \times 10^{-40} \text{gm cm}^2$$

$$I_C = 24.62 \times 10^{-40} \text{gm cm}^2$$

Hence CH_2O is an asymmetric top rotor or a nearly prolate symmetric top. We can describe the behaviour of an asymmetric rotor in terms of a parameter known as asymmetry parameter. It is given by

$$\kappa = \frac{2B - A - C}{A - C}$$

where A, B. C are the rotational constants given by

$$A = \frac{h}{8\pi^2 I_A}$$

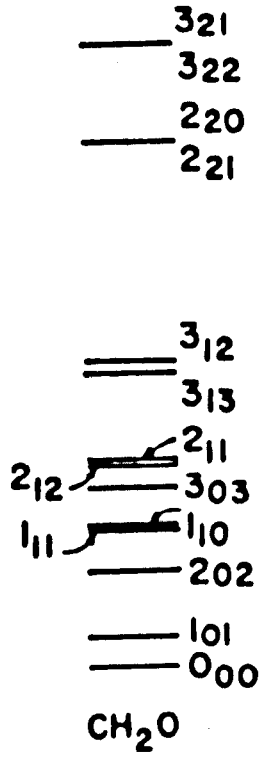

Fig. 3.2 Lower rotational levels of formaldehyde.

$$B = \frac{h}{8\pi^2 I_B}$$

$$C = \frac{h}{8\pi^2 I_C}$$

where h is the Planck's constant.

For a prolate symmetric top $\kappa = -1$.

For an oblate symmetric top $\kappa = +1$.

In the case of $C^{12}H_2O^{16}$:

A = 282,106 Mc

B = 38,834 Mc

C = 34,004 Mc.

$\therefore$ Asymmetry parameter $\kappa = \frac{2B - A - C}{A - C} = -0.961067$

Rotational energy levels of CH_2O

In the case of asymmetric top molecules, the rotational frequencies can no longer be expressed in convenient equations as in linear and symmetric top molecules. Only for certain low J values can the energy levels of the asymmetric rotor be expressed in a closed form.

King, Hainer and Cross[38] have published extensive tables from which energy levels for various degrees of asymmetry can be obtained to a useful degree of approximation for J values up to 12. The lower rotational levels of CH_2O, calculated in the rigid rotor approximation are shown in Fig. 3.2.

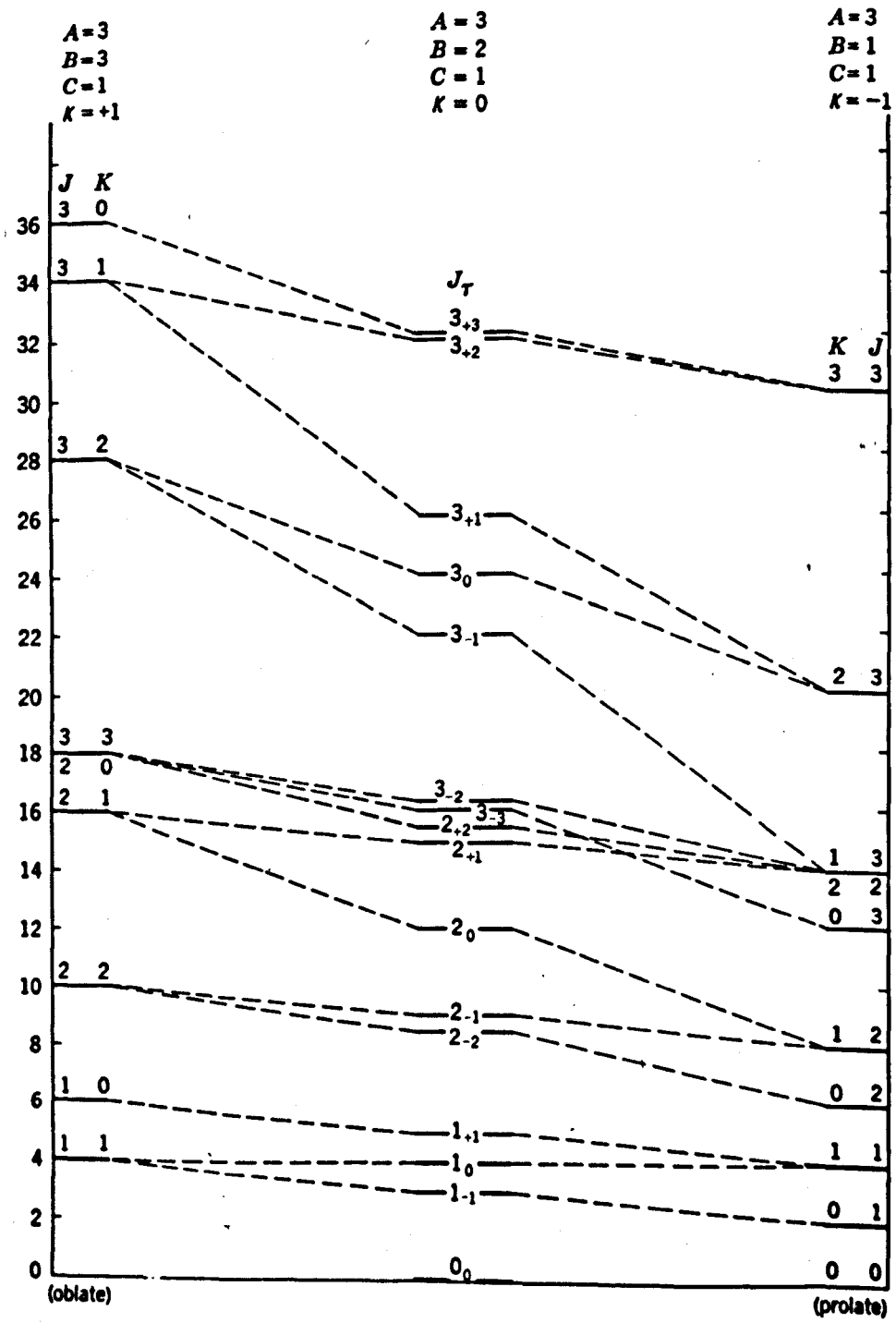

Fig. 3.3 Correlation of energy levels of an asymmetric rotor with those of the limiting symmetric tops.

Double subscript system of King, Hainer and Cross

Their system is best understood by a comparison of the limiting prolate and oblate symmetric tops. The energy expression for the symmetric rotor is

$$E_{JK} = h\left[BJ(J + 1) + (A - B)K^2\right] \quad \text{Prolate Symmetric Top}$$

$$E_{JK} = h\left[BJ(J + 1) + (C - B)K^2\right] \quad \text{Oblate Symmetric Top}$$

The energy levels of slightly asymmetric rotor ($\kappa \approx -1$ or $+1$) differ from the limiting symmetric top ones only in that the levels corresponding to -K and +K which are always degenerate in the symmetric rotor, are separated in the asymmetric rotor. An asymmetric rotor has (2J + 1) distinct rotational sublevels for each value of J whereas a symmetric rotor has only J + 1 rotational sublevels for each value of J. With the increase in asymmetry, the "K splitting" increases until there is no longer any close correspondence between the two levels and the degenerate K levels of the symmetric top.

Nevertheless, by connecting the K levels for a given J of the limiting prolate symmetric top with those of the oblate symmetric top in the ordered sequence - highest to highest, next highest to next highest and so on, as shown in Fig. 3.3, one can obtain a qualitative indication of the levels of an asymmetric rotor. Energy levels are indicated as $J_{K_{-1}\ K_1}$.

3.2.1 Properties

Formaldehyde is a colourless gas which condenses on chilling to give a liquid that boils at -19°C and freezes to a crystalline solid at -118°C. Both liquid and gas polymerize readily at ordinary and low temperatures and can be kept in the pure monomeric state only for a limited time. Because of these factors formaldehyde is sold and transported only in solution or in the polymerized state. When required, monomeric formaldehyde is prepared from the commercial solution or polymer at the point of use.

Monomeric formaldehyde gas is characterised by a pungent odour and is extremely irritating to the mucous membranes of the eyes, nose, and throat even when present in concentrations as low as 20 parts per million. In this connection it should be noted that the polymeric vapours of Trioxane $(CH_2O)_3$ the little known trimer of formaldehyde, are not irritating but possessa pleasant chloroform-like odour. Pure, dry formaldehyde gas shows no visible polymerization at temperatures of 80 - 100°C and obeys ideal gas laws without pronounced deviation. However, its stability is dependent on purity, even a trace of water provoking rapid polymerization. At ordinary temperatures the dry gas polymerizes slowly, building up a film of polyoxymethylene on the walls of the containing vessel. Kinetic studies indicate that this transformation takes the form of a surface reaction, unimolecular at high pressures and polymolecular below 200mm. In the presence of water vapour and other

polar impurities formaldehyde gas is stable only at pressures of 2 to 3 torr or concentrations of about 0.4 per cent at ordinary temperatures.

Formaldehyde gas that is 90 to almost 100 per cent pure must be kept at temperatures in the neighbourhood of 100 to 150°C or above, if polymerization is to be avoided. Chemical decomposition of formaldehyde gas is not appreciable at temperatures below 400°C.

Formaldehyde gas is flammable, having a heat of combustion of 4.47Kcal per gram. It forms explosive mixtures with air or oxygen. Formaldehyde-air mixtures containing from 7 to 73 per cent formaldehyde should be regarded as potentially explosive.

3.2.2 Preparation

Formaldeyhde gas is not an article of commerce. It must be prepared at the site of use. Although monomeric formaldehyde is obtained whenever formaldehyde solution or its linear polymers are subjected to vapourisation, gas having a high formaldehyde concentration is best obtained by the action of heat on paraformaldehyde, which contains 95-96 per cent available formaldehyde, or from the more highly polymerized polyoxymethylenes, which contain less than one per cent of combined water. However, gases obtained in this way contain small proportions of water and polymerize rapidly below 100°C.

Dry gas is best prepared from pure anhydrous liquid formaldehyde. Chemical drying agents cannot be used for removing moisure from formaldehyde gas, because they function as polymerization catalysts. Formaldehyde gas is readily soluble in water and polar solvents such as alcohols, but is only slightly soluble in such liquids as acetone, benzene, chloroform and ether.

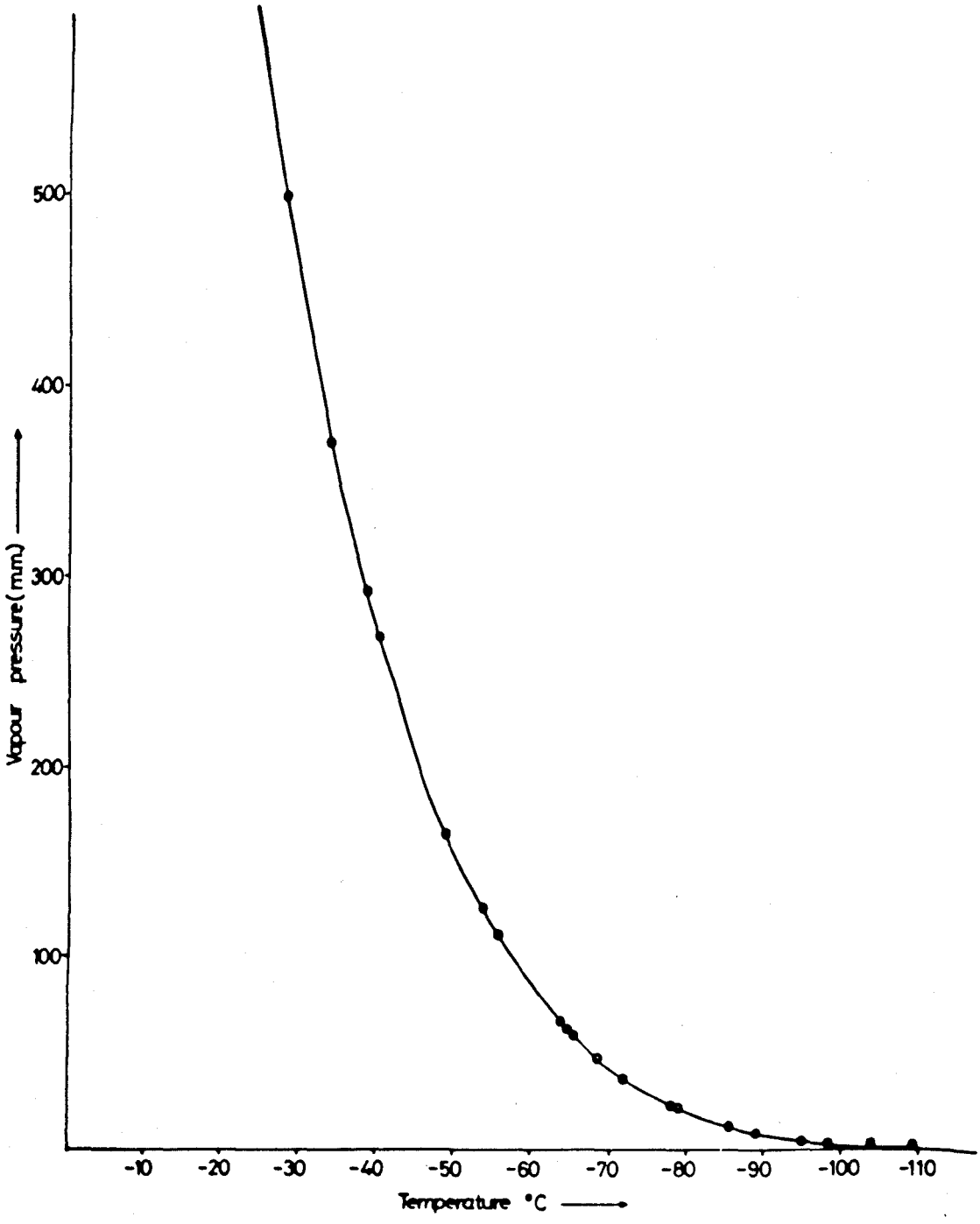

Fig. 3.4 Vapour pressure curve of formaldehyde

Alkali-precipitated polyoxymethelenes are superior to paraformaldehyde for the preparation of liquid formaldehyde because it contains only about 0.1 per cent combined water, whereas paraformaldehyde contains as much as 2 - 4 per cent water even after desiccation. Acid-precipitated alpha-polyoxymethelene cannot be used for liquid formaldehyde preparation because traces of acid present in the vapour produced from this polymer accelerate polymerization to such an extent that little or no liquid is obtained. The vapour pressure curve of formaldehyde is shown in Fig. 3.4.

3.2.3 Experimental

Gaseous formaldehyde was prepared by vapourization of liquid monomeric formaldehyde which is extraordinarily unstable. Liquid formaldehyde was prepared by heating paraformaldehyde to about 110°C in an oil bath and condensing the vapour in a cold trap at -80°C using dry ice. The connecting tubing was heated electrically to about 90°C to prevent polymerization on the walls. The paraformaldehyde had previously been dried by standing in a desiccator over Phosphorous Pentoxide (P_2O_5) in vacuum for a few days.

Initially, the apparatus used was made of Pyrex glass of Quickfit type with glass stop-cocks. It was found that polymer formation was much more pronounced in a glass surface in spite of precautions and the glass stop-cocks got blocked with the polymer. Hence a metallic system was constructed using copper tubes and Edwards High vacuum taps.

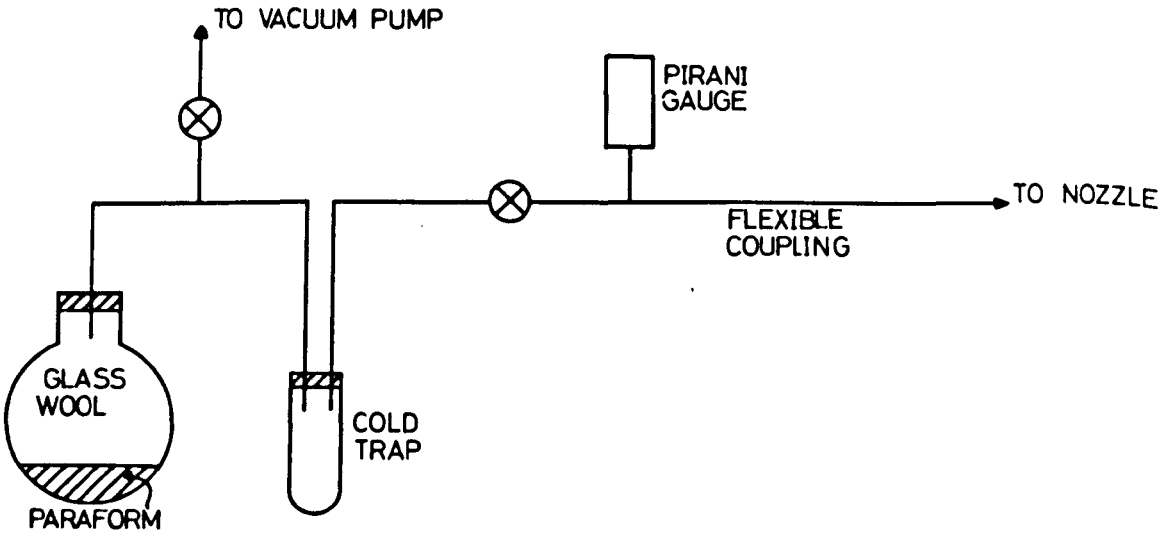

Fig. 3.5. FORMALDEHYDE SYSTEM.

This system was found to be more rugged and satisfactory. The flask containing paraformaldehyde and the cold trap were made of glass so that the formation of liquid formaldehyde could be watched from the outside. India rubber bungs were used for connecting the flask and cold trap to the $\frac{1}{2}$ inch copper tubing. M5Cl Pirani-gauge head (Edwards High Vacuum Ltd.) was used for monitoring the gas pressure.

It was found that formaldehyde gas obtained from paraformaldehyde in this way is contaminated by small quantities of water, methylal and methyl formate which catalyse rapid polymerization at temperatures below 100°C which contaminated the apparatus.

Hence Trioxane, the cyclic trimer of formaldehyde was used to generate anhydrous formaldehyde gas. This eliminated the contamination of the apparatus and made it possible to make repeated starts without cleaning the contaminated parts.

The layout is shown in Fig. 3.5.

3.3 Ammonia (NH_3)

Ammonia is unique among molecules investigated by microwaves. Since Cleeton and Williams[39] observed its spectrum in 1934 and thus began microwave spectroscopy, more experiments on this molecule have been reported than any other molecule studied by microwave methods. The large amount of data on the infra-red and Raman spectra of the ammonia molecule[35] shows that it has the general dynamical properties of a

vibrating, non planer, non-rigid symmetric top molecule and its general shape is that of a pyramid. The three hydrogen atoms form the base of a shallow triangular pyramid while the nitrogen atom lies at its apex. The symmetric top molecules have the property of having equal moments of inertia about two out of their three principal axes. The rotational motion of these molecules is such that while the whole molecule rotates about its main axis of symmetry, this axis itself precesses about the direction of the total angular momentum vector.

The nitrogen atom has two equally possible positions of equilibrium - one on either side of the plane in which the three hydrogen atoms lie. It is found that the nitrogen atom can pass from one equilibrium position to another. In this process, however, it has to cross the plane of the hydrogen atoms and consequently it has to overcome the potential barrier formed by the close proximity of these atoms. In the ground vibrational state of ammonia, the molecule has not enough energy to allow the nitrogen atom to be found in the plane of the hydrogen atoms due to the large potential barrier and classically the penetration of this barrier is not possible. However, quantum mechanical treatment shows that the nitrogen atom can tunnel through the potential barrier, and thus it can move to and fro between its two equilibrium positions, in which the molecule has slightly different energies. This to and fro vibrational motion of the nitrogen atom is called inversion. Usually vibrations produce frequencies in the infra-red region, but in this case the

vibration is so much slowed down by the potential barrier that the inversion frequency due to the transitions between the two energy levels corresponding to the two positions of the nitrogen atom, lies in the microwave region. On the simplest theory of inversion only one resonant frequency is to be expected. However, the centrifugal distortion produced by the molecular rotation changes the interatomic distances which in turn alter the height of the potential barrier. This shifts the inversion frequency so that a series of lines corresponding to different rotational states are obtained. If nuclear hyperfine structure is neglected, a total of 64 lines of $N^{14}H_3$ has been observed[40,41] for rotational quantum numbers up to J = 17, K = 15, and frequencies ranging from 16,800 Mc to 40,000 Mc. The strongest of these lines (J = 3, K = 3) has a peak absorption of $7.2 \times 10^{-4} cm^{-1}$. This line has been used during the investigations reported here.

3.3.1 Experimental

Ammonia is commercially available as a compressed gas. The cylinder is connected to a pressure reducing valve. The vacuum connecting pipes are made from ½ inch diameter copper pipe with 'Yorkshire' lead solder sealed junctions and 'Genevac' or 'Edwards' pressure actuated hand valves are used. The ammonia is frozen in a liquid nitrogen trap and water vapour and air impurities removed by pumping. It is then stored at a pressure greater than atmospheric in a large reservoir. The flow from the reservoir to the nozzle is

controlled by a fine control needle valve and the pressure (0.5 to 10 torr) is measured by an Edwards Pirani thermal gauge (head M5C, 10^{-3} torr to 10 torr). The layout is similar to Fig. 3.1.

CHAPTER IV

DESIGN OF MILLIMETRE SPECTROMETERS

Introduction

The design of spectrometers used for observation and measurement of absorption lines depends upon several factors such as frequency, the gas under examination and the nature of the information required. The basic elements are (a) an absorption cell or container; (b) a tunable microwave source; (c) a frequency modulator for the absorption line or signal source; (d) a microwave detector; (e) an amplifier of the detector signal; (f) a signal indicator and (g) a frequency meter. The design of a millimetre wavelength spectrometer is severely limited by the availability and high cost of millimetre components. The difficulties of constructing 4 millimetre and 2 millimetre components are considerable because of the small dimensions and tolerances involved. The consideration in the design was to keep the number of these millimetre components to a minimum. An 8 millimetre klystron was chosen as the fundamental source of power. In order to achieve high signal-to-noise ratio in the millimetre region where low power is available a confocal-type Fabry-Perot resonator was designed as a high Q tunable cavity for the 4 millimetre transitions. The cavity could be tuned mechanically from outside the vacuum system. The details about its design are given in Chapter II.

The resonance of a cavity is affected when an absorbing gas is introduced into the cavity. The quality factor Q is decreased due to the increased losses. Thus, microwave absorption can be detected by the change in a transmitted or reflected wave in the cavity. For high sensitivity, the Q value should be large; however, it is limited to a value such that the width of the cavity resonance is wide enough to display the entire line and possibly any fine structure if present. Using a high Q cavity as an absorption spectrometer, very long path lengths can be achieved from the relation[42] $\frac{Q\lambda}{2\pi}$, which gives equivalent absorption path length in free space. For the 2 millimetre transition a 9 inch Q-band waveguide cell was used rather than a cavity. Conventional waveguide techniques were employed to propagate the power. Carbonyl sulphide and Formaldehyde were chosen to test the spectrometer because of the strong transition of OCS at 72976 Mc (Intensity $1.4 \times 10^{-3} cm^{-1}$) and the weaker transition in CH_2O at 72838.14 Mc (Intensity 9.8×10^{-5}). The particular components of the four and two millimetre spectrometers will now be discussed in some detail.

4.1 The 8mm Klystron

The klystron used in the spectrometer is the Elliott 8RK17 operating in the frequency range of 33.81Kmc/s to 36.50Kmc/s. It has a maximum output of 1100 milliwatts although this power decreases as the klystron ages. The klystron is operated with the cathode at -2.5 kilovolts, the reflector between -700 to -900 volts relative to the cathode and the grid at -40 volts relative to the cathode.

The current drawn from the power supply is of the order of 22mA, but this value falls as the valve ages. The klystron requires a forced air cooling at 13 cu.ft./min.

The power supply used was a commercial one of the type D.H.7 (KSM Electronics Limited), but this proved to be most unsatisfactory. The resonator voltage switched on with a transient in excess of -3KV even when the resonator voltage was kept to a minimum. On switching on the klystron, transients in the power supply output caused arcing in the klystron which resulted in "stripping" of the cathode and the cathode emission fell to zero and rendered the klystron useless. After repairs by the manufacturers the power supply still was unsatisfactory. Circuit modifications made by ourselves resulted in a satisfactory solution. A thermistor CZ1A and a reset contactor were used in the primary of the resonator supply transformer. The thermistor controlled the transient so that it was always less than -2.5 kilovolts and the reset contactor switched off the resonator if the current exceeded 25mA. A 330K resistor was also connected in the grid lead. With these modifications the power supply worked satisfactorily.

The klystron could be reactivated by overrunning the filament at about 7.5 volts, starting the resonator at 500 volts. The resonator voltage tapping was changed in steps of 500 volts up to 2500 volts, carefully monitoring the resonator current throughout. The heater voltage was also reduced from 7.5 volts to 6.3 volts in steps until the cathode current was restored to its normal or near normal value. This reactivation process normally took several hours.

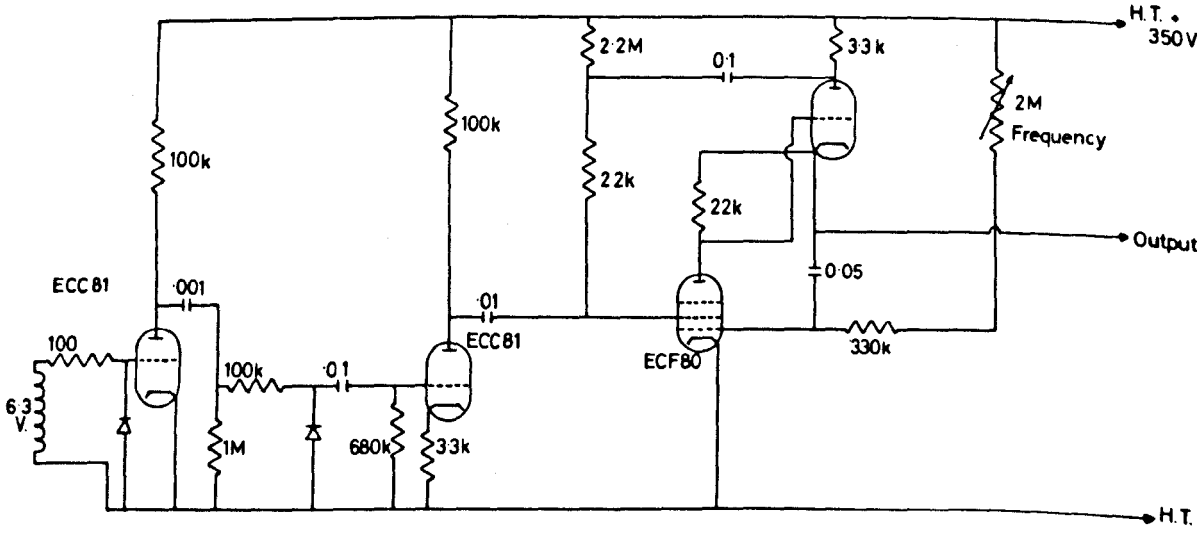

Fig. 4.1. SWEEP UNIT.

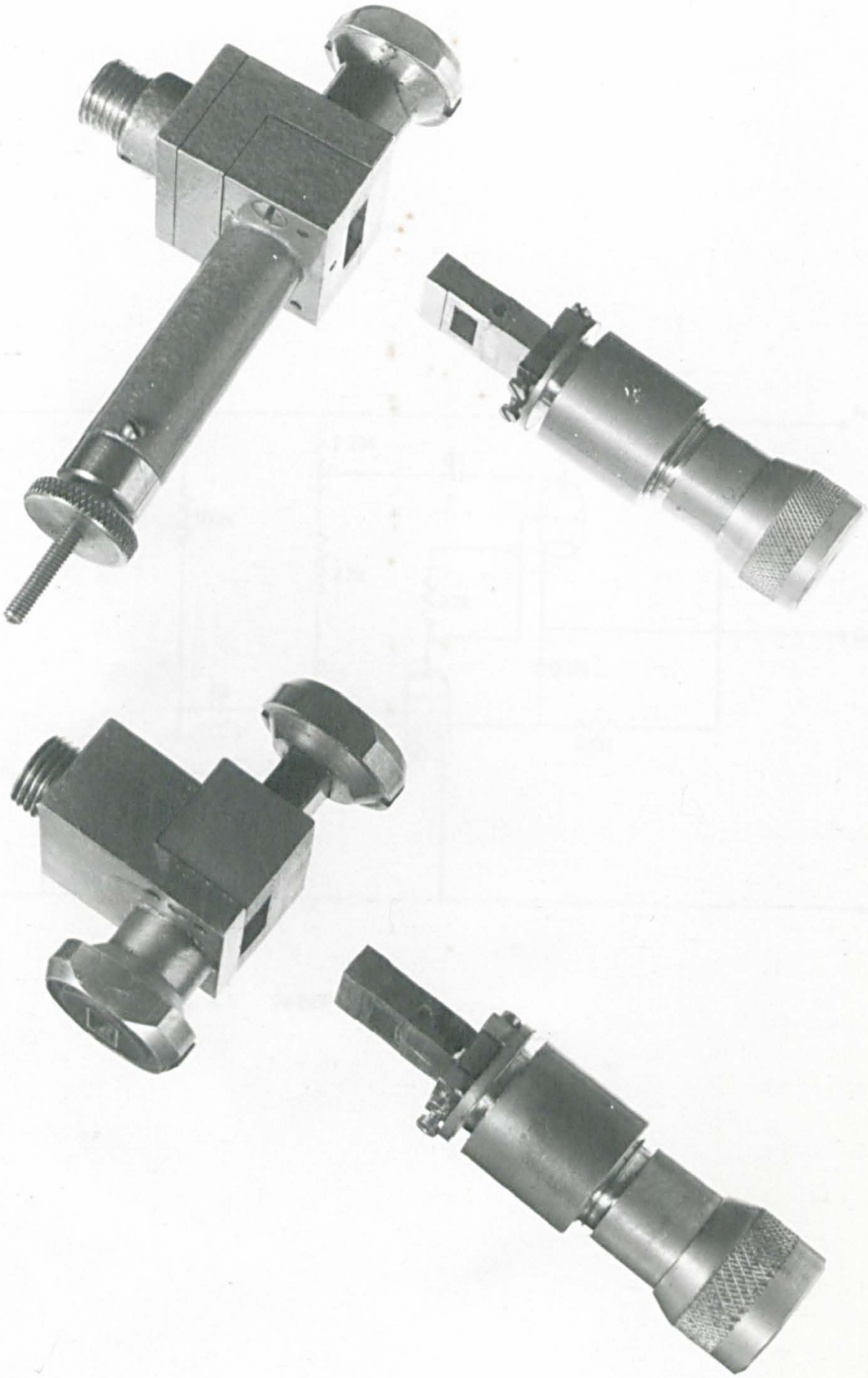

Fig. 4.2 Harmonic generators.

4.1.1 Sweep unit

A triode-pentode time base circuit was designed to obtain a linear sweep with a large amplitude to be applied to the reflector of the klystron for modulation. The sweep unit is synchronised at the mains frequency. Spiky pulses for this purpose are obtained by feeding 6.3 volts at 50 c/s through a double triode-pentode circuit using an ECC81 valve. As a large amplitude sweep is obtained with this circuit and no cathode resistor need be used with the pentode, the initial step at the start of the rundown is negligible. The screen-grid stopper resistor is necessary in order to avoid the onset of low amplitude high-frequency oscillation when large values of pentode control-grid resistor are inserted. In the absence of the screen-grid stopper, the high frequency oscillation can cause a small flat portion to appear at the bottom of the output waveform.

Unlike most Miller time-bases, the one shown here has no other anode load than the capacitor and the resistors in series with it, so that the effective gain during the rundown is very high. Consequently the linearity of the waveform is excellent. A peak-to-peak amplitude of 200 volts is obtained with a h.t. supply voltage of 350 volts. An EHT isolating transformer is used for coupling to the reflector.

4.2 Harmonic Generator

The harmonic generator used during these investigations is a modified Q band tunable crystal holder which takes standard Q-band cartridges (G.E.C. Pattern, type SIM 8). In this unit it was designed

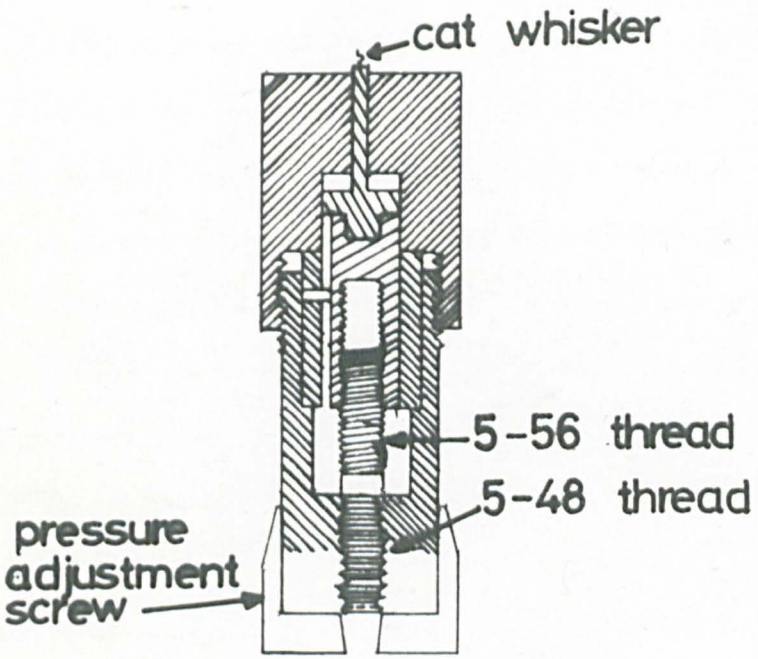

Fig. 4.3. Differential screw mechanism.

such that the pressure of cat-whisker against the crystal could be adjusted by advancing or retracting the whisker. This is a most critical adjustment and is made by means of a differential screw mechanism, details of which are shown in Fig. 4.3. Provision is made for rotation of the crystal mount so that different points of contact can be made. For operation at the shorter millimetre wavelengths the point of the whisker is very critical. It is necessary that the point be very sharp, i.e. with a radius of curvature at the tip of the order of one ten-thousandth of an inch or less. An equipment was set up for electrolytically sharpening the point of the whisker to the form which would give best results. The end to be pointed is allowed barely to make contact with the surface film of a 10N solution of potassium hydroxide. The concentration is not critical. An a.c. current is then passed through the whisker and solution until action at the end of the whisker ceases, usually about less than one second. The other electrode used was a copper plate. After the pointing, the solution is washed off, and the point is examined under a microscope. Often it is necessary to repeat the process a number of times in order to obtain a satisfactory point. A resharpening of the whisker is necessary after a few readjustments of the point of contact. Sometimes the point of the whisker is blunted by excess pressure, and sometimes it is burned off in the multiplier unit by excess power. If for unknown reasons the performance of the unit drops, it is advisable for one to examine the whisker point under the microscope.

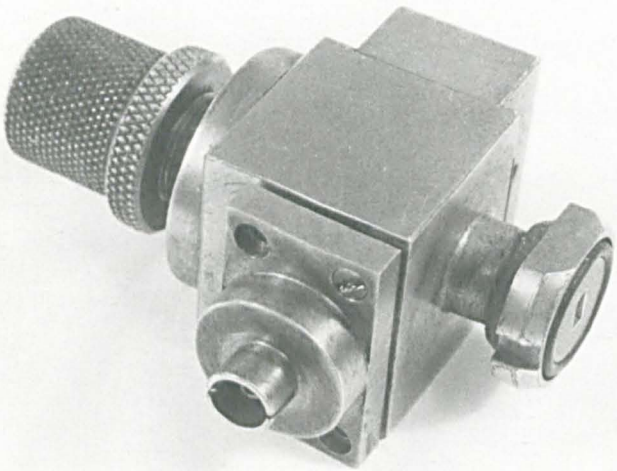

Fig. 4.4 Crystal detector.

The whiskers were made from 1.5mil (.0015" diameter) tungsten wire. The shape of the whisker and its size influence both the stability and the figure of merit of the crystal. A die was therefore made to shape the whiskers.

One side of the crystals was coated with gold by vacuum deposition techniques. These could then be soldered onto the post and polished. Soldering of tungsten is difficult. Hence a small hook was made in the wire which could be trapped in the solder. Full wave harmonic generation was used. Biasing of the harmonic generators was also tried but the improvement appeared to be a function of the specific run-in conditions.

4.3 Detector

The crystals used for detection and related purposes are probably the most inefficient of the components used and their relatively low sensitivity is the chief factor at present limiting the performance of microwave spectrometers. It is for this reason that much effort was devoted to the improvement of their performance. The crystal detector used was of the type WO 948 (Microwave Instruments Ltd.). The whiskers were made from 1.5 mil tungsten wire. The same crystal detector was used for detection of two millimetre waves. Tapers from 4 millimetre to 2 millimetre wavelength along with a length of 2 millimetre waveguide and matching unit were used to filter the 2 millimetre waves. The initial procedures for electropolishing and pointing the tungsten wire and setting

Fig. 4.4a Whisker assembly for the Crystal detector.

up a contact for the detector are exactly the same as those for a harmonic generator. However, in this case only very light contact pressures are used, because the contact area must be kept down to a minimum for good millimetre wave performance. After the first contact, the semiconductor crystal is rotated so that the pointed metal whisker scrapes over it and produces brief bursts of rectified output from the incident radiation. The magnitude of these bursts gives some indication of the best performance to be expected, and they should be followed up by a slight increase of pressure and more rotation until a stable output is obtained. Usually a slow withdrawal of the crystal after this process, without further rotation, will result in a series of near-optimum contacts that are reproducible but depend critically on the contact pressure. The whole process is very much more tedious and time consuming than setting up a harmonic generator, and experience is the only guide as to when the point of diminishing returns is reached. Good contacts are very susceptible to mechanical shock, unlike those of harmonic generators, and it is rare for them to survive overnight. However, they can be remade by a slight alteration in contact pressure without further adjustment and in this sense are stable for weeks. Best results for longer wavelengths are obtained when the crimp in the whisker almost enters the detector waveguide, but for wavelengths much shorter than cut-off the wire length should be optimised experimentally. One irritating feature of a good contact is that its output tends to drift down to about two thirds of the value when first made over the course of some minutes, and

that during this period the amplitude flickers noticeably at the rate of a few cps. Contacts which show exceptional instability of this kind may be improved by "tapping", a sharp blow to the crystal mount parallel to the whisker. This invariably leads to a loss of output, but a change in contact pressure then results in a contact more stable than before.

The sensitivity of the crystal, when used as a detector depends on three factors:

(i) the relative forward and reverse impedances;

(ii) the conversion gain;

(iii) the noise factor.

The relative forward and reverse impedances determine the proportion of the incident microwave power which can be rectified.

The conversion gain is a measure of the efficiency with which the rectification takes place. A figure of about 25% is typical; this corresponds with a loss of about 6db. At low powers (10^{-5} to 10^{-4}watt) the conversion gain increases with increasing incident power, becoming approximately constant about 10^{-4}watt. Useful results, however, can be obtained at a power of a few microwatts.

The electical noise is the most important factor in crystal performance and determines the smallest quantity of microwave power which can be detected. The noise, S, may be expressed for most purposes by

$$S = kT\Delta\nu + \frac{CI^2}{\nu}\Delta\nu \qquad (4.1)$$

Here the first term, $kT\Delta\nu$, is the 'Johnson' or 'thermal' noise associated

with a range of frequencies $\Delta\nu$ in width, and arises from the thermal agitation of electrons; k is the Boltzmann constant and T the absolute temperature. The second term, known as the 'crystal noise' is largely empirical, and is peculiar to crystal detectors; I is the rectified crystal current, ν the value of the modulation frequency which is often impressed on the microwave signal, and C a constant. $\Delta\nu$ is the bandwidth and is a measure of the range of frequencies which can pass through a given circuit, such as a filter or amplifier. It is a parameter of great importance in the design of electronic equipment.

Johnson (thermal) noise is present in all circuits, since it depends on $\Delta\nu$ and T, both of which must be finite. Its magnitude determines the weakest signal which can be detected or amplified with electronic apparatus when all other sources of noise have been eliminated. The term $kT\Delta\nu$ does not contain the absolute frequency, so neglecting other sources of noise, crystals and other electronic components at the same temperature and with the same bandwidth, but operating at different frequencies, produce the same Johnson noise. The second term of equation (4.1) is unlike that for the Johnson noise in that it is dependent on the frequency. Its value is inversely proportional to the modulation frequency impressed on the microwave signal which, after rectification, provides the crystal output. It is proportional to the bandwidth, and to the square of the crystal current I. When the crystal power is greater than about 10^{-4}W the crystal operates as a square-law detector, i.e. $I = cV^2$ where c is a constant and V is the voltage developed across the

crystal. In this event the output power from the crystal is also proportional to the square of the crystal current. It follows that if the crystal noise is the principal source of noise, then the precise value of the crystal current will not affect the signal-to-noise ratio to a great extent, as both signal and noise power vary with crystal current in the same way. The crystal noise may be reduced by operating at lower power, but since the conversion gain then falls off sharply it is not possible to realize this potential advantage in sensitivity. Much of the complexity of sensitive spectrometers depends upon the methods used to reduce crystal noise.

4.4 Detecting Systems

The three basic methods of detection used in gaseous microwave spectrometers are

(1) Crystal-video

(2) Stark modulation

(3) Source modulation

Any of these three methods can be combined with a second microwave oscillator to produce a superheterodyne system of detection. This removes the low-frequency crystal noise completely, but has the disadvantage of great complexity. Greater sensitivity can also be obtained with any of these methods by employing phase-sensitive (or lock-in) amplifiers. These will reduce the bandwidth of the detecting systems and for this reason it is normal to use pen-recorders of bandwidths less than 1c/s with them, rather than oscilloscopes.

In the millimetre region there is less advantage in using Stark modulation than at lower microwave frequencies. The chief advantage of the Stark method is that it permits the amplification at high frequencies of the crystal output, so that the low frequency crystal noise is eliminated. The microwave powers generated at centimetre wavelengths are large enough to ensure that a high proportion of the microwave energy is rectified by the crystal. In the millimetre region, however, there is usually so little power available, that even at low modulation frequencies, the noise is largely Johnson (thermal) noise. The attenuation produced by a Stark electrode further reduces the power reaching the crystal, which is then operating under conditions such that its conversion efficiency is low. For these reasons it is preferable to use the simple video method, or, for the highest sensitivity, source modulation together with phase sensitive detection. Measurements at millimetre wavelengths are favoured by the fact that absorption coefficients are appreciably higher than at centimetre wavelengths and shorter absorption cells, sometimes only a few inches long, are satisfactory.

Two methods of detection were used during the investigations reported here. These are the crystal-video detection and the superheterodyne detection. It is of interest to compare the theoretical sensitivities of the two systems.

4.4.1 Crystal-video detection

The sensitivity of a low power crystal-video detector can be calculated by the method of Beringer[43], and Torrey and Whitmer[44]. With no d.c bias and with the microwave power of the order of a microwatt where the crystal operates as a square law detector, the noise generated in the crystal is essentially the Johnson noise of a resistance equal in value to the d.c. impedance of the crystal. Because of the high conversion loss, the input impedance of the crystal square-law detector is relatively insensitive to the output load impedance. Beringer has shown that the output r.m.s. noise voltage N_o from a crystal-video receiver operating in the square law region is given by

$$N_o = G\left[4kT(R + R_A)B\right]^{\frac{1}{2}} \qquad (4.2)$$

where R is the video resistance of the crystal and R_A is a resistance which in series with the grid of the input stage of the amplifier would generate a noise equivalent to that generated by the amplifier, G is the gain, and B the bandwidth of the amplifier. In the square law region the voltage detected by the crystal, V_α, is

$$V_\alpha = SV_s^2 \qquad (4.3)$$

where S represents sensitivity of the detector and V_s is the r.m.s. input voltage. The output voltage of the receiver is

$$V_o = GSV_s^2 \qquad (4.4)$$

and for a small change in power P

$$\Delta V_o = GS(2V_s \Delta V_s) = GS(R\Delta P) \tag{4.5}$$

since G, the voltage gain, and S are constants.

To meet the usual criterion of detectibility

$$\Delta V_o = GS(R\Delta P) = G\left[4kT(R+R_A)B\right]^{\frac{1}{2}}$$

$$\therefore \quad \Delta P = \left[4kT(R+R_A)B\right]^{\frac{1}{2}}/RS = \left[4kTB\right]^{\frac{1}{2}}/M \tag{4.6}$$

where $RS/(R+R_A)^{\frac{1}{2}} = M$, the figure of merit of the receiver.

If a power P_i is introduced into a waveguide it will be attenuated by the losses in the waveguide walls and also by possible gas absorption. These two sources of attenuation are designated by attenuation coefficients α_c and α_g respectively. The power after traversing a length L of the waveguide will therefore be

$$P = P_i e^{-(\alpha_c+\alpha_g)L}$$

If the gas is removed, the power P is $P = P_i e^{-\alpha_c L}$ so that the change in power due to the gas is

$$\Delta P = P_i e^{-\alpha_c L}(1 - e^{-\alpha_g L}) = \alpha_g L P_i e^{-\alpha_c L} \tag{4.7}$$

if $\alpha_g << 1$, as is usually the case.

Substituting this value of ΔP in equation (4.6) we obtain

$$\alpha_g = (4kTB)^{\frac{1}{2}}/MLP_i \exp(-\alpha_c L) \tag{4.8}$$

If it is assumed that M is independent of the received power $P_i \exp(-\alpha_c L)$, then it is appropriate to determine L_{opt} from equation (4.8) by setting $\partial/\partial L(\alpha_g) = 0$. This assumption is not valid, however, for powers above the microwatt range. In this way we obtain $L_{opt} = \alpha_c^{-1}$ and

$$\alpha_g(\min) = 2e\alpha_c(kTB)^{\frac{1}{2}}/MP_i \qquad (4.9)$$

The figure of merit M is a measure of the detecting efficiency of the crystal and its noise properties. Substitution of typical values into equation (4.9) give a minimum detectable α_g of about 10^{-7}cm^{-1}, showing that this method is not nearly as sensitive as superheterodyne detection, but it has the advantage of simplicity and is often used in the millimetre region where not enough local oscillator power is available to operate a superheterodyne receiver without great conversion loss. The appearance of $\alpha_g(\min)$ as an inverse function of power suggests that one may increase sensitivity indefinitely by increasing the source power. This is not true because M, the figure of merit, remains constant for only a small range of powers in the microwatt region.

4.4.2 Superheterodyne detection

At low microwave power levels, crystals are inefficient detectors, as their output voltage is approximately proportional to the square of the radio-frequency amplitude. It is then advantageous to use superheterodyne detection to produce a signal as large as possible relative to noise in the amplifiers. Moreover, if the intermediate frequency is reasonably high (e.g. 30 to 60 Mc) crystal noise within

the intermediate-frequency amplifier bandwidth is reduced practically to the thermal noise.

The significant difference between video and superheterodyne detection is that the latter restricts the detector response to a very narrow range of wavelengths. In defining the noise figure of a receiver the usual reference level is the available Johnson noise power kTB. If we assume that the minimum detectable signal power, P_{min}, is that which at receiver output just equals the noise power, then

$$P_{min} = F_r kTB$$

where F_r is the noise figure of the receiver, which incorporates the conversion loss and noise of the detector as well as the noise arising from the amplifier, k is the Boltzmann's constant, T is the absolute temperature, and B is the effective noise bandwidth of the receiver. The receiver in microwave spectroscopy is not required to detect small amounts of signal power, but rather to detect small variations, or decrements in a relatively large signal power. One can, however, use r.f. balancing to cancel the power around the absorption line and thus cause the spectrum line to appear as a small amount of unbalanced power $(\Delta P)'$. It is easy to show that

$$(\Delta P)' \approx (\Delta P)^2/4P_i \exp(-\alpha_c L) \qquad (4.10)$$

where ΔP is the power absorbed by the gas, P_i the input power to the cell, L the equivalent cell length, and α_c the attenuation coefficient of the cell.

When the input impedance of the receiver is coupled to a source, there is an additional $F_s kTB$ of available noise power (where F_s is the noise figure of the power source) so that

$$(\Delta P)'_{min} = F_r kTB + F_s kTB = FkTB \qquad (4.11)$$

where F is now the overall noise figure of the spectrometer. Combining (4.10) and (4.11) one obtains

$$(\Delta P)_{min} = \left[4FkTBP_i \exp(-\alpha_c L)\right]^{\frac{1}{2}} \qquad (4.12)$$

where $(\Delta P)'_{min}$ is the minimum detectable unbalanced and $(\Delta P)_{min}$ is the minimum detectable absorption of power by the gas.

To obtain the optimum cell length and the minimum detectable absorption coefficient of a gas with this type of receiver, one must maximise the detected power $(\Delta P)'$.

Now

$$(\Delta P)' = (\Delta P)^2/4P_i \exp(-\alpha_c L) = P_i \exp(-\alpha_c L)/4(\alpha_g L)^2 \qquad (4.13)$$

as $\Delta P = \alpha_g L P_i \exp(-\alpha_c L)$.

By setting $\partial/\partial L(\Delta P)' = 0$ and solving, it is seen that $L_{opt} = 2/\alpha_c$ which yields with equation (4.13) $(\Delta P)' = P_i(\alpha_g/e\alpha_c)^2$. Substituting this value in equation (4.11)

$$FkTB = P_i(\alpha_g(min)/e\alpha_c)^2$$

or

$$\alpha_g(min) = e\alpha_c(FkTB/P_i)^{\frac{1}{2}} \qquad (4.15)$$

for the minimum detectable absorption coefficient, α_g, of a gas.

Though r.f. balancing is assumed in the above analysis, essentially the same results are obtained for a receiver employing linear detection without r.f. balancing. Detection in the usual superheterodyne receiver is linear. Also, the detection in a crystal-video receiver for large signal reception is approximately linear. For these we have

$$V_o = GV_s \tag{4.16}$$

where V_o is the output voltage, V_s is the r.m.s. signal voltage, and G is a constant which incorporates the gain of the amplifier and the conversion gain (or loss) of the detector. For a small change in V_s

$$(\Delta V_o) = G(\Delta V_s) \tag{4.17}$$

The output noise voltage N_o of the receiver is

$$N_o = G(4FkTBR)^{\frac{1}{2}} \tag{4.18}$$

where F again is the overall noise figure and R is the input impedance. To meet the usual criterion for detectability, we equate ΔV_o to N_o. By combining equations (4.17) and (4.18) we obtain

$$(\Delta V_s)_{min} = (4FkTBR)^{\frac{1}{2}} \tag{4.19}$$

It is easily shown that

$$(\Delta V_s) = R(\Delta P)/2V_s = (R/4P)^{\frac{1}{2}}\Delta P \tag{4.20}$$

which with (4.19) yields

$$(\Delta P)_{min} = (16FkTBP)^{\frac{1}{2}} = \left[16FkTBP_i \exp(-\alpha_c L)\right]^{\frac{1}{2}} \qquad (4.21)$$

This expression, except for a factor of 2, is identical with equation (4.12) obtained with r.f. balancing. The optimum cell length is again $2\alpha_c^{-1}$, and

$$\alpha_g(min) = 2\alpha_c e(FkTB/P_i)^{\frac{1}{2}} \qquad (4.22)$$

The result indicates that there is no significant gain in r.f. balancing as long as it is assumed that the overall noise figure is independent of the power received. This assumption is not justified except for relatively low signal power, and r.f. balancing could be an advantage when high power sources are available if cells are employed which have sufficiently large volume to prevent molecular saturation.

In equation (4.22) B is the bandwidth of the detecting system, and F is the overall noise figure of the crsytal, including Johnson noise and excess crystal noise varying as 1/f, the local oscillator and intermediate frequency amplifier noise, and also the effect of conversion loss in the crystal. It will have a value of about 50db in a typical case, but this can be improved by the use of a balanced mixer to eliminate the local oscillator noise which is an additional source of noise in millimetre wave systems. Whether the local oscillator power is generated electronically or by harmonic generation process, its spectrum is that of a single frequency surrounded by noise sidebands which spread out to several

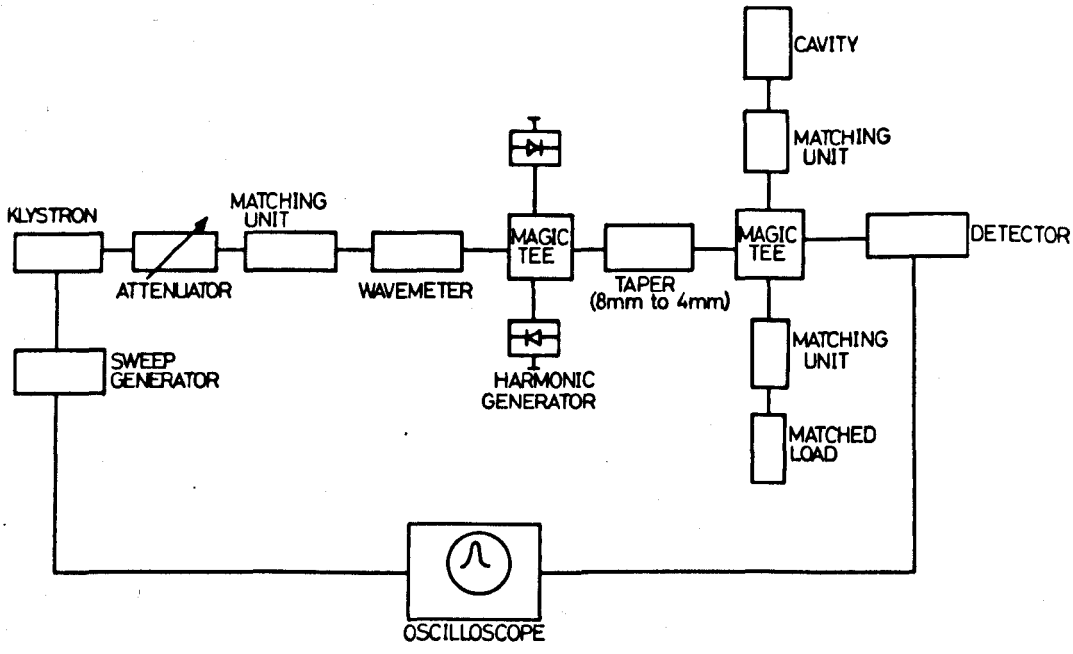

Fig. 4.5. 4mm SPECTROMETER.

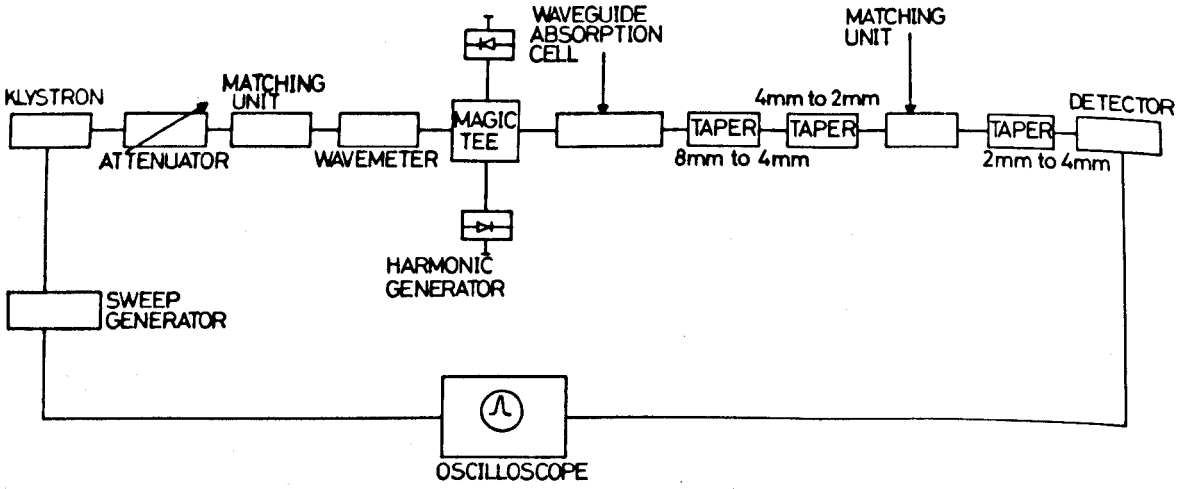

Fig. 4.6. 2mm SPECTROMETER.

hundred Mc/s on each side at millimetre wavelengths. Unless these noise sidebands are supressed by a balanced mixer or in some other way, they are a predominant source of detector noise. The value of B will depend on the recording system employed, 100c/s being the minimum possible for oscilloscope presentation, but well under 1c/s can be used if phase sensitive detection with a pen-recorder is incorporated. Substitution of these figures in equation (4.22) gives values for α_g(min) of about $10^{-8}cm^{-1}$ and $5 \times 10^{-10}cm^{-1}$, respectively for (i) oscilloscope presentation and (ii) pen recorder with a balanced crystal detector.

4.5 Experimental Results

The block diagrams of 4 millimetre and 2 millimetre spectrometers are shown in Figs. 4.5 and 4.6.

The absorption of OCS at 72976.8Mc is sbown in Fig. 4.7.

Fig. 4.8 shows the absorption line of OCS at 145946.82Mc using the 2 millimetre spectrometer.

Fig. 4.9 shows a simultaneous display of both the lines.

Results with CH_2O are shown in Chapter VII.

The microwave klystron is frequency modulated by a sawtooth wave of variable frequency. This sawtooth wave is also connected to the oscilloscope in such a manner that it synchronizes the sweep of the oscilloscope. Since the frequency variation of the klystron is approximately linear with voltage, the horizontal axis of the oscilloscope represents a frequency scale. The power from the klystron is transmitted

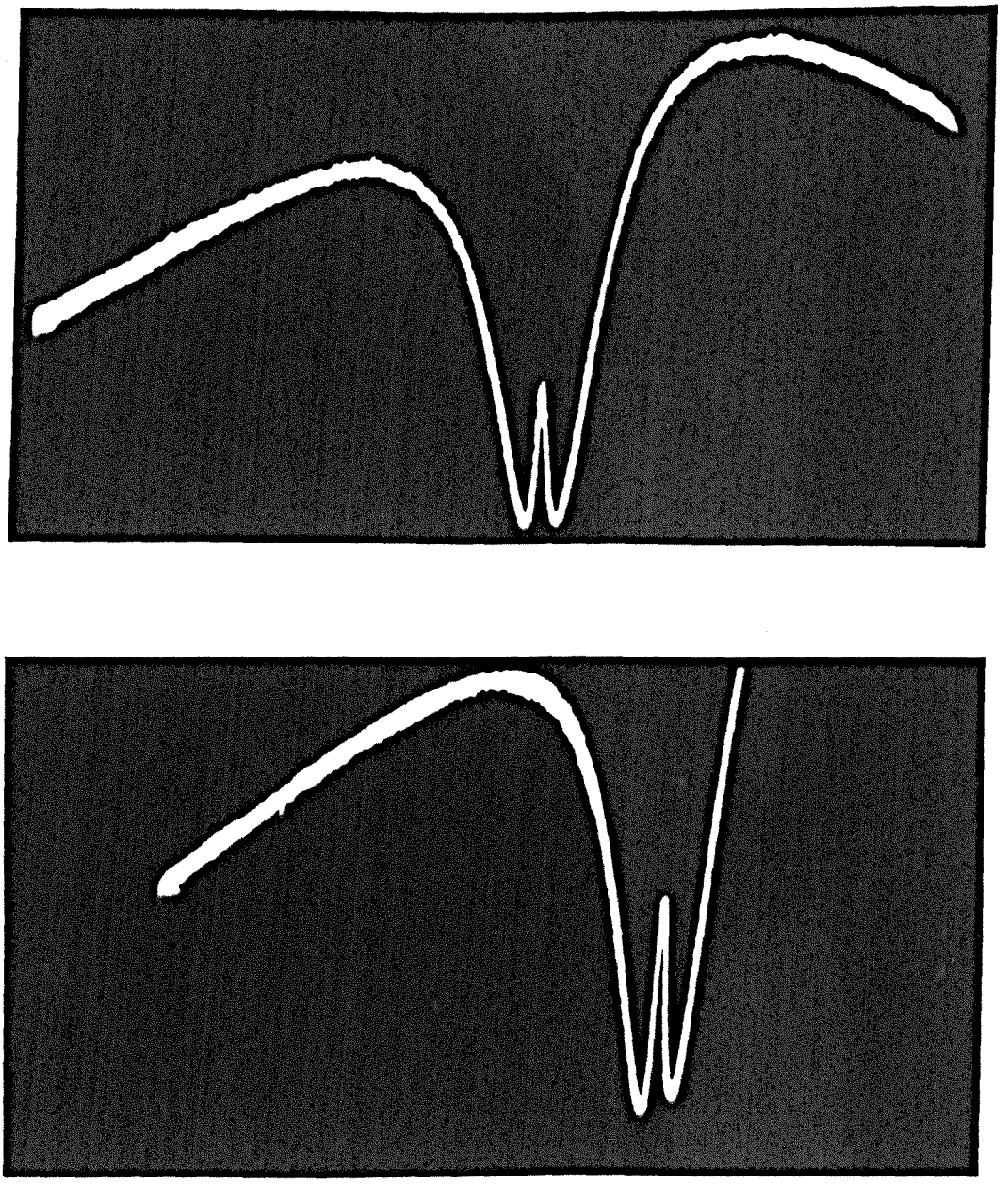

Fig. 4.7 OCS rotational line at 72.976kMc/s (4mm wavelength).

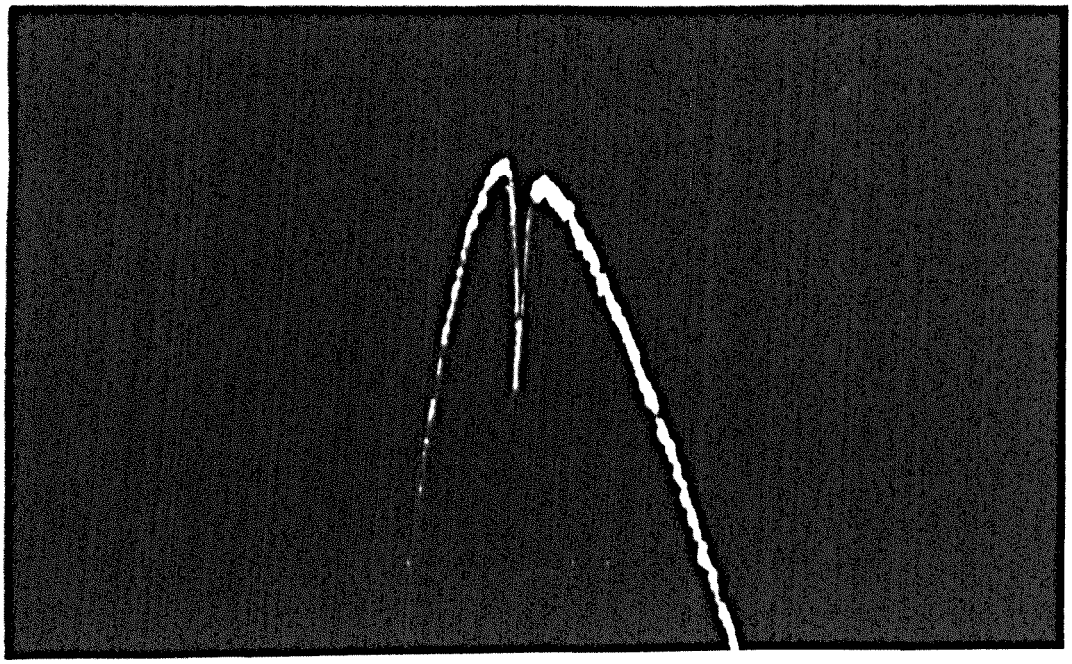

Fig. 4.8 OCS rotational line at 145.946kMc/s (2mm wave length).

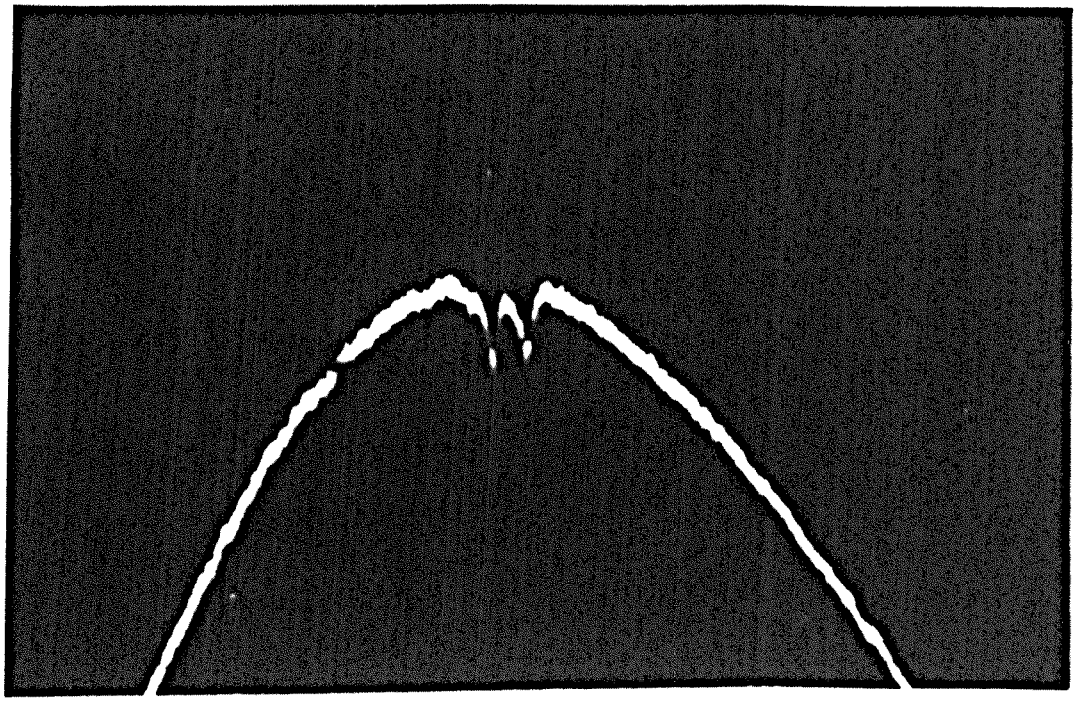

Fig. 4.9 Multiple display of OCS rotational lines at 72.976kMc/s and 145.946kMc/s.

down the guide, and the envelope of the klystron mode of oscillation is detected by the crystal detector. This wave is then amplified and fed to the vertical input of the oscilloscope. The vertical axis now represents a signal intensity scale. In effect, the oscilloscope screen is a graph of the energy of the microwave signal received at the detector crystal as a function of frequency. If the molecules of gas present in the waveguide absorb a certain frequency of microwave energy, then the envelope of the mode which is detected will contain a dip at this frequency. Energy of the frequencies not absorbed by the molecules will be equal to the energy output of the klystron at this frequency less the attenuation of the waveguide. It is this dip in the detected mode which is presented. When the cavity is used the mode of the klystron is displayed with a dip corresponding to the microwave cavity absorption. The absorption due to the gas produces an absorption dip superimposed on the cavity absorption in antiphase.

Fig. 4.9 illustrates the broadbanded coverage of the harmonic generator and detector. To understand this it is necessary to realize that the different harmonics of the klystron are exact integral multiples, whereas the rotational frequencies of the linear molecules are almost integral multiples, but not exactly so. The departure by the molecular frequencies from the exact harmonic relationship is caused by centrifugal distortion. By careful adjustment of the various tuning knobs, one can alter significantly the relative strengths of the lines "seen" with the

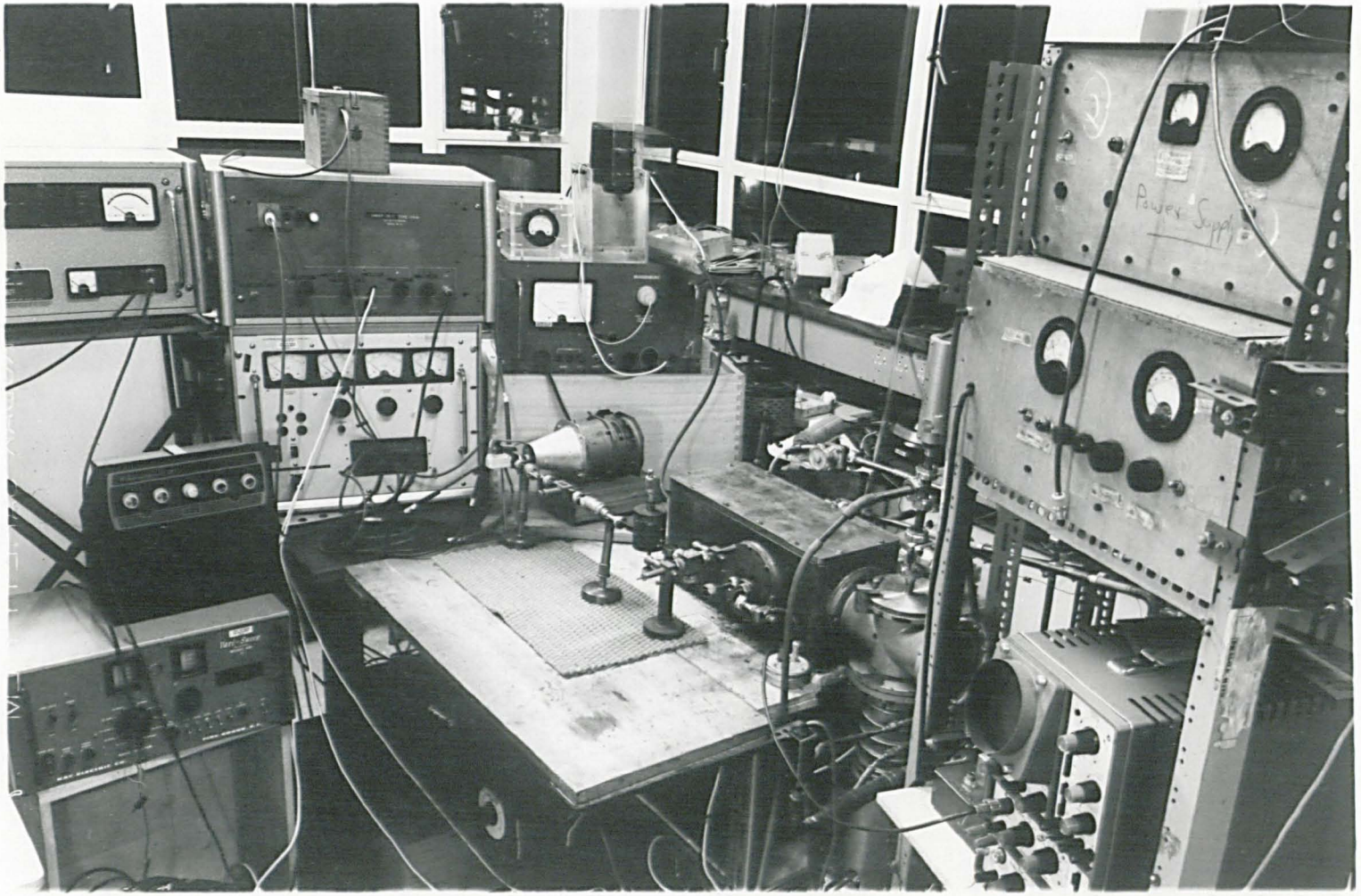

A general view of the detection system

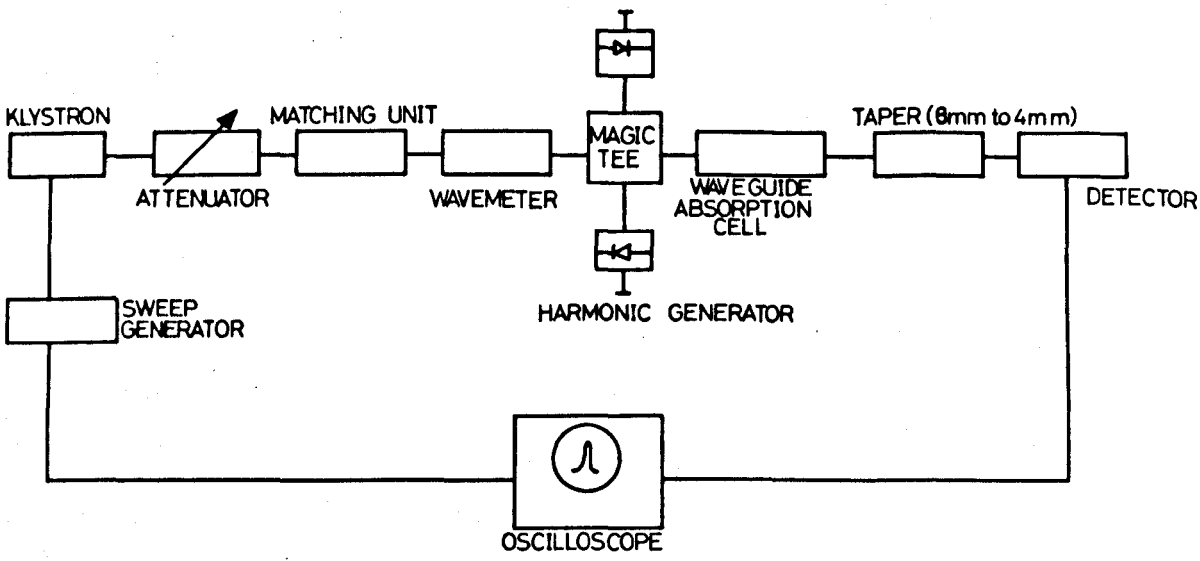

Fig. 4. 9a. Spectrometer for multiple display of rotational lines.

different harmonics. This multiple display of rotational lines has useful applications. It can be used as an aid to tuning, for accurate evaluation of centrifugal stretching, and for measurement of line breadths as a function of rotational quantum number.

CHAPTER V

COHERENCE PHENOMENA IN ELECTRIC DIPOLE SYSTEMS

Introduction

A sizeable part of the effort in Physics during this century has been devoted to the study of the interaction of electromagnetic radiation with matter. From these studies emerged our present ideas of energy levels and energy bands as well as the concepts of stimulated absorption, stimulated emission and spontaneous emission which were developed by Einstein in 1917. It was the development of these ideas which provided the foundation upon which the concepts on coherence phenomena in molecular systems are based.

Molecules in certain of their energy states can interact with a microwave radiation field of appropriate frequency and either absorb energy from the radiation field while jumping to a state of greater internal energy, or, under the influence of the radiation field, can give up some of their internal energy and drop to a state of lower energy. The amount of internal energy thus transferred, i.e. the difference in energy of the two energy levels, $E_1 - E_2$ is linearly related to the frequency of the radiation field:

$$E_1 - E_2 = h\nu$$

Here h is Planck's constant and ν is the frequency. Consider two energy levels of a molecule whose energy difference corresponds to a microwave

frequency. If a molecule in the lower energy state is placed in a microwave field of this frequency, it will absorb energy and hop up to the higher state. A molecule in the upper state, on the other hand, will give up energy to the microwave field and drop to the lower level. The probability for both transitions is the same. Therefore, whether a system of many molecules exhibits a net absorption or emission of energy depends on whether more molecules are in the lower or upper energy state. All molecular systems when allowed to come to thermal equilibrium have more molecules in the lower of each pair of states, and hence are absorptive. However, it is possible to build devices that will disturb the molecular system and put it in an emissive condition. Several methods of producing an emissive condition have been devised. One of them is the molecular-beam maser[45] in which the upper and lower state molecules are physically separated. The upper-state molecules are then used in a resonant cavity as the emissive molecular system. Other methods of exciting such systems by interchanging the population of two levels are (1) Excitation by applying a short controlled pulse of microwave power at the transition frequency and (2) Excitation by adiabatic fast passage where a strong exciting microwave field is swept in frequency past the transition frequency. The emission of radiation produced when a molecule returns from a higher to lower energy in the absence of any external stimulus is known as spontaneous emission. In the case of spontaneous emission, the presence of similar radiating molecules have

negligible effect on the emission, and the molecules emit independently of each other in an incoherent fashion. Molecules may be induced to give up their internal energy by locating them in a microwave field which is either generated by neighbouring radiating molecules, or is externally applied, emit radiation that is coherent, i.e., phase related to the general radiation field. Amongst other methods of interest in the study of coherence phenomena are the transient effects in which coherent radiation is produced by the excitation of super-radiant states.

5.1 Basic Physical Properties and Relaxation Mechanisms in molecular systems

To understand the basic physical processes involved in a molecular system, let us consider a system of many molecules. If the system is in thermal equilibrium at an absolute temperature T, the ratio of number of molecules with energy E_1 to the number of molecules with energy E_2 is given by

$$N_1/N_2 = \exp(E_2 - E_1)/kT$$

where k is the Boltzmann's constant. The Boltzmann distribution has the properties that states of lower energy are more highly populated than states of higher energy and that the population ratio of any two states can be enhanced by lowering the temperature and reduced by raising it. The Boltzmann distribution of molecules among the various possible energy states is an equilibrium one; that is, as long as the temperature

of the system is held constant. Once this distribution is attained, it will remain the same indefinitely. This corresponds to a state of maximum entropy, or maximum disorder. Any distribution whatever, if it is left undisturbed for a sufficient length of time, will spontaneously change until it is an equilibrium one. The processes that produce such changes in an arbitrary distribution are known as relaxation mechanisms. Interaction with a black body radiation field, collisions between molecules, and electric and magnetic dipolar interactions are such processes of importance in molecular systems.

The relaxation processes are divided into two classes which are not necessarily mutually exclusive. These correspond to the two different ways a system can deviate from equilibrium. If the total energy of the molecular system E differs from its thermal equilibrium value E_{eq}, spontaneous changes will occur that result in a net transfer of energy between the internal degrees of freedom of the molecular system and its surroundings. Those processes that contribute to this exchange of energy are called longitudinal relaxation processes. In many cases of practical importance, the displacement of the molecular internal energy E from its equilibrium value E_{eq} decreases exponentially with time:

$$d(E - E_{eq})/dt = -\frac{1}{T_1}(E - E_{eq})$$

The reciprocal of the decay constant, which has the dimensions of time, is known as the longitudinal or spin-lattice relaxation time. It is conventionally designated T_1. This symbolism arose in the field of nuclear-magnetic resonance, where the internal energy is the magnetic dipolar or spin orientation energy of nuclei in an applied magnetic field. The term spin lattice relaxation also arose in nuclear magnetic resonance, where the crystal lattice constitutes the heat reservoir.

There is another kind of relaxation process. Since the equilibrium state is one of complete randomness or molecular chaos, any coherence or definite phase relationship between the various molecules constituting the system corresponds to a (partially) ordered, and hence non-equilibrium, state. In this case, the energy of the system (E) need not depart from its equilibrium value E_{eq} to produce a non-equilibrium state. Relaxation processes that tend to destroy such order in the system are known as transverse processes, and where they can be adequately described by an exponential decay of the order are describable phenomenologically by a transverse or spin-spin relaxation time T_2. Examples of this type of relaxation process can be found that either can simultaneously transfer energy between the system and surroundings, or can involve only members of the system itself, and hence cannot exchange energy with the heat reservoir. A collision between two gas molecules, where internal energy can be transformed to kinetic energy of the molecules is an example of the former; the magnetic dipolar interaction between two localized spins in a crystal is an example of the latter.

The three basic types of radiation field-molecule interaction are: absorption, induced or stimulated emission, and spontaneous emission. These types of interaction were treated on a phenomenological basis by Einstein[47] before an adequate microscopic quantum picture was available. His "B coefficient" gives the probability for either absorption or induced emission; his "A-coefficient" gives the spontaneous emission probability.

A very important point about absorption and emission must be made. Both a microscopic quantum mechanical treatment and Einstein's phenomenological treatment give the result that, for a given microwave field strength, the probability of a molecule in the lower of two energy states absorbing a photon is exactly equal to the probability of a molecule in the upper of the same two states giving out a photon by induced emission. This has the consequence that any macrosystem that is in a state where two energy levels are equally populated will be completely transparent to radiation at the frequency corresponding to their energy difference. Neglecting the usually insignificant spontaneous emission effects, it is only an imbalance in populations that produces an observable effect. For computational purposes it is therefore possible, when considering transitions between two energy levels, to pair off the molecules as far as possible and to deal only with excess molecules in the more highly populated state.

An electromagnetic field of the proper frequency can induce transitions between energy levels. It must be remembered, however, that while this is going on, the relaxation mechanisms are operative, tending to restore the system to thermal equilibrium. For weak transition-inducing fields, the relaxation mechanisms are strong enough to maintain the system in an absorptive state not much different from that of thermal equilibrium. However, if the electromagnetic field strength is increased, molecules tend to undergo induced transitions to the upper energy state faster than the relaxation processes can restore them to the lower state. The effective pairing off of molecules is then shifted from that at equilibrium, and there are fewer molecules now in the excess to absorb. It does reach a limit, however, determined by the maximum rate that the relaxation processes can remove the internal energy from the molecular system thus supplied by the microwave field. Under these conditions, the microwave absorption is said to be saturated.

The above discussion has assumed that the energy levels are perfectly sharp, that is, that only one (monochromatic) frequency couples two energy levels. This is not strictly true: transitions may be induced by a band of frequencies centred at the frequency given by $E_i - E_j = h\nu$. Thus absorption or emission spectral lines have a finite frequency width which can be ascribed to a width of the corresponding energy levels. The physical reason for this width is that because of relaxation processes, a molecule interacts with the radiation field for only a finite time before it is dephased and effectively the interaction

stops momentarily. But in the interaction time of the order of T_2, a molecule will "see" essentially the same number of cycles of the microwave field as long as the frequency lies in a band of frequencies of width $\Delta\nu \approx \frac{1}{T_2}$. In other words, a molecule is not able to tell what frequency is acting on it to within a range $\Delta\nu$ in the time T_2 before the interaction is interrupted. The spectral width of a molecular resonance should thus be given by $\Delta\nu T_2 \sim 1$, with short relaxation times leading to broad lines and conversely. This is as observed: in a gas, where T_2 is inversely proportional to the pressure, the observed line width is also proportional to the pressure. In some cases it happens that certain frequencies couple more than one pair of states. This may happen because two or more internal states correspond to the same energy (degeneracy), or because two or more pairs of levels are separated by the same energy gap. The first of these cases is the more common. However, in many systems of interest neither occurs. To simplify, it will be assumed that neither occurs in the following discussion. It is a good approximation to ignore the effects of all energy states but the two that are directly coupled. This reduces the situation to a relatively simple two state case.

If a molecule is in either one of the energy states at t=0, at a time t the probability that it has undergone a transition and is in the other state is given by

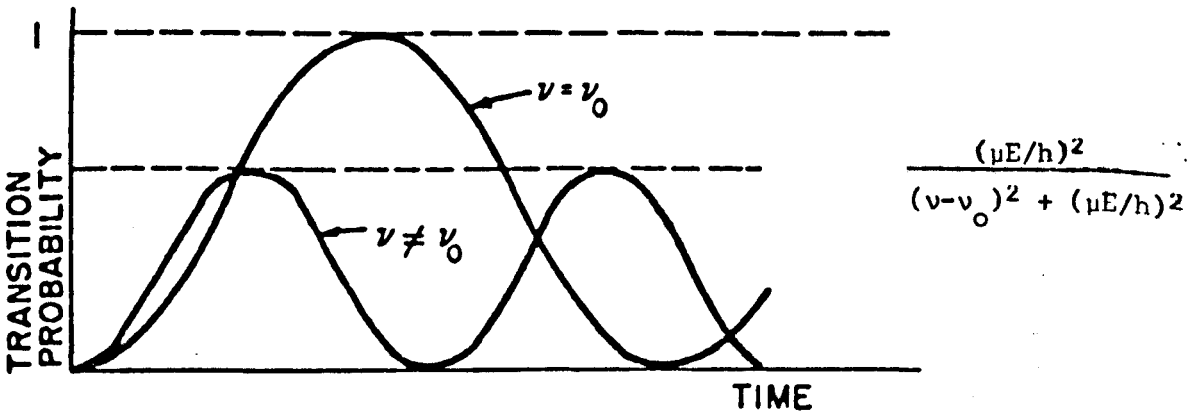

Fig. 5.1 -Transition probabilities between energy states as a function of time for molecules initially in one of two microwave-coupled states when subjected to microwave radiation at or near the resonant frequency.

$$\text{Transition probability} = \frac{\left(\frac{\mu E}{h}\right)^2}{(\nu-\nu_o)^2 + \left(\frac{\mu E}{h}\right)^2} \sin^2 \pi\left[(\nu-\nu_o)^2 + \left(\frac{\mu E}{h}\right)^2\right]^{\frac{1}{2}} t \qquad (2)$$

where μ = electric dipole moment

E = amplitude of the applied microwave field

ν = frequency of the applied field

$\nu_o = E_2 - E_1/h$

A plot of equation (2) is shown in Fig. 5.1. The transition probability oscillates between zero and

$$\left(\frac{\mu E}{h}\right)^2/(\nu-\nu_o)^2 + \left(\frac{\mu E}{h}\right)^2$$

On resonance, ($\nu = \nu_o$), a molecule oscillates between the two states, while somewhat off resonance, a molecule that starts in one state never quite gets to the other (with certainty) before the process is reversed.

The principle of producing coherent radiation in the microwave region is bound up with the possibility of producing an inverted population between the energy levels. Amongst the various methods devised for obtaining such inversion of energy level populations is the molecular beam maser which will be discussed in some detail in Chapter VII. Other methods of producing an emissive condition consist of pulsed resonance excitation and rapid passage technique. From equation (2) it follows that if a system is exposed to a pulse of microwave power on resonance ($\nu = \nu_o$) of such strength and duration that

$$\mu ET/h = \tfrac{1}{2} \qquad (3)$$

molecules originally in the lower state will be raised to the upper state and vice versa; i.e., the state populations will be inverted. Thus such a pulse transforms an absorptive system into an emissive one. The pulse duration must be short compared to the relaxation times, or complete inversion is not achieved. This is not a serious limitation, however, as with readily available powers, pulses of under a microsecond duration satisfy equation (3). Two conditions are critical in obtaining an emissive state; (i) if the pulse frequency is off resonance, complete inversion will not be obtained; (ii) the product of pulse strength and duration must be accurately adjusted. A serious fault of this method of achieving state-population inversion is that it depends on a critical adjustment of frequency and pulse strength and duration. These difficulties are overcome in connection with a second pulse method of obtaining an emissive state, i.e., adiabatic fast passage. This method was used by the Stanford group as a means of reversing the nuclear magnetization by sweeping the d.c. field through the resonance in the first observation of proton resonance in water. Bloch[48] has shown that spin systems in a static magnetic field can be inverted by adiabatic fast passage. His results can be generalized to show that state populations in an arbitrary two-level system can be inverted by a similar technique. In adiabatic fast passages, the molecular system is subjected to a strong

microwave field of amplitude E and variable frequency. The frequency of this field starts far off resonance and is slowly swept through the resonant frequency until it is far off resonance on the other side. When this has been done, the state populations are inverted. Three conditions must be met for this to occur.

(1) The passage must be adiabatic; that is, the frequency must be changed slowly compared to the internal motions of the molecule in response to the driving field E. This condition can be expressed as $\frac{d\nu}{dt} << \frac{\mu E}{h}$.

(2) The passage must be fast compared to the relaxation time; the time required to sweep the frequency from one side of resonance to the other must be short compared to the relaxation time of the system.

(3) The driving field E must be larger than the maximum radiation field of the system. During the passage through resonance, the molecular system develops an oscillating dipole moment; the maximum radiation field of this moment must be smaller than the driving field or population inversion cannot be achieved.

A physical explanation can be given for each of these requirements. In an adiabatic fast passage, the molecular system goes through a series of quasi-stationary states. If the sweep rate is too large, the system cannot follow the changes adiabatically, and non-stationary states, such as are possible for pulse inversion, are induced. The second condition merely assures that the inversion is completed before the competing relaxation processes can restore the system to thermal

equilibrium. The third condition arises because the radiation field and driving field become out of phase as they approach each other in magnitude, and at equality of magnitudes, they just cancel each other in their effects.

Two other points of importance should be mentioned. One is that it does not matter in which direction the frequency sweep traverses the resonance: the initial frequency can be either above or below the resonant frequency. The second is that, if the resonant frequency of the molecular system can be altered by the application or change of an applied electric or magnetic field, for example, the inversion can be achieved by keeping the frequency of the applied microwave field fixed and sweeping the resonant frequency from one side of the applied frequency to the other.

5.2 Transient Effects

An interesting transient effect named "wiggles" by Bloembergen[49], Purcell and Pound was first observed in nuclear magnetic resonance. The wiggles were observed after sweeping through the resonance line in a time short compared with the three relaxation times, T_1, the spin-lattice relaxation time, T_2, the spin-spin relaxation time and $(\gamma\delta H_o)^{-1}$, where δH_o is the inhomogeneity of the steady field H_o over the specimen and γ is the nuclear gyromagnetic ratio. The wiggles were beat signals between the applied radiofrequency signal and the changing precession

frequency of the nuclei which possessed phase coherence as they followed the changing magnetic field. A theoretical analysis of the wiggles was given by Jacobshon[50] and Wangness.

Further work on transient phenomena was done by Bloch and Hahn[51] to measure nuclear relaxation times. Studies of transient nutations of the nuclear magnetic moment under the action of radio-frequency pulses have been reported by Torrey[52]. Work on spin echoes have been reported by Hahn[53] and Oraevskii[54]

The analogous effects to spin echoes in the optical region have been observed by Kurnit[55] et al., Abella[56] et al. and McCall[57] and Hahn. This phenomenon called 'photon echoes' was first observed for two ruby laser pulses incident on an absorbing ruby sample. These echoes result from the coherent excitation of the electric dipoles of a two level absorbing medium. Photon echoes in gases have been observed by Patel[58-59] and Slusher following two pulses of CO_2 laser radiation incident on SF_6 gas. Homogeneous relaxation times for SF_6 colliding with SF_6, He, Ne and H_2 are shown to be easily measurable from the decay of photon-echo amplitude.

The analogous transient effects in the microwave region have also been reported. Coherent spontaneous emission (molecular ringing) has been reported by Lainé[60] in an ammonia beam maser using a single cavity. A frequency scanning rate which allows passage of the applied exciting signal through the molecular emission spectrum in a time

shorter than the mean transit time of the molecules passing through the microwave cavity was used. Thus immediately after the rapid passage, the molecules within the cavity possess an oscillating net polarization at the molecular resonance frequency. They subsequently radiate spontaneously and coherently at a diminishing rate until they finally pass out of the cavity, or collide with the cavity walls. The decaying ringing signal beats with the applied signal and produces alternate maxima and minima following the emission signal.

A super-radiative transient has also been observed following rapid passage of an exciting signal through the absorption resonance of a molecular beam of ammonia[61]. The relatively weak absorption of a thermal molecular beam necessitates sensitive methods of detection which usually preclude an examination of transient properties. The experimental technique used to produce the effect following rapid passage through a molecular beam absorption was similar to that reported previously by Lainé for the beam maser, but with the modification that the upper state separator was replaced by an alternate-gradient focuser which had been found to enhance the sensitivity of ammonia beam absorption spectrometer. Under these conditions a weak decaying beat signal which increased in frequency away from the molecular resonance was observed between the decaying oscillating polarization carried by the beam and the frequency swept excitation signal.

Coherent spontaneous emission has also been reported in some detail in ammonia beam masers using two cavities in cascade[62-63] or for a single cavity beam maser of the atomic hydrogen type[64].

Methods of exciting gases to emit coherent spontaneous radiation in the microwave region have been described by Dicke and Romer[65]. The excitation was produced by application of short pulses of microwave power. The process of spontaneous emission from a gas is usually an incoherent process and the resulting signal power in the microwave region is much less than that obtainable in a coherent absorption process. However, the pulse excitation of a volume of gas causes it to emit spontaneous radiation in a coherent way, the resulting signal power being comparable to the signal power available in an absorption experiment. For these experiments the 3-3 line of ammonia was used. It was pointed out that this technique of pulse excitation of a volume of gas to coherently radiating states can be applied to high resolution spectroscopy. In absorption or emission spectrometers operating in the microwave region the signal is usually superimposed upon a carrier wave. For the most sensitive detection possible, in order to avoid masking the signal, the carrier must be eliminated. This can be achieved by balancing it out in a bridge, but spurious low-frequency modulation of the bridge or of the carrier limits the overall sensitivity of detection. On the other hand, where the technique of coherently radiating states is used, as in Dicke and Romer's experiments, no carrier is present and the signal

itself can be detected directly by beating it with a local oscillator in a superheterodyne receiver and an improved sensitivity over conventional spectrometers is obtained.

Lainé[66] pointed out that the technique used by Dicke and Romer of a pulse excitation of a volume of gas to coherently radiating states can be applied to high resolution spectroscopy using molecular beams. A two cavity maser-like system without a state separator is proposed, where the molecular beam is polarized by a pump field in the first cavity and the coherent spontaneous emission radiated in a second pick-up cavity detected by a superheterodyne receiver.

Coherent microwave emission from pulse-excited ammonia molecules using the 7,7 line have been reported by Norton[67]. Coherent and periodic pulses of near resonance frequency and 1-μsec duration excited the gas from its initial thermal equilibrium condition. Self-induced coherent emission (molecular ringing) continued after the excitation field was removed. This radiation was observed during a period of 10μsecs.

Coherent ringing was also observed by Hill[68], Kaplan, Herrmann and Ichicki in OCS excited by short microwave pulses. J = 0-1 transition was used at 12.16 Gc/sec. A spectrometer consisting of a tunable CW oscillator gated by a travelling wave tube amplifier which provided pulses 10^{-7} - 10^{-6} sec long and 10 W peak power were used along with an S-band gas cell, and a superheterodyne receiver connected through a ferrite circulator. With a small amount (10^{-10}W) of CW oscillator allowed to be present in the waveguide, the beat phenomenon was observed.

In the investigations reported here molecular ringing have been observed following rapid passage of an exciting signal through the absorption resonance in bulk gas using a simple crystal video technique. Experimental results are discussed in Chapter VI.

5.3 Theoretical Approach

The transient phenomena discussed in section 5.2 can be explained in terms of Dicke's[69] theory. He has treated the problem in a detailed and rigorous fashion. The gas as a whole is considered as a single quantum-mechanical system. The molecules are interacting through a common radiation field and hence cannot be treated as independently. Spontaneous transitions between highly correlated states lead to coherent emission. These coherent states may be excited by either the emission of photons by the gas or the absorption of photons from an externally applied radiation pulse.

Omitting the radiation field, the Hamiltonian for an n molecule gas can be written as

$$H = H_o + E \sum_{j=1}^{n} R_{j3} \qquad (4)$$

where $E = h\nu$ = molecular excitation energy

H_o represents the translational and intermolecular interaction energies of the gas

ER_{j3} is the internal energy of the jth molecule and has the eigenvalues $\pm\frac{1}{2}E$.

H_o and all the R_{j3} commute with each other. Hence, energy eigenfunctions may be chosen to be simultaneous eigenfunctions of H_o, R_{13}, R_{23}, $\ldots R_{n3}$. Let a typical energy state be written as

$$\psi_{gm} = U_g(r_1 \ldots . r_n) \left[+ + - + \ldots . \right] \qquad (5)$$

Here $r_1 \ldots . r_n$ designates the centre-of-mass coordinates of the n molecules, and + and - symbols represent the internal energies of the various molecules. If the number of + and - symbols are denoted by n_+ and n_- respectively, then m is defined as

$$m = \tfrac{1}{2}(n_+ - n_-),$$

$$n = n_+ + n_- = \text{number of gas molecules.}$$

If the energy of motion and mutual interaction of the molecules is denoted by E_g, then the total energy of the system is

$$E_{gm} = E_g + mE$$

It is evident that the index m is integral or half-integral depending upon whether n is even or odd. Because of the various orders in which the + and - symbols can be arranged, the energy E_{gm} has a degeneracy

$$\frac{n!}{(\tfrac{1}{2}n+m)!\ (\tfrac{1}{2}n-m)!}$$

This degeneracy has its origin in the internal coordinates only. In addition, the wave function may have additional degeneracy from the centre-of-mass coordinates. It should be noted in this connection that

the degeneracy of the total wave function will depend upon whether or not the molecules are regarded as distinguishable or not. It is assumed that there is insufficient overlap in the wavefunctions of separate molecules to require that wave functions be symmetrized.

Of the Hamiltonian equation (4), H_o operates on the centre-of-mass coordinates only and gives

$$H_o U_g = E_g U_g$$

whereas R_{j3} operates on the plus or minus symbol in the jth place corresponding to the internal energy of the jth molecule.

It is also convenient to define the operators

$$R_k = \sum_{j=1}^{n} R_{jk} \quad , \qquad k = 1, 2, 3$$

and the operator

$$R^2 = R_1^2 + R_2^2 + R_3^2$$

In this notation the Hamiltonian becomes

$$H = H_o + ER_3$$

and

$$R_3 \psi_{gm} = m\psi_{gm}$$

To complete the description of the dynamical system, there must be added to the Hamiltonian the interaction term H_1, that of the radiation field and interaction between field and the molecular system. The total

interaction energy is of the form

$$H_1 = -\Sigma_j A(r_j).(e_1 R_{j1} + e_2 R_{j2}) \qquad (6)$$

Assuming the dimensions of the gas cell small compared with wavelength, the dependence of the vector potential on the centre of mass of the molecules can be omitted and the interaction energy becomes

$$H_1 = -A(0).(e_1 R_1 + e_2 R_2) \qquad (7)$$

e_1 and e_2 are constant real vectors the same for all molecules.

Since the interaction term equation (7) does not contain the centre-of-mass coordinates, the selection rule on the molecular motion quantum number g is $\Delta g = 0$. Consequently there is no Doppler broadening of the transition frequency. This results solely from the small size of the gas container.

The operators R_1, R_2 and R_3 obey the same commutation relations as the three components of angular momentum. Consequently, the interaction operator equation (7) obeys the selection rule $\Delta m = \pm 1$. In general, it has non-vanishing matrix elements between a given state equation (5) and a large number of states with $\Delta m = \pm 1$. In order to simplify the calculation of spontaneous radiation transitions, it is desirable that a set of stationary states be selected in such a way that the interaction term has matrix elements joining a given state with, at most, one state of higher and lower energy, respectively. Because of the very close

analogy between this formalism and that of a system of particles of spin $\frac{1}{2}$, known results can be taken over from the spin formalism.

In a manner similar to an angular momentum formalism[70], the operations H and R^2 commute; consequently, stationary states can be chosen to be eigenstates of R^2. These new states are linear combinations of the states of equation (5). The operator R^2 has eigenvalues r(r+1). r is integral or half integral and positive, such that

$$|m| \leq r \leq \tfrac{1}{2}n$$

The eigenvalue r is called the "Cooperation number" of the gas. Denote the new eigenstates by

$$\psi_{gmr}$$

Here

$$H\psi_{gmr} = (E_g + mE)\psi_{gmr}$$

$$R^2\psi_{gmr} = r(r+1)\psi_{gmr}$$

The degeneracy of the stationary states is not completely removed by introducing R^2. The state (g,m,r) has a degeneracy

$$\frac{n!(2r+1)}{(\frac{1}{2}n+r+1)!\ (\frac{1}{2}n-r)!}$$

The complete set of eigenstates ψ_{gmr} may be specified in the following way: the largest value of m and r is

$$r = m = \tfrac{1}{2}n$$

This state is non-degenerate in the internal coordinates and may be written as

$$\psi_{g,\frac{1}{2}n,\frac{1}{2}n} = U_g.[+ + ... +]$$

All the states with this same value of $r = \frac{1}{2}n$, but with different values of m, are non-degenerate also and may be generated as[71]

$$\psi_{gmr} = \left[(R^2 - R_3{}^2 - R_3)^{-\frac{1}{2}}(R_1 - iR_2)\right]^{r-m}\psi_{grr} \qquad (8)$$

The operator $R_1 - iR_2$ reduces the m index by unity every time it is applied and the fractional power operator is to preservethe normalization of the wave function[72]. The fractional power operator is defined as having positive eigenvalues only.

The state $\psi_{g,\frac{1}{2}n-1,\frac{1}{2}n}$ is one of n states with this value of m. The remaining n-1 states should be chosen to be orthogonal to this state, orthogonal to each other, and normalized. Since these remaining n-1 states are not states of $r = \frac{1}{2}n$, they must be states of $r = \frac{1}{2}n-1$, the only other possibility. Again the complete set of states with this value of r can be generated using equation (8) where now $r = \frac{1}{2}n-1$; and the operator in equation (8) is applied to each of the n-1 orthogonal states of $r = m = \frac{1}{2}n-1$. This procedure can be repeated until all possible values of r are exhausted, in which case all the stationary states have been defined.

Spontaneous radiation probability will be

$$I = I_o(r + m)(r - m + 1)$$

When $r = m = \frac{1}{2}$, it is evident that I_o is the radiation rate of a gas composed of one molecule in its excited state.

If $m = r = \frac{1}{2}n$ (i.e. all n molecules excited)

$$I = nI_o$$

Coherent radiation is emitted when r is large but $|m|$ small. For example, for even n let

$$r = \tfrac{1}{2}n,\ m = 0; \quad I = \tfrac{1}{2}n(\tfrac{1}{2}n + 1)I_o \tag{9}$$

This is the largest rate at which a gas with an even number of molecules can radiate spontaneously. It should be noted that for large n it is proportional to the square of the number of molecules.

States with a low "cooperation number" are also highly correlated but in such a way as to have abnormally low radiation rates. For example, a gas in the state $r = m = 0$ does not radiate at all. This state, which exists only for an even number of molecules, is analogous to a classical system of an even number of oscillators swinging in oppositely phased pairs.

The energy trapping which results from the internal scattering of photons by the gas appears naturally in the formalism. As an example, consider an initial state of the gas for which one definite molecule, and only this molecule, is excited. The gas at first radiates at the normal incoherent rate for a short time and thereafter fails to radiate. The probability of photons being emitted during the radiating period is

1/n. These results follow from the fact that the assumed state is a linear superposition of the various states with $m = 1 - \frac{n}{2}$, and that $\frac{1}{n}$ is the probability of being in the state $r = \frac{1}{2}n$. The probability that the energy will be "trapped" is $\frac{n-1}{n}$. This is analogous to the radiation by a classical oscillator when n-1 similar unexcited oscillators are near. The solution of this classical problem shows that only $\frac{1}{n}$ of the excitation energy is radiated. The remainder appears in non-radiating normal modes of the system.

The gas which is radiating strongly because of coherence is called "super radiant" by Dicke. There are two obvious ways in which a "super radiant" state may be excited. First, if all the molecules be excited, the gas is in the state characterized by

$$r = m = \tfrac{1}{2}n$$

As the system radiates it passes to states of lower m with r unchanged. This will take the system to "super radiant" region $m \sim 0$.

Another way in which such a state can be excited is to start with the gas in its ground state,

$$r = -m = \tfrac{1}{2}n$$

and irradiate it with a pulse of radiation[73-74]. If the pulse is sufficiently intense, the system is lifted to energy states with $m \sim 0$ but with r unchanged, and these states are "super radiant".

If there is a large difference between the populations of two particular single-molecule energy states, then the molecular assemblage need not be considered as a single quantum system. For with a large population imbalance, a net macroscopic polarization exists which oscillates in time and whose radiation rate can be computed classically. Bloom[75] has attacked the problem of molecular ringing by using semi-classical radiation theory. Instead of dealing with a macroscopic polarization, the simple and well known time-dependent perturbation theory is used to compute the population variation of an assemblage of two-state molecules driven by a classical electromagnetic field. This driving field orders the state phases of the various molecules, which before the application of the field had random phases. When the field is suddenly removed, the assemblage does not immediately become quiescent; it continues to radiate in diminishing amounts. This coherent molecular-ringing radiation persists until the molecular populations return to the values they had at the beginning of the driving pulse. The effects of molecular impacts, which tend to destroy the phase coherency of the radiating molecules produced by the driving field are also calculated. According to Bloom, molecular ringing is related to the operation of molecular oscillators. When an empty cavity is struck by a resonant electromagnetic field it continues to ring depending upon its Q. If a molecular system capable of making a resonant radiative transition and having a large population imbalance is introduced, the

cavity will ring longer. This is due to the ringing of molecules themselves. To prevent this composite ringing from dying out one must replenish the supply of such molecules to the high Q cavity. This is what occurs in the maser oscillator[76].

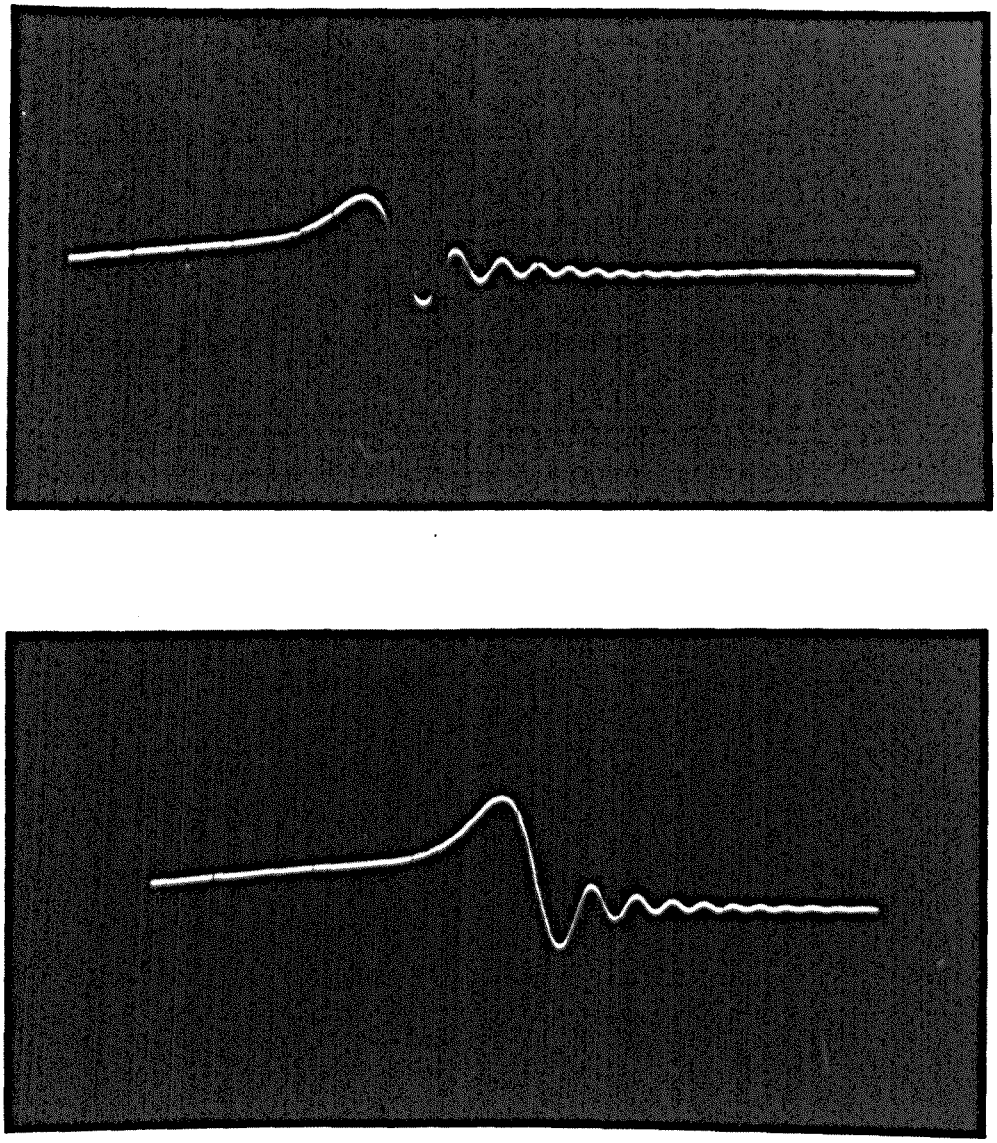

Fig 6.1

Molecular ringing in OCS at 72.976 Gc/s using a wave guide cell. (Pr = .06 - .07 mm of Hg)

CHAPTER VI

EXPERIMENTAL RESULTS

6.1 Molecular Ringing

Coherent spontaneous emission (molecular ringing) was observed in $O^{16}C^{12}S^{32}$ using $J = 5 \rightarrow 6$ transition at 72976.8Mc/sec. This phenomenon which is the electric dipole analogue of the so called 'wiggles' of n.m.r. results from the molecules being excited to decaying super-radiative states. The effect was observed after sweeping through the resonance line in a time short compared to the relaxation times. A simple crystal video spectrometer was used.

A Q-band waveguide gas cell 250cm long was used in transmission. The results are shown in Figure 6.1. The results shown in Figure 6.2 were obtained by using a high Q confocal resonator in reflection. The resonator could be tuned mechanically from outside the vacuum system. The applied exciting signal frequency was scanned with 87 - 120kc/sec sine wave sweep. Since the frequency of the applied signal changes with time, the beat signal frequency increases with time and eventually passes beyond the pass band of the amplifiers. The signal is then not registered on the oscillograph even though the phase coherence may not have been fully destroyed. Hence a wide band (20Mc bandwidth) Hewlett Packard Model 175A oscilloscope was used in conjunction with a high pass filter to avoid instrumental accentuation of the signal decay. The molecular ringing was observed

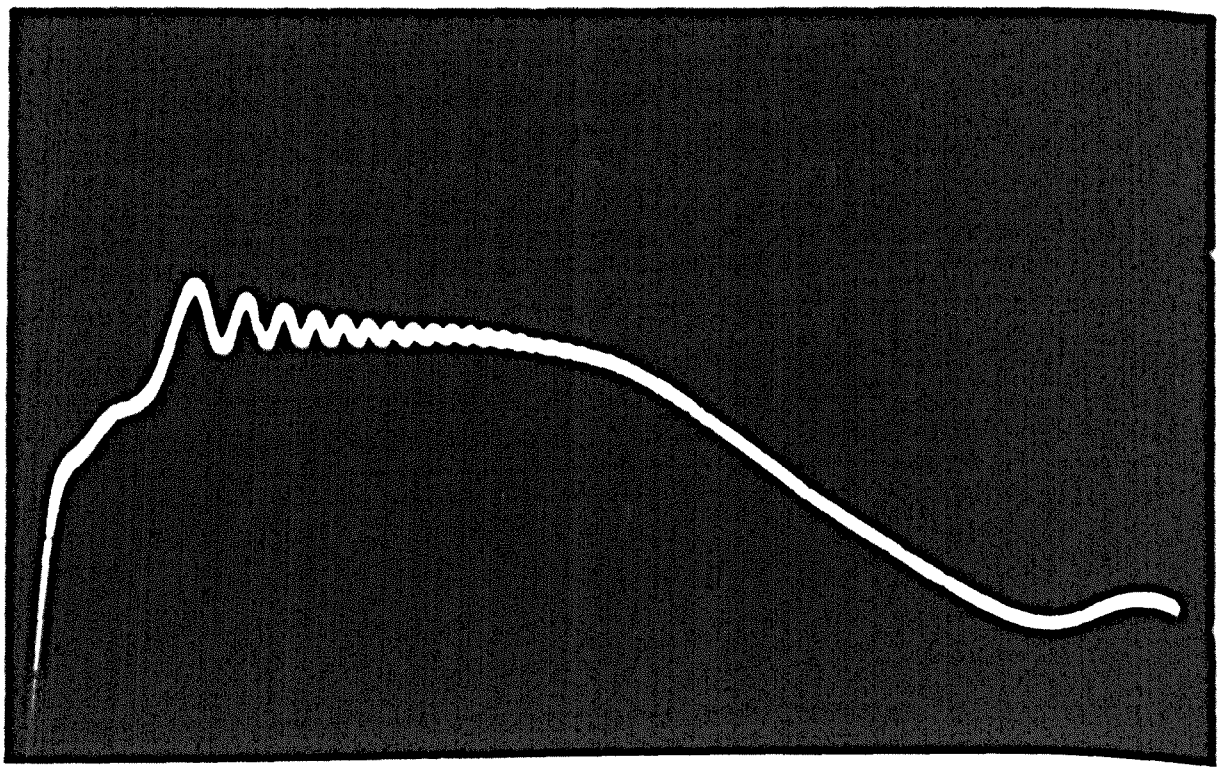

Fig. 6.2 Molecular ringing in OCS at 72.976 Gc/s using confocal resonator (Pr. = .09mm of Hg).

at gas pressures of .02mm to 0.2mm of Hg. The pressures were measured by means of a McLeod gauge.

The gas system can be assumed to be excited from thermal equilibrium to a super-radiant state. The wiggles are beat signals between the applied microwave signal and the coherent spontaneous emission from the molecules. The duration of the phase memory is limited by T_2. The decay time T_2 of the oscillating polarization is measured from the amplitude of the decay envelope of the 'wiggles' which has the form $A = A_o \exp(-t/T_2)$ and is analogous to the transverse relaxation time in magnetic resonance. If radiation damping is small, the decay is a direct measure of the loss of coherence of the radiating molecules by collision with other molecules, or walls of the gas cell or by diffusion along the direction of propagation. The pressure dependent part of the decay measurement shows agreement with line width measurements by others[77].

6.2 Relaxation Processes and Line Widths

The relaxation processes are divided into classes which correspond to different ways a system can deviate from equilibrium. Super-radiative states are non-equilibrium states. Every sort of relaxation process leads to destruction of a super-radiating state.

Relaxation processes due to exchange of energy between the molecular system and the surroundings (lattice) lead to an approach of the energy of the system to its equilibrium value which depends upon the temperature of the lattice. Although a single time constant does not

adequately describe the trend of the molecular system towards equilibrium with the lattice, such a constant is usually introduced to give at least the time scale of the process, and is given the name spin-lattice relaxation time. Bloch has given it the name of longitudinal relaxation time. Another type of relaxation process is due to exchange of energy between the molecules. The time for this process is commonly called T_2, the spin spin or transverse relaxation time. The physical meaning of T_1, as the time constant measuring the rate of progress of the molecular system towards thermal equilibrium with the lattice is clear. An unambiguous definition of T_2 is more difficult and conflicting interpretations of its meaning are found in the literature. The symbolism arose in the field of nuclear magnetic resonance where the internal energy is the magnetic dipolar or spin orientation energy of the nuclei in an applied magnetic field. The crystal lattice constitutes the heat reservoir.

Usually $T_2 << T_1$, so that a coherent super-radiative state of the system is destroyed much more rapidly than the molecular system returns into the thermodynamic equilibrium with the lattice. Here, T_2 is determined by a number of factors which include homogeneous (energy dissipating) and inhomogeneous (non-energy dissipating) relaxation processes which have characteristic relaxation times T'_2 and T^*_2 respectively. The latter relaxation process is due to the difference in the resonance frequencies of the individual radiators.

The shapes of spectral lines have long been a subject of theoretical interest, a subject intimately connected with the development of both classical and quantum mechanical radiation theory. Theoretical treatments usually start with the concept of a single isolated radiating oscillator with a natural line breadth determined classically by radiation damping and quantum mechanically by the probability of spontaneous emission of radiation. The natural width is negligible - only a fraction of a cycle - at microwave frequencies. For widths greater than the Doppler width (~50Kc) collisions with other molecules (pressure broadening) become the principal factor for determining line widths in the microwave region. At very low pressures where the mean free path becomes comparable with the dimensions of the gas cell, collisions with the cell walls increase the line width.

Pressure broadening is usually by far the most important. The theory of pressure broadening is somewhat complicated but has been approached in general terms by Van Vleck and Weisskopf who considered the random interruption of an assemblage of harmonic oscillators. The line width between half-power points is found to be $2\Delta\nu = \frac{1}{\pi\tau}$ where τ is the average time between collisions and $\Delta\nu$ is the line breadth parameter.

The detailed derivation of linewidths from intermolecular forces is a complicated problem which has attracted the attention of many theorists. The general nature of the problem, however, is straightforward. A molecule in a precisely defined energy state is disturbed by the force

field of a passing molecule which may shift the energy state by a Stark effect type of interaction, or may induce a transition to some other energy state. Both the energy shift and the transition probability may be calculated by time-dependent perturbation theory, and both contribute to the observed line width. The Stark perturbation broadens the line in an obvious manner, whereas the induced transitions decrease the lifetime in the energy state and produce a broadening based upon the uncertainty principle. This principle may be stated in the form $\tau\Delta E = \frac{h}{2\pi}$. Hence $\Delta\nu = \frac{\Delta E}{h} = \frac{1}{2\pi\tau}$, where τ is the life time in the state. The expression for line width predicts that it is inversely proportional to the time between collisions, or directly proportional to the pressure of the gas. Experimentally this is true over a wide range of pressures.

Collisions of the molecules with the walls of the gas cell will produce line broadening in exactly the same way as collisions between the gas molecules themselves. The average number of collisions per second with the walls for each molecule can be found from kinetic theory to be equal to $\frac{S}{V}(\frac{RT}{2\pi M})^{\frac{1}{2}}$ where S is the surface area of the waveguide cell and V is its volume. M is the molecular weight of the gas. These collisions will produce a line broadening given by

$$2\Delta\nu = 1.15 \times 10^{3} \cdot \frac{S}{V}(\frac{T}{M})^{\frac{1}{2}} \text{ c/s}$$

Such broadening becomes noticeable when the molecular mean free path is comparable with the waveguide dimensions, i.e. at pressures below 10^{-3}mm of Hg. As it is seldom greater than 15Kc/sec in magnitude it is not usually serious.

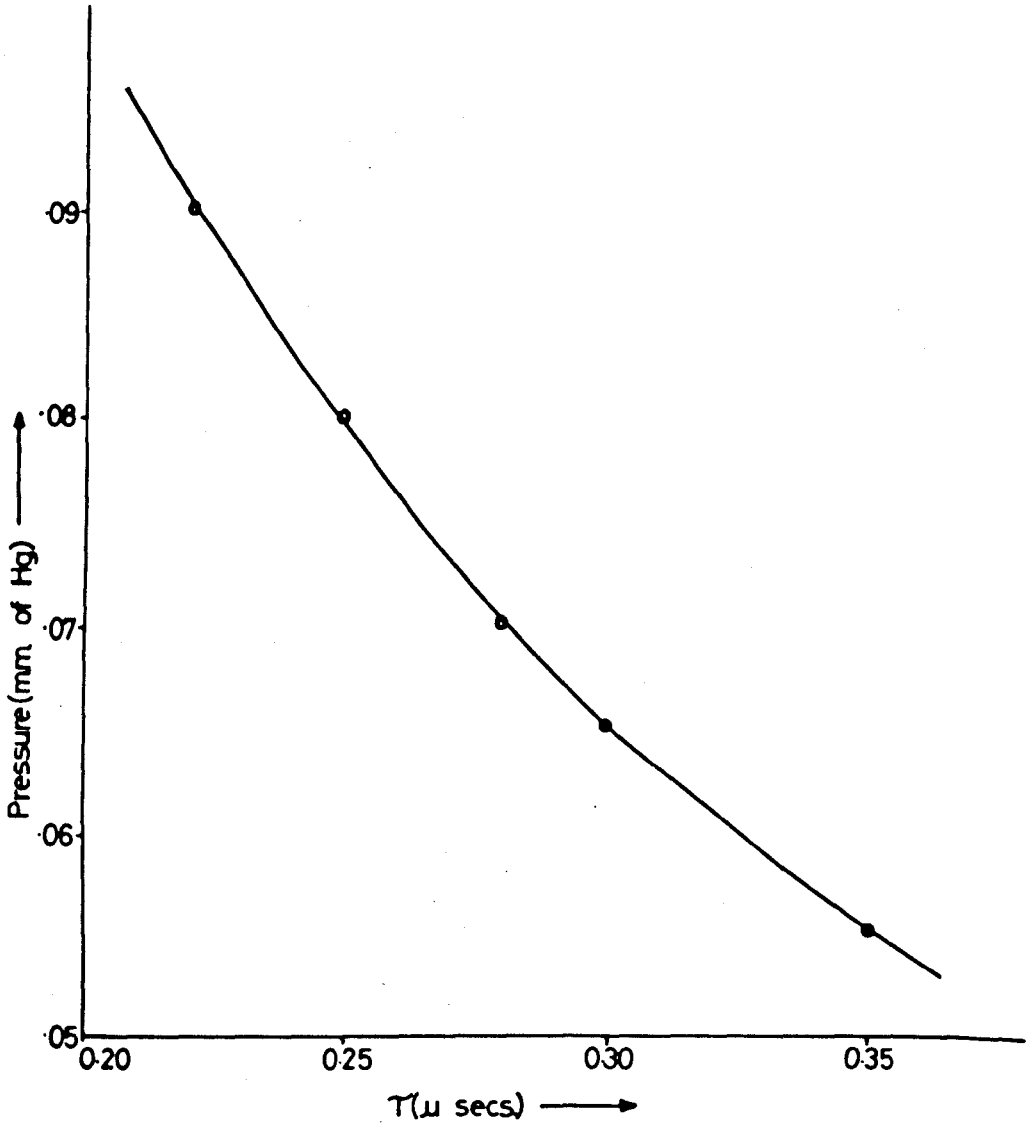

Fig. 6.3. Variation of relaxation time with pressure. (OCS)

6.3 Relaxation Times and Line Width Measurements

The decay envelope of the wiggles is of the form $A = A_o \exp(-t/T_2)$ and is analogous to the transverse relaxation time in magnetic resonance. The relatively high gas pressures used in these measurements ensure that the relaxation processes are predominantly collision induced. Typical signal displays for $O^{16}C^{12}S^{32}$ are shown in Figures 6.1 and 6.2. The relaxation time has been obtained for a number of different pressures and the results are given in Figure 6.3. The line width is given by the relation $2\Delta\nu = \frac{1}{\pi T_2}$. The line breadth parameter $\Delta\nu$ for the $J=5 \rightarrow 6$ transition at room temperature is found to be 8.06 ± 0.20 Mc/mm which checks with the value inferred from the results of Johnson and Slager[77]. Successful comparison of the line width measurements are rather limited as not much experimental data is available except in the case of ammonia which is so far the only microwave case for which extensive quantitative agreements between theory and experiment seems to have been achieved.

6.4 Molecular Ringing in Ammonia

Signal display for molecular ringing in ammonia in bulk gas is shown in Figure 6.4. The 3-3 line of ammonia was used. The experimental technique is similar to the one used for $O^{16}C^{12}S^{32}$. The effect was observed by using a simple crystal video spectrometer with an X-band waveguide cell 100cm long operated in transmission. A klystron scan repetition frequency in the range of 60 - 120KHz/sec was used to give a frequency

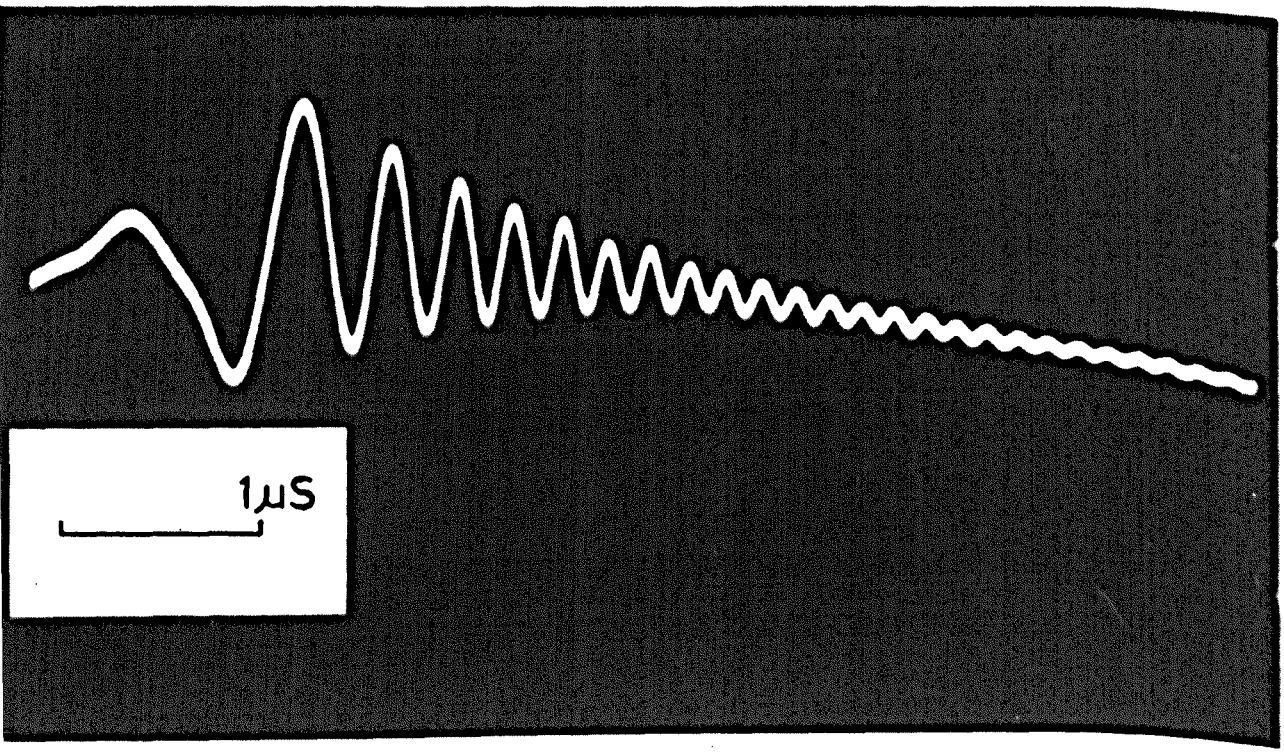

Fig. 6.4 Molecular ringing in bulk gas due to the NH_3, J=K=3 transition (23.87 GHz).

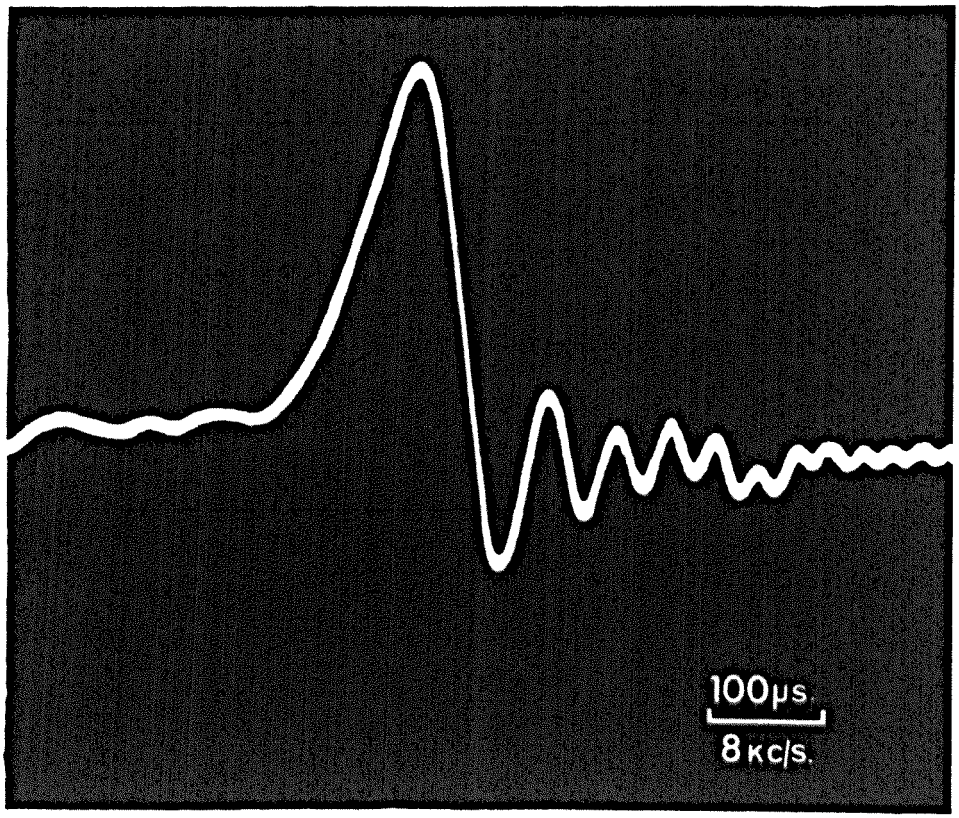

Fig. 6.5 Molecular ringing in the ammonia beam maser (23.87 GHz).

scanning rate of 10^{12}Hz/sec. The scan rate and the exciting signal power were not critical for observation of the effect, provided that the spectral line was scanned in a time shorter than the relaxation time. A fast oscilloscope (20MHz bandwidth) was used for signal display. The relaxation time is found to be 1.3μs at a pressure of 2×10^{-3}torr.

Figure 6.5 shows molecular ringing in the ammonia beam maser (23.870GHz). The ammonia beam maser used for this experiment was operated with a single hole nozzle, a ring state separator and a microwave cavity 10cm long operated in E_{010} mode. A single klystron superheterodyne system was used to detect the power emitted by the molecular beam. Assuming a mean molecular velocity of 5×10^{4}cm/sec, a linear frequency scanning rate >30MHz/sec allows passage of the driving signal through the molecular emission spectrum in a time shorter than the mean transit time of the molecules passing through the resonator. When the maser was operated below oscillation threshold with exciting signal frequency scanning rate less than 30MHz/sec, the normal stimulated emission of ammonia was observed. On increasing the frequency scanning rate, molecular ringing was observed as shown in Figure 6.5. The line width is found to be of the order of 10KHz. The slow axial molecules can be expected to give a longer ringing time. A detailed study of the decay envelope of the ringing signal after excitation by rapid passage can give information about the contribution which these molecules make to the oscillation conditions of a beam maser.

CHAPTER VII

INVESTIGATIONS ON THE $0_{00} - 1_{01}$ TRANSITION OF FORMALDEHYDE

7.1 Introduction

The $0_{00} - 1_{01}$ transition of formaldehyde was used in an attempt to observe molecular ringing, but was found to be too weak for this effect to be observed. The suitability of this transition for beam maser operation was then studied to solve a number of basic problems involved in the construction of such a device.

Normally the population distribution amongst the various energy states of a molecular system in thermal equilibrium is given by Boltzmann's Law and there are always more molecules in the lower energy states than in the higher ones. However, with suitable techniques this population distribution between the various energy states of a molecular system can be altered such that there is an excess population of molecules in a higher energy state over a lower one. Under such conditions stimulated emission can be obtained and incident radiation will be amplified. If the stimulated emission is sufficient to overcome losses a coherent oscillation may be obtained. The necessary condition for oscillation is that the energy emitted due to stimulated emission must be greater than the energy losses in the resonant structure (e.g. microwave cavity) and the associated coupled systems. Various schemes have been proposed to achieve an excess population in the higher-energy state and thereby produce amplification

and oscillation. The first such device which produced oscillation at the microwave frequency of 23.87Gc/s was operated by Gordon, Zeiger and Townes[80] in 1954 using the J=K=3 inversion transition of ammonia. The non equilibrium population condition was obtained by passing a beam of molecules through a very strong inhomogeneous electric field which both created a second order Stark effect for the molecules and physically separated them in various energy states. By using an electric quadrupole deflection field, the upper state molecules were concentrated along the axis of the beam and the lower state molecules moved away from the axis. After state separation, the beam entered a resonant cavity and oscillations were obtained with a power output of about 10^{-11} watts. The success of the beam maser provided impetus in three directions:

(1) High resolution spectroscopy.

(2) Frequency standards.

(3) Low noise amplification.

The J=K=3 line, while it is the most intense line of ammonia inversion spectrum, has the serious disadvantage that even its strong central $\Delta F = \Delta F_1 = 0$ component is split by quadrupole hyperfine structure into three unresolved components separated by about 1KHz[81]. This small splitting is undoubtedly responsible in part for many of the frequency instabilities such as variation with gas pressure behind the nozzle, with focuser voltage etc. Measurements of oscillation on the 3-2 line[82] of a ammonia (22.83GHz) which has no quadrupole splitting showed considerable

improvement in the frequency stability achieved. Isotope N^{15} has also been used, since N^{15} has a spin of $\frac{1}{2}$ and therefore no quadrupole moment.

The recent interest in extending the useful spectrum to the millimetre and submillimetre waves makes it worthwhile to consider the feasibility of extending the techniques developed for the ammonia beam maser at 23.87Gc to the millimetre and submillimetre wave regions. In extending these techniques it is hoped that it will be possible to obtain a very stable maser oscillator which can be used as a high precision frequency standard. Additionally, masers of this type may be useful as narrow band low noise amplifiers.

In general, similar techniques can be used for higher frequency beam masers provided that a resonant structure can be made for the appropriate frequency and that the energy levels are appropriate for magnetic or electrostatic state separation. In the beam maser the function of the state separator is to increase the inequality of the populations of molecules in the pair of energy states used for the maser transition; the greater the excess population in the upper energy state, the greater the emission. Focussing action of the molecules for satisfactory maser action can only be achieved for molecules with low values of rotational quantum number J, except for some molecules with large permanent dipole moments and small rotational constants. The difficulty of separating out molecules in different energy states associated with higher J values arises from the increasing number of Stark sub-levels and

also from the decreasing sensitivity of the molecules to electric field gradients as the rotational frequency is increased. For many molecules with strong transitions in the millimetre wave spectral region conventional beam maser operation may be difficult due to poor separator action, necessitating techniques for more effective state separation. Schulten[83] has pointed out that a conventional electrostatic separator is not necessary if a field perturbation is applied for a carefully calculated length of time, and has proposed an OCS maser at 73GHz by passing the beam first through an inverting pump field and then through a signal cavity.

The interesting feature of the formaldehyde transition at 72.8GHz is its simplicity. In CH_2O the spins of the nuclei C and O are zero, while the spin of H is $\frac{1}{2}$. Consequently there is no nuclear quadrupole hyperfine structure. In the case of $0_{00} - 1_{01}$ transition, the spins of the H nuclei are oppositely directed and the resulting spin of the molecule is zero. Hence the magnetic fine structure is also absent. The absence of any fine structure favours the frequency stability of the maser operated on this line. The form of the Stark effect also favours the frequency stability. Hence, there is a possibility that formaldehyde maser may prove to be an interesting frequency standard. The interest in the formaldehyde maser also lies in the investigation of focusing efficiency of asymmetric top molecules and the usefulness of Fabry-Perot interferometers in this range. Moreover it will be possible to evaluate the usefulness of a number of other molecular transitions in the frequency ranges

where at present there are neither amplifiers nor signal sources. With this in view, it was proposed to construct a molecular generator on the basis of the transition $0_{00} - 1_{01}$ of the formaldehyde molecule.

7.2 Stark Effect

The presence of a molecular electric dipole moment is the most important criterion for the existence of a pure rotational spectrum. The intensities of the transitions are closely related to its magnitude. When an external electric field is applied to a polar gas, it interacts with the electric dipole causing a splitting of the rotational energy levels, which results in the appearance of a fine structure in the rotational spectrum. This is known as the Stark effect.

In considering the molecular Stark effect, the relative directions of the dipole moment and of the angular momentum vector must be taken into account. Thus, in linear molecules the dipole moment is perpendicular to J, the total angular momentum of rotation, provided that the molecule is not in an excited vibrational bending mode, and that it is in $^1\Sigma$ electronic state. The great majority of stable molecules are normally in such an electronic state, since their electrons are fully paired. In symmetric tops, the dipole moment is directed along the figure axis (except in the case of accidental symmetry) and hence it has a component along J, except when K = 0.

Generally speaking, if the dipole moment is perpendicular to J, the splitting of the rotational levels by an electric field depends on

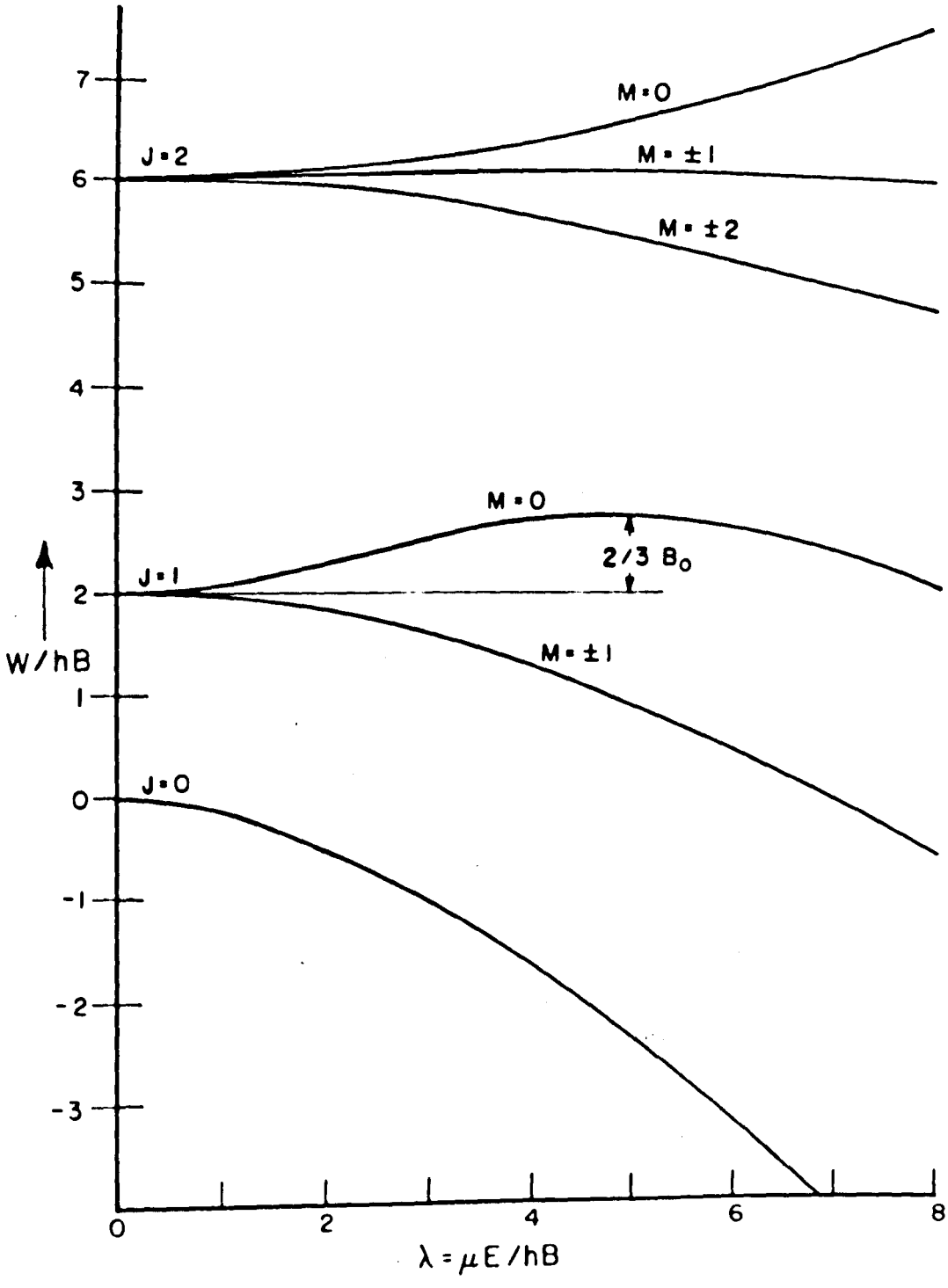

Fig. 7.1 *Stark effect for a linear molecule*

the square of the field intensity E, giving what is known as a second order Stark effect. If the dipole moment has a component along J, the splitting is directly proportional to E, giving a first order Stark Effect.

A formaldehyde molecule is a slightly prolate and slightly asymmetric top with a rather large dipole moment having μ_a = 2.31 Debye, $\mu_b = \mu_c = 0$. The asymmetry parameter is equal to -0.96107. Because of the slight asymmetry of the CH_2O molecule, the Stark effect may be considered (to a good approximation) to be of the form of the Stark effect for the J=1, K=0 transition of a symmetric top. The Stark effect for the K=0 levels of a symmetric top is in turn identical with the Stark effect of a linear molecule[84].

The Stark effect for the lower rotational levels of a linear molecule is shown in Figure 7.1. It is seen that the J=0 and J=1, M = ±1 levels experience a depression of energy in an electric field but that J=1, M=0 level rises in energy to a maximum value of $\frac{2}{3}B_o$ at a field strength such that $\frac{\mu E}{hB_o} \simeq 5$. Of course, here for the rotational constant B of the linear molecule it is necessary to use the average of the rotational constants B and C of the formaldehyde molecule. The form of the Stark effect favours level sorting of the beam of molecules. The energy of molecules of the lower level decreases in the field E and the energy of molecules in the upper level with M=0 increases and has a maximum for E = 156.7KV/cm. There exists an optimum field intensity in the sorting system, corresponding to the maximum Stark energy of the

active molecules, which is best for sorting. The presence of a point $\frac{\partial W}{\partial E} = 0$ makes it possible, apparently, to reduce greatly the influence of the changes in the sorting voltage on the number of active molecules at the output of the sorting system, and this should influence favourably the frequency stability of the maser.

The maximum value of $^2/_3 B_o$ for the increase in energy in turn corresponds to the radial K.E which a molecule possesses at room temperature when it is moving at an angle of about 2^o to the focuser axis, so that all molecules in the J=1, M=0 state travelling at an angle less than this can be expected to be focused.

It follows that the form of the Stark effect of the levels under consideration is favourable for the sorting of the molecules. All molecules in states increasing their energy with increasing field intensity experience forces directed towards decreasing electric field intensity and vice versa. It follows that all ground state molecules as well as molecules with J=1, M=±1 will move towards increasing field intensities while molecules with J=1, M=0 will move towards decreasing field intensity. The beam consequently splits into two parts and population inversion can be achieved.

7.3 State Separators

In the case of electric dipoles the upper and lower state molecules can be separated by passing the molecular beam through a non-uniform electric field. Molecules in different energy states assume

different trajectories and the field may be so arranged that upper and lower state populations are almost completely separated from each other. For the CH_2O molecules in an inhomogeneous electric field the Stark energies are such that all molecules in states J=0 and J=1, M=±1 move towards increasing field intensities while molecules with J=1, M=0 move towards decreasing field intensities. The kind of configuration envisaged can be obtained by having a multipole focuser consisting of an even number of alternately charged parallel rods located symmetrically about the beam axis. Such state separators have been used in beam masers by Gordon et al. and others[85-90]. Theoretical analysis have been given by Shimoda[91], Vonbun[92], Hirono[93] and Shimuzu[94]. More recently ring and spiral focusers have been developed[95-98]. The advantages of the ring and spiral focusers are that the units can be smaller than the rod systems and that better efficiencies can be obtained. In a ring separator the beam passes through a series of equally spaced identical rings which are alternately charged positively and negatively. The field produced is inhomogeneous and increases from the axis to the periphery in the same way as the field in the 2n-pole focuser. The optimum ratio of the ring radius R_o to the distance X_o between rings should be of the order of unity

$$\zeta_{opt} = \left(\frac{R_o}{X_o}\right)_{opt} \approx 1$$

since when $\zeta \ll 1$ the field is almost uniform in cross section and when $\zeta \gg 1$ the whole field is concentrated at the periphery of the system and axial molecules are not state separated at all.

The field in a ring system is given by[99]

$$E = \frac{V_o}{I_o(\frac{2\pi R}{L})} \frac{\sin\frac{\pi}{2}(1 - \frac{2\delta}{L})}{\frac{\pi}{2}(1 - \frac{2\delta}{L})} \frac{2\pi}{L} Z$$

where

$$Z^2 = I_o^2 (\frac{2\pi r}{L}) \cos^2 \frac{2\pi Z}{L} + (I_o')^2(\frac{2\pi r}{L}) \sin^2 \frac{2\pi Z}{L}$$

and

$$I_o(X) = 1 + \frac{X^2}{4} - \frac{X^4}{2^4(2!)^2} + ...$$

is a modified Bessel function of the first kind of zero order, which becomes $\simeq 1 + \frac{X^2}{4}$ if X is small. L is the period of the ring system, δ is the ring thickness and Z the axis along the separator. Letting $\delta = 0$

$$E = \frac{4V_o Z}{\left[1 + \frac{\pi^2 R^2}{L^2}\right] L}$$

with Z varying periodically from $(\cos \frac{2\pi Z}{L})(1 + \frac{4\pi^2 r^2}{L^2})$ to $\frac{8\pi^2 r}{L^2}$ along the Z direction. If R = 0.17cm, L = 0.5cm and V_o = 30,000 volts on the axis the field varies from 0 to 120,000 volts/cm. Thus an important advantage of ring separators is that they produce an inhomogeneous field along the axis of the separator, thus axial molecules are well separated.

Becker[100] has shown that the diameter, z, of the molecular beam of upper state molecules is given by

$$z = \frac{eB}{a}\left[1 - \frac{a(e-a)}{ef}\right]$$

where e is the distance between the source nozzle (diameter d) and the diaphragm (diameter D) at the entrance to the resonator, a is the distance between the nozzle and the centre of the separator (internal diameter B), f is the focal length of the 'lens equivalent' of the separator given by

$$B/f = bmU$$

where U is the potential difference between the rings or spiral wires, m is the number of rings (or windings of a single wire) and b is a constant, being 0.87×10^{-6} per volt for ring and 1.03×10^{-6} per volt for spiral separators. Thus if m = 6 for a ring separator with U = 20kV, f = 3.5cm and if e = 10cm and a = 2.0cm, z is about 0.4cm. Thus it is seen that such a narrow diameter separator can produce a highly directional narrow beam.

Some other interesting variants of the focusing systems are (i) an annular system[101] to be used with a higher mode resonator in order to increase the power of a maser, (ii) grid type separators consisting of two sets of parallel rods as used by Becker[102] and Shimoda[103]. This type produces a flat beam and is particularly suited for use with plane parallel Fabry-Perot resonators.

7.4 Oscillation Conditions

If a CH_2O molecule makes a transition from one rotational energy to another, it may either radiate or absorb energy, depending on whether it is going from a state of higher to lower energy or vice versa.

Thus a molecule going from J=1 to J=0 rotational energy level radiates a quantum of energy ΔE at a frequency ν given by $\nu = \Delta E/h$. A radiative transition may be either spontaneous or induced by an external electromagnetic field. The spontaneous emission occurs with random phase and orientation and is the limiting source of noise in maser amplifiers. For oscillators, the spontaneous transition probability can be made sufficiently small to be neglected compared to the induced emission probability.

Probabilities for absorption and induced emission are equal and proportional to the power density in the vicinity of a molecule. Thus, the net interaction with an applied electromagnetic field is determined by the difference between the number of molecules in the upper and lower energy states. In a beam maser a molecular beam with an excess of molecules in the higher energy state enters the resonant cavity. The condition for maser oscillation can be found by equating the power lost in the cavity to the power supplied by the molecular beam.

Power supplied by the molecular beam is given by

$$P = N.h\nu_o|a|^2$$

where ν_o is the resonant frequency of the molecular transition

N is the number of upper state molecules entering the cavity per second

$h\nu_o$ is the energy per transition

$|a|^2$ is the transition probability.

$$\text{Power lost in the cavity} = \frac{\text{Energy stored in the cavity}}{\text{Energy lost per radian}}$$

$$= W/Q_{/\omega} = \frac{W\omega}{Q}$$

where W is the energy stored in the cavity.

The oscillation condition is

$$Nh\nu_o|a|^2 = \frac{\omega_o W}{Q}$$

Now

$$|a|^2 = \frac{(\frac{\mu\varepsilon_1}{h})^2}{(\frac{\mu\varepsilon_1}{h})^2 + (\nu-\nu_o)^2} \sin^2\left[\pi t\{(\frac{\mu\varepsilon_1}{h})^2 + (\nu-\nu_o)^2\}^{\frac{1}{2}}\right]$$

where ε_1 = electric field strength of the r.f.

μ = electric dipole moment

ν_o = resonant frequency of the molecular transition

ν = frequency of the r.f. field.

At resonance $\nu = \nu_o$

$$|a|^2 = \sin^2 \pi t(\frac{\mu\varepsilon_1}{h}) \qquad 7.1$$

For small values of time and electric field, a good approximation is

$$|a|^2 = \{\pi t(\frac{\mu\varepsilon_1}{h})\}^2 = (\frac{\pi\mu\varepsilon_1 t}{h})^2 \qquad 7.2$$

Therefore, the condition for oscillation is

$$Nh\nu_o|a|^2 = \frac{\omega_o W}{Q}$$

or $$N h\nu_o \left(\frac{\pi\mu\varepsilon_1 t^2}{h}\right) = \frac{\omega_o W}{Q} = \frac{2\pi\nu_o W}{Q}$$

$$= \frac{2\pi\nu_o}{Q} \cdot \frac{\varepsilon^2_1 V}{8\pi} = \frac{\varepsilon^2_1 V\nu_o}{4Q}$$

(as $W = \frac{\varepsilon^2_1 V}{8\pi}$, where V = volume of cavity).

Using the assumption that r.f. electric field in the cavity is uniform and polarized in the proper direction to induce transitions, the value of N may be determined.

The number of molecules per second needed for oscillation can be found from the equation

$$N h\nu_o \frac{\pi^2\mu^2\varepsilon^2_1 t^2}{h^2} = \frac{\varepsilon^2_1 V\nu_o}{4Q}$$

or $$N = \frac{hV}{4\pi^2\mu^2 t^2 Q}$$

It may be noted that the electric field no longer appears here. This is as a result of approximation 7.2.

Now

$$t = L/v$$

where L = length of cavity

v = velocity of the molecules.

Therefore $$N = \frac{hV}{4\pi^2\mu^2L^2/v^2Q} = \frac{hALv^2}{4\pi^2\mu^2L^2Q}$$

$$= \frac{hAv^2}{4\pi^2\mu^2LQ} \qquad \text{as } V = AL \qquad (7.3)$$

where A = area of cross section of the cavity

L = length of the cavity

For the formaldehyde molecules

$v = 0.34 \times 10^5$ cm/sec

L = 4.5 cm

r = 0.1574 cm

$\mu = 2.34$

Substituting these values in equation 7.3 one gets

$$N \simeq 10^{11} \text{ molecules/sec}$$

Since only .03% of the molecules are in the J=1, M=0 state, a beam flux of about 10^{15} molecules/sec will be required. Allowing for the beam divergence about 10^{17} molecules per second are required.

7.5 Experimental

The essential parts of a maser are a reservoir or source of formaldehyde gas, a nozzle or collimator which produces a molecular beam, an electrostatic separator which separates out the higher energy molecules, and a resonant microwave cavity; all these being enclosed in a vacuum envelope. In addition, microwave and electronic equipment is also required to monitor the output signal. These various parts will now be described briefly.

7.5.1 Formaldehyde supply and molecular-beam source

Formaldehyde gas is not available commercially. It must be prepared at the site of use. Gaseous formaldehyde was obtained by vaporization of liquid monomeric formaldehyde which was prepared by heating paraformaldehyde to about 110°C in an oil bath and condensing the vapour in a cold trap at -80°C using dry ice. The connecting tubing was heated electrically to about 90°C to prevent polymerization on the walls. To avoid contamination of the apparatus a much purer polymer was used. The details are given in Chapter III.

Formaldehyde gas then passes through a valve to tbe beam source into the main vacuum chamber. The directional beam was obtained by using a nozzle consisting of a single hole 0.6mm in diameter. The beam source was cooled to about -60°C which is slightly above the dew point of formaldehyde. Since the working levels are lower rotational levels, the dependence of their population upon temperature is determined by the dependence of rotational sum upon temperature. When the temperature is lowered to about -60°C, the population of chosen levels is increased by a factor of 1.65 and the molecular velocity is reduced by a factor of 1.2. Controlled cooling of the source was accomplished by connecting the nozzle to the liquid nitrogen cold trap by means of a metal rod. A heating coil was mounted on the rod for temperature control. A copper-constantan thermocouple was used for temperature measurements.

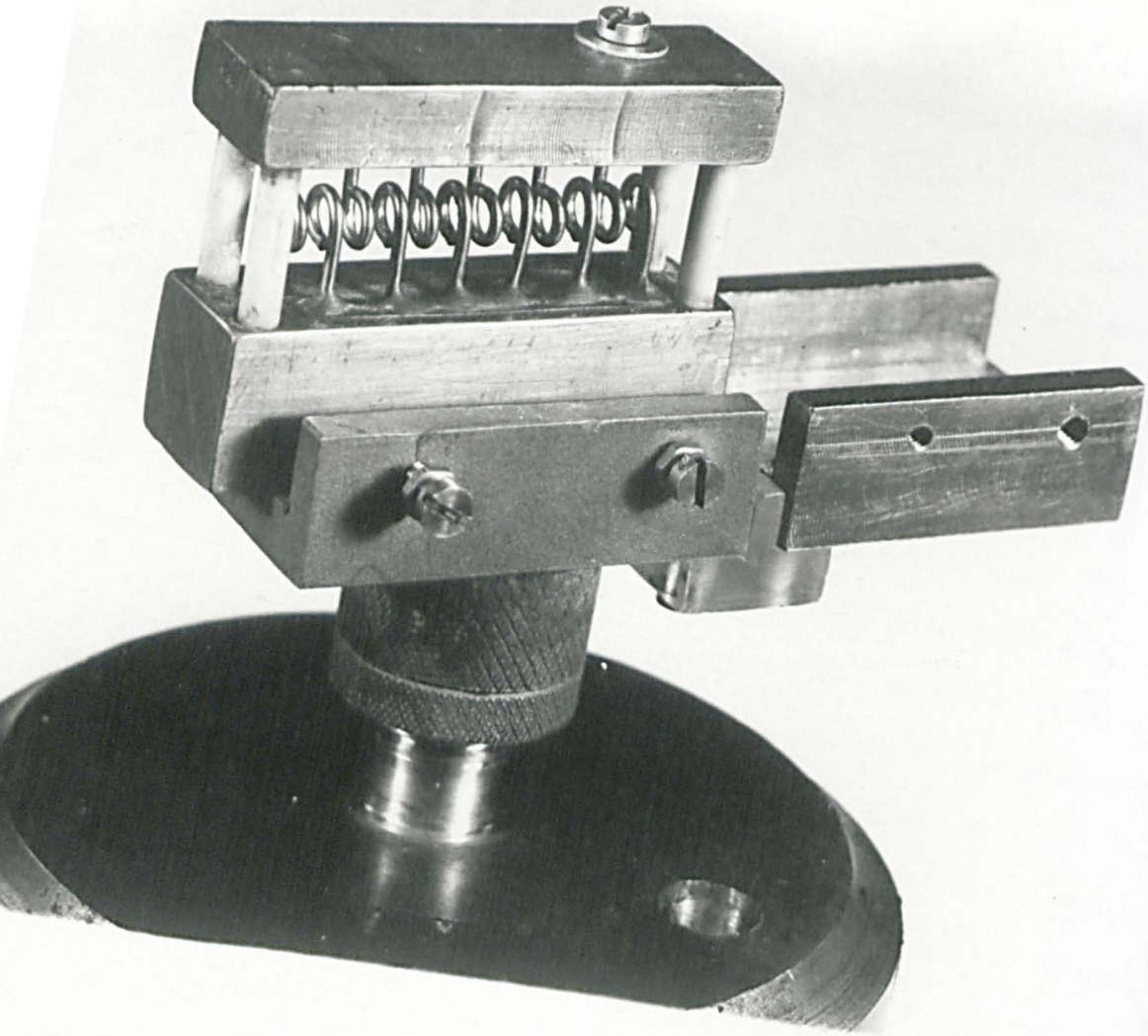

Fig. 7.1a State Separator

7.5.2 State separator

A ring separator (Figure 7.1a) was used having internal diameter of 0.30mm, the separation between the rings being 0.25cm. Since voltages up to 30KV may be applied to the state separator, care was taken to avoid sharp points, and the separator was carefully cleaned before assembly.

7.5.3 Microwave cavity

A cylindrical cavity of length 4.5cms was used. The cavity was designed to resonate in the TM_{010} mode where the resonant frequency is a function of the bore diameter only. The cavity was formed by electro-forming on stainless steel mandrel. The Mandrel was ground from S80 stainless steel and copper was electro-deposited from an acid copper bath. The cavity was tuned to the appropriate transition frequency by heating it electrically. A temperature control unit 'Airmec' type 299 was used. The loaded Q of the cavity was 2400. The cavity was used in transmission. The details are given in Chapter II.

7.5.4 Vacuum requirements

The vacuum in a maser is important in two respects. Firstly, it makes it possible to obtain a molecular beam from the source and secondly it permits a spatial separation of molecules of higher energy from the lower energy ones for time intervals long enough before equilibrium is restored by collision processes. To fulfil these requirements it is desirable to have a background pressure of 4×10^{-6}mm of mercury or less. In order to achieve this pressure, formaldehyde gas has to be

removed from the chamber at least at a rate equal to the influx from the source. This is achieved by using three oil diffusion pumps together with two rotary backing pumps. A copper coil containing liquid nitrogen surrounds the separator and assists in the maintenance of high vacuum as most of the defocussed formaldehyde molecules are trapped as solid formaldehyde on the cold surface of the coil.

The main body of the vacuum system was cast in aluminium bronze with various 'O ring' demountable plates. All the maser components were mounted horizontally on a half inch thick brass optical bench. This system being horizontal rather than vertical had a good vision along the axis from the microwave cavity end. Hence a laser beam was used for alignment of the maser components.

The maser vacuum housing was mounted on a portable trolley and consisted of two 2" diffusion pumps (40 litres per sec.) operating in parallel, backed by a Genevac two stage GRD4 (1.88 litre/sec) rotary pump. The diffusion pumps were suitably baffled to prevent pump oils reaching the cavity. To increase the pumping speed another 4" oil diffusion pump backed by a Metrovac rotary pump type DR1 was coupled to the system. This system together with a separator nitrogen jacket reduced the approximately 3.5 cubic feet volume of the high vacuum system to about 1×10^{-6} torr in a few hours. The nitrogen jacket consisted of hollow copper tube coils (which fitted either side of the state separator) attached to the base of a liquid nitrogen reservoir which was double insulated from its

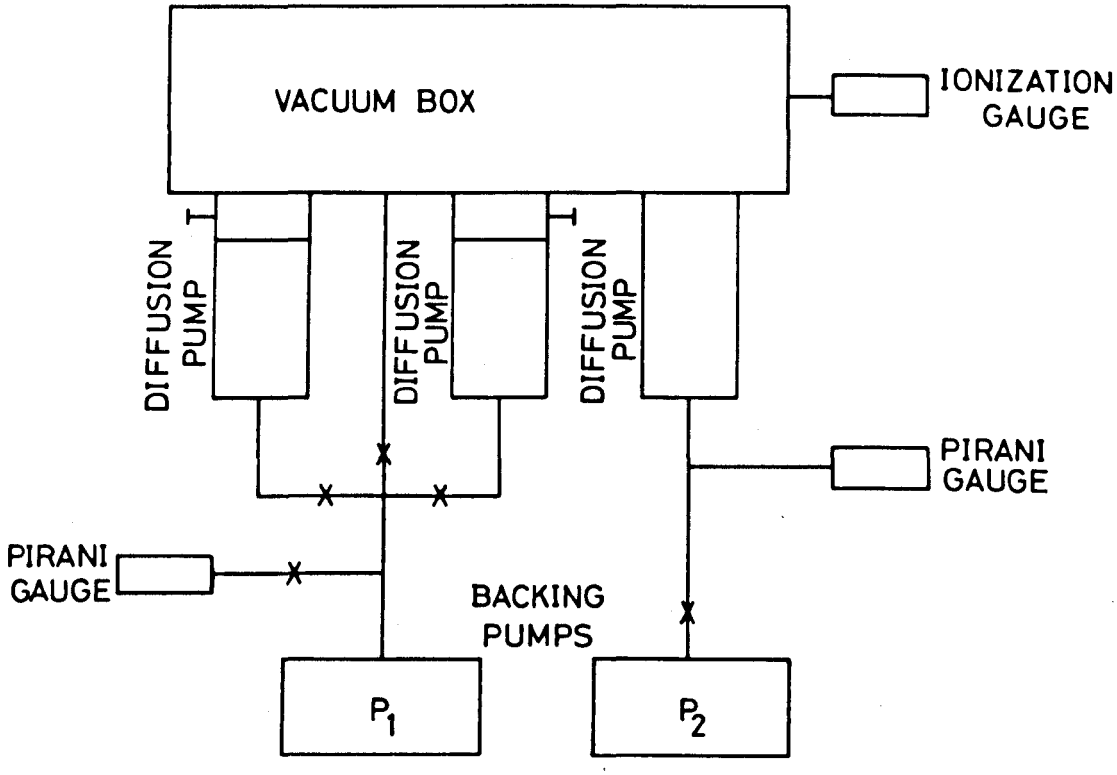

FIG. 7.2 VACUUM SYSTEM.

surroundings by copper-nickel tube. Pirani gauge heads, type M5C1 (Edwards High Vacuum Ltd.) were used for monitoring the backing pressure and ionization gauge heads IG2HB (Edwards High Vacuum Ltd.) were used for monitoring the high vacuum in the chamber.

The vacuum connecting pipes were made from copper pipe with 'Yorkshire' lead solder sealed junctions, and for isolating different sections 'Genevac' or 'Edwards' pressure actuated hand valves were used. All the connections and electrical lead-ins were sealed with appropriate 'O' rings. The E.H.T. lead-in was a long reach sparking plug suitably machined and with the atmospheric end extended with an araldite casting. The liquid nitrogen pipes were connected to the vacuum chamber by cupro-nickel tubes to provide a thermal break between the liquid nitrogen coil and the rest of the system. This prevented the freezing of the 'O' rings in the neighbourhood. A block diagram of the vacuum system is shown in Figure 7.2. The whole apparatus is demountable. Rubber 'O' ring seals were used to couple the components into the vacuum chamber. In the absence of a vacuum inside the chamber the whole assembly could be dismantled for modifications.

7.5.5 Microwave detection and display system

Two methods for measuring the level of microwave power leaving the cavity are used. These are the crystal video and superheterodyne detection.

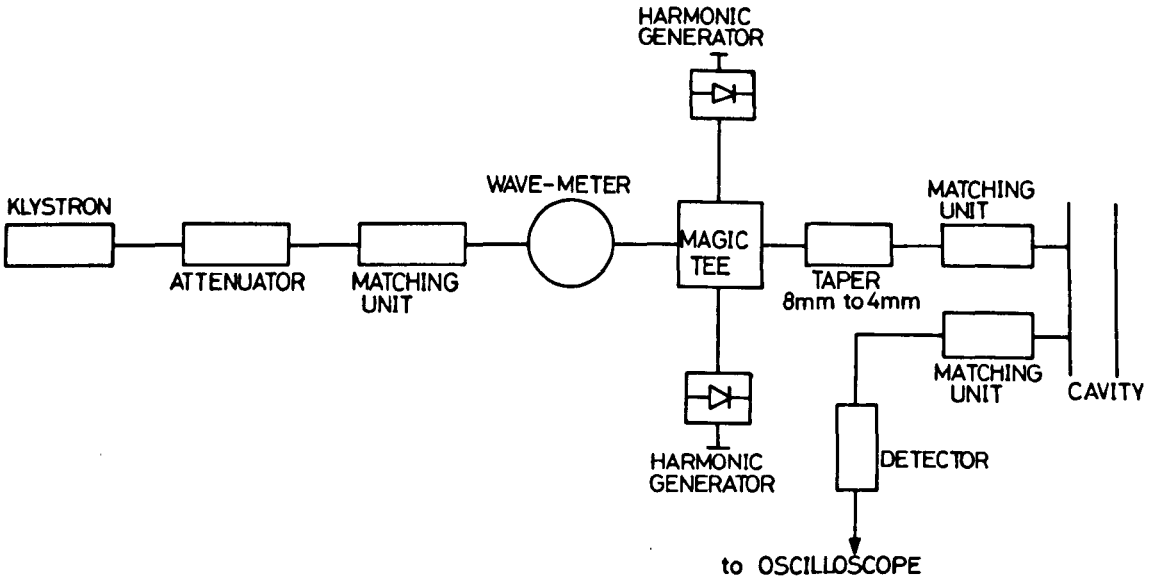

Fig. 7.3. CRYSTAL VIDEO DETECTION.

Crystal Video Detection

A block diagram of the experimental scheme used is shown in Figure 7.3. The Bridge was balanced for maximum power transmission through the cavity. Klystron power was frequency modulated by a 50 cycle saw tooth voltage of about 100 to 150 volts. A part of this saw tooth voltage was also connected to the oscilloscope in such a manner that it synchronized the sweep of the oscilloscope. Since the frequency variation of the klystron was approximately linear with voltage, the horizontal axis of the oscilloscope represented a frequency scale. Formaldehyde gas at 10^{-1} to 10^{-3} torr was introduced into the microwave cavity and an absorption dip superimposed on the cavity transmission was observed. The temperature controller was then adjusted so that the cavity was exactly tuned to the transition frequency. The $0_{00} - 1_{01}$ transition of formaldehyde was observed with a signal-to-noise ratio of 2:1. A Q band wave meter was calibrated against this transition. This transition is much weaker than the J=K=3 line of ammonia or $J_{5\to6}$ transition in OCS. Hence sensitive methods of detection should be used.

Superheterodyne Detection

The power output from the maser is expected to be of the order of 10^{-11} watts. The thermal noise power from the cavity is kTB (where B is the bandwidth of the cavity) and is of the order of 10^{-13} watts. Hence only a sensitive method such as superheterodyne detection is feasible for maser output detection. A block diagram of the microwave circuit used is shown in Figure 7.4.

General view of the maser assembly and detection system

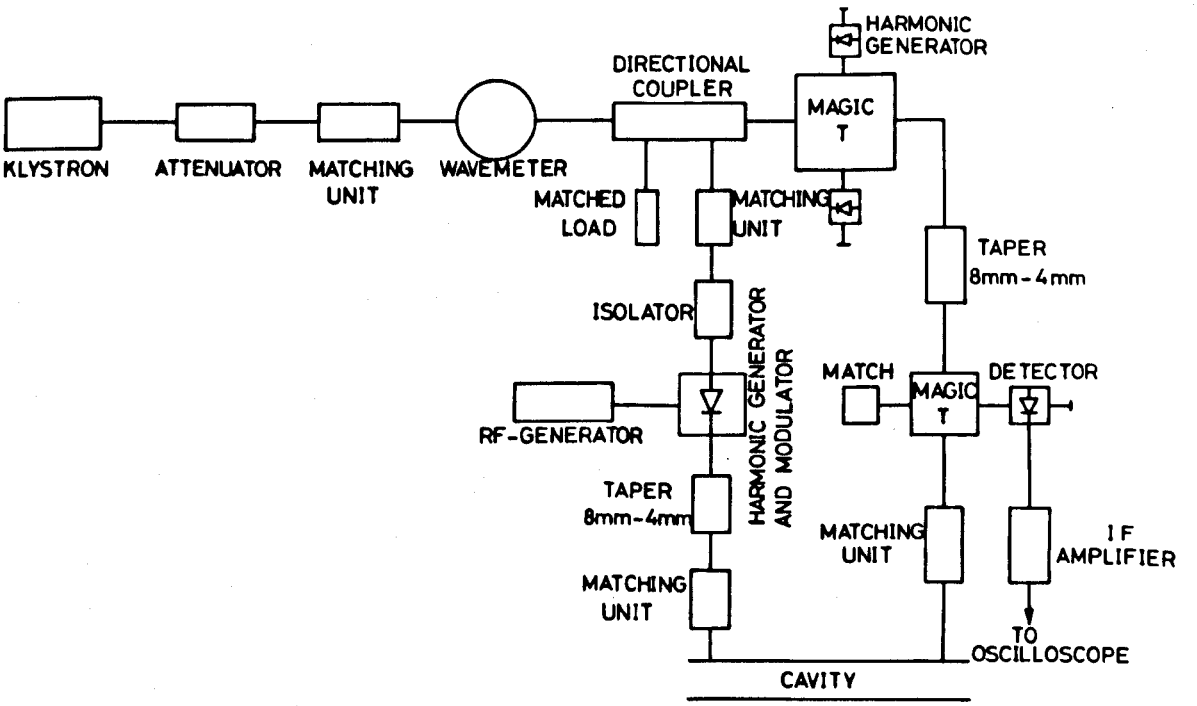

FIG. 7.4 SUPER-HETRODYNE DETECTION.

A part of the power of the heterodyne klystron was removed by a 6dB directional coupler and fed to a multiplier crystal which also acted as a modulator to produce side bands at 60Mc. It was found that the process of modulation was considerably more efficient in the case of germanium crystals than silicon ones. The carrier and two sidebands, separated by 60Mc from the carrier frequency passed through the cavity which filtered out one side band and the carrier so that only one side band was used as a signal. This signal was mixed with the local oscillator power obtained from the same klystron (using two separate multipliers as harmonic generators) which produced a signal of 60Mc at the mixer. This was amplified by an I.F. amplifier, detected and fed to the oscilloscope.

The output from the mixer crystal was matched to the input of the I.F. amplifier. The I.F. amplifier operating at 60Mc/s with a bandwidth of 3Mc and 80db gain was followed by diode detection. The output from the diode was applied to the Y plates of the CRO through a low pass filter.

To observe the formaldehyde absorption the klystron frequency was swept by a sawtooth reflector voltage modulated at 50 cycles/sec. The centre frequency of the klystron was adjusted to be either 60Mc above or below the formaldehyde absorption frequency. The klystron sideband was swept repetitively across the absorption line which was displayed on the C.R.O. screen.

The klystron frequency was offset by 60Mc with the help of a high Q confocal Fabry Perot resonator which was used as a wavemeter. The details

of fabrication of this tunable high Q cavity are discussed in Chapter II. The Q band wavemeters could not be used for this purpose because of their low Q value.

The pressure in the vacuum chamber was first reduced to .01mm of mercury by the backing pumps. The pressure was then further lowered to the region of 10^{-5}mm of mercury by the diffusion pumps. When this pressure was reached, the cooling jacket was filled with liquid nitrogen, so that it acted as a cold trap and condensed any residual gases within the vacuum chamber. By this technique a pressure better than 2×10^{-6}mm of mercury was attained. This pressure was maintained even with a large formaldehyde beam flux. The cavity was thermally tuned by careful adjustment of the temperature control unit to the formaldehyde absorption frequency by the help of the wavemeter calibration. The formaldehyde gas pressure was adjusted to about 1mm of mercury at the input to the nozzle and the separator voltage to about 25KV. The output from the crystal detector was amplified in the I.F. amplifier, demodulated in a diode detector and finally passed through a low pass filter to the Y plates of the C.R.O.

When the maser oscillates, the klystron signal will mix with the maser output at the detector crystal, to produce a beat signal at 60Mc/s. Since the klystron frequency is modulated about its mean frequency, the beat signal will pass across the amplifying band of the I.F. amplifier and the trace can be displayed on the oscilloscope, which will then be

Fig. 7.5

CIRCUIT DIAGRAM OF 60M/cs VARIABLE GAIN I.F. AMPLIFIER.

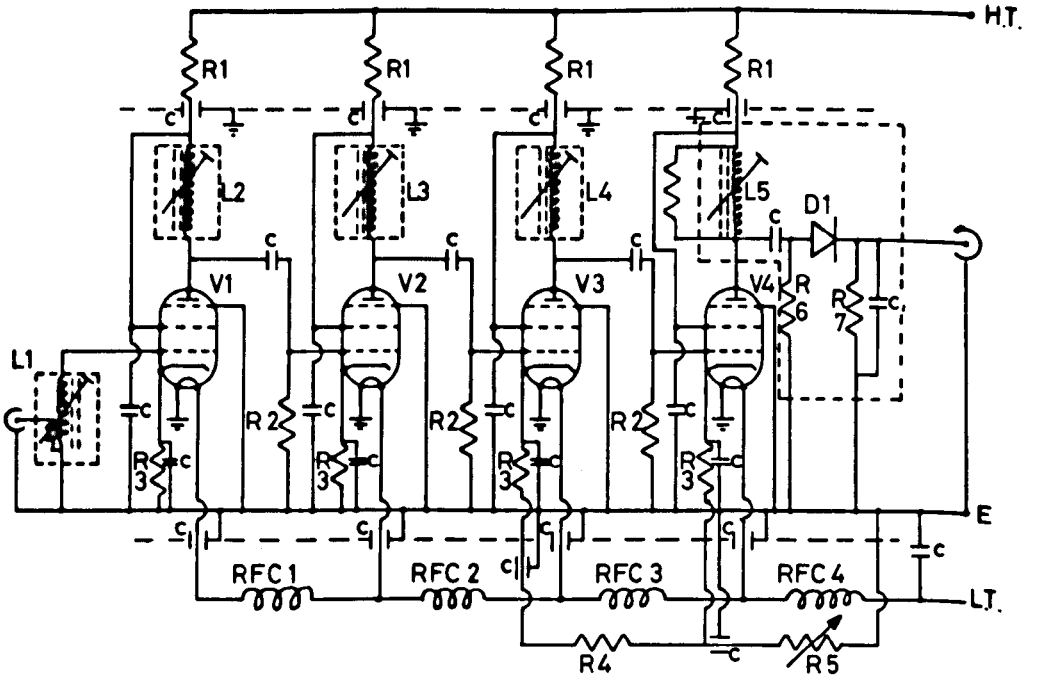

$V_{1,2,3,4}$ - E 180 F

D1 - OA 81

$RFC_{1,2,3,4}$ - 8 TURNS, 20 s.w.g.

R1 - 3·3 kW
R2 - 2·7 k
R3 - 680 Ω
R4 - 100 Ω
R5 - 2·5 k
R6 - 27 k
R7 - 15 k
c - 1000 pF
c. - ·002 μF

that of the I.F. amplifier frequency response. Power level and the matching can then be adjusted to get the maximum output signal on the oscilloscope.

7.5.6 General electronics

(a) Power Units

A commercial stabilised power supply is used for the 8RK17 klystron. Modulation of the frequency of the klystron is achieved by applying a saw-tooth voltage to the reflector. A sweep unit was built for this purpose. The output from the sweep unit was fed to the reflector through an EHT isolating transformer.

Stabilised power supply units are also used to supply the d.c. line voltage to the I.F. amplifier and the sweep generator.

For exciting the state separator a 'Brandenberg' S. 0530 EHT unit is used. This provides 0 - 30KV potential difference with a stability better than 0.25% and a ripple of less than 0.1% at full output.

(b) Intermediate Frequency Amplifier

The I.F. amplifier is centred upon 60Mc/s and has a bandwidth of 3Mc/s with a gain of 80db. In order to have a high gain and low noise in the first stage of the amplifier an E180F pentode is used. This valve has a low noise and high g_m. To achieve a wider bandwidth, damping resistances across the r.f. tuned coils have been used. The amplified output of 60Mc/s is demodulated in a diode detector. The video signal is then passed through a low pass filter and is displayed on the oscilloscope. The circuit diagram is shown in Figure 7.5.

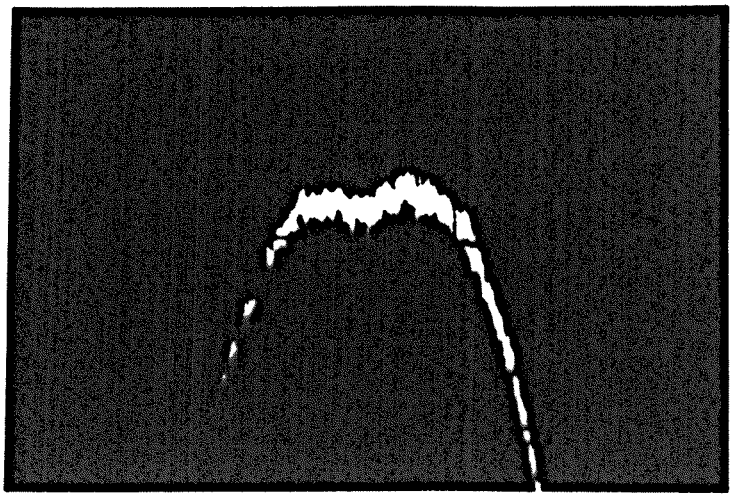

(a)

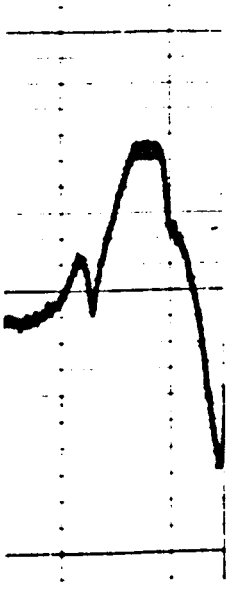

(b)

Fig. 7.6 Formaldehyde absorption at 72.838 Gc/s using crystal video detection

(a) with cylindrical cavity; (b) with confocal resonator.

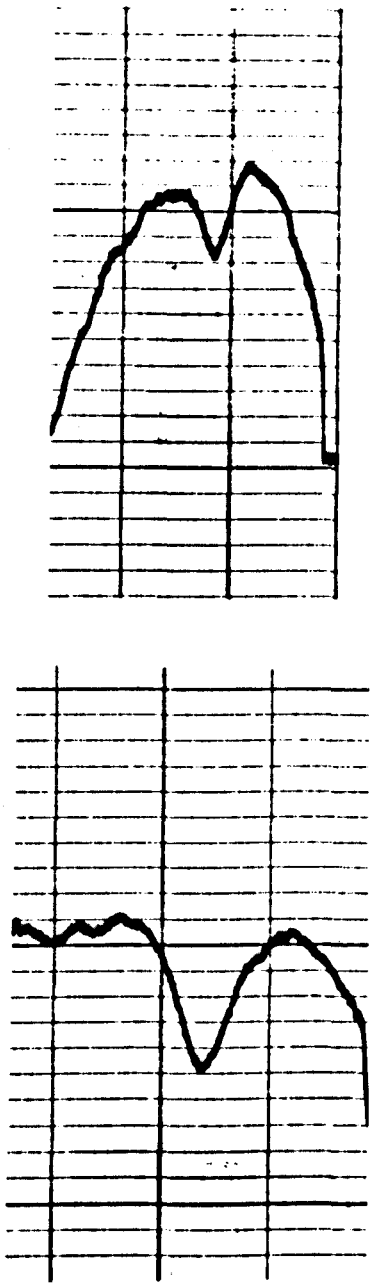

Fig. 7.7 Formaldehyde absorption at 72.838 Gc/s using superheterodyne detection with cylindrical cavity (TM_{010} mode).

(c) Cavity Temperature Stabilisation Unit

The cavity resonator is thermally expanded until it is tuned to the $0_{00} - 1_{01}$ transition of formaldehyde. The cavity is heated by a current flowing in a 10 ohm bifilar coil of glass insulated "Eureka" wire around it. The coil is supplied from a 20 volt tapping of a transformer. The input potential is switched on and off by a relay system ('Airmec' type N299) operated by a copper resistance thermometer (8.8 ohm at 20°C) attached to the cavity. The cavity can be set and stabilised at any temperature between 20°C and 30°C to within 1/10°C.

(d) For display, normally a double beam 'Telequipment' oscilloscope along with a two channel preamplifier, type P.A.3, have been used.

7.6 Experimental Results and Discussion

The experimental results are shown in Figures 7.6 and 7.7. The signal-to-noise ratio was about 2:1 in crystal video detection. This was increased to about 10:1 by using the superheterodyne scheme shown in Figure 7.4. The signal-to-noise ratio was further enhanced by using a digital memory oscilloscope which could additionally provide a chart recorder output of the oscilloscope display.

A 4.5cm long cavity was used in transmission with E_{010} mode and coupling holes of about .132cms. The Q of the cavity was about 2400. A single unstabilized Q-band klystron was used. A part of the power of the heterodyne klystron was removed by a 6db directional coupler and fed to a multiplier crystal which also acted as a modulator to produce side-

bands at 60Mc/s. The carrier and two side bands passed through the cavity which filtered one side band and the carrier so that only one sideband was used as a signal which when mixed with the local oscillator power obtained from the same klystron produced a signal of 60Mc at the mixer. This is then fed to the oscilloscope through the I.F. amplifier. A single beam source was used with a diameter of about 0.6mm. In order to increase the intensity of the line the source was cooled to about $-70^{\circ}C$. Formaldehyde absorption could be observed down to a pressure of 1×10^{-4}mm of mercury with a pressure of 0.9mm Hg behind the nozzle.

The only work so far published in which a formaldehyde maser has been operated using $0_{00} - 1_{01}$ transition is by Krupnov and Skvortsov[105-107] of the Soviet Union. The sensitivity of their apparatus is quite high. Molecular beam absorption could be observed down to a pressure of about 10^{-5}mm of mercury as compared to 10^{-4}mm of mercury in this work. It is evident that an improvement to the present sensitivity of detection is required to verify that the present system is operating as a maser. The $0_{00} - 1_{01}$ transition of formaldehyde is much weaker as compared to J=K=3 line of ammonia or the $J_{5\to6}$ transition of OCS. Moreover the cavity Q is about $\frac{1}{3}$rd of that at K band frequencies. Hence special techniques are required to increase the sensitivity which has been one of the basic difficulties. The following modifications are suggested. The signal-to-noise ratio can be improved by use of a balanced mixer to eliminate the local oscillator noise which is an additional source of noise in a millimetre wave system. When the local

oscillator power is generated by a harmonic generation process, its spectrum is that of a single frequency surrounded by noise sidebands. Unless these sidebands are suppressed by a balanced mixer or in some other way, they are a predominant source of detector noise. Secondly, stabilized klystron sources should be used so that narrow band amplification can be incorporated. The increase of harmonic power can be achieved by the use of bombarded silicon in harmonic generators. This material can be made by bombardment of silicon with 40,000eV positive ions. Use of isolators for Q band and O band could also make an improvement to the present system.

REFERENCES

1. Pierce, J.R., Physics Today, 3, 1950, p.24.
2. Karp, A., Proc. I.R.E., April 1957.
3. King, W.C. and Gordy, W., Phys. Rev. 93, 1954, p.407.
4. Johnson, C.M., Slager, D.M. and King, D.D., Rev. Sci. Instrum., 25, 1954, p.213.
5. Gordy, W., Rev. Mod. Phys., 20, 1948, p.668.
6. Gordy, W. and Jones, G., Phys. Rev. 135A, 1964, p.295.
7. Smith, A.G., Gordy, W., Sommers, J.A. and Smith, W.V., Phys. Rev., 75, 1949, p.266.
8. Ohl, R.S., Budenstein, P.P. and Burrus, C.A., Rev. Sci. Instrum., 30, 1959, p.765.
9. Burrus, C.A. and Gordy, W., Phys. Rev., 93, 1954, p.897.
10. North, H.Q., NDRC 14-328, G.E. Co., Mar. 26, 1945.
11. Angello, S.J., Westinghouse Research Report SR-176, April 21, 1943.
12. Pfann, W.G., BTL Report, Case 24026, Dec. 3, 1942.
13. Mathias, L.E.S. and Crocker, A., Physics Letters, 13, 1964, p.35.
14. Becker, R.C. and Coleman, P.D., Proc. Symp. on mm Waves, New York, 1959.
15. Sommers, G., Proc. I.R.E., 47, 1959, p.1201.
16. Froome, K.D., Proc. 3rd Int. Conf. on Quantum Electronics, 2, 1963, p.1527.
17. Nicholls, E.F. and Tear, J.D., Proc. Natl. Acad. Sci. U.S., 9, 1923, p.221.

18. Langenberg, N., Scalpino, D.J. and Taylor, B.N., Scientific American, 214, 1966, p.530.

19. Klein, J.A., Loubser, J.H.N., Nethercot, A.H. and Townes, C.H., Rev. Sci. Instrum., 23, 1952, p.78.

20. Connes, P., Revue d'Optique, 35, 1956, p.37.

J. Phys. Radium, 19, 1958, p.262.

21. Jackson, D.A., Proc. Roy. Soc., A263, 1961, p.289.

22. Fox, A.G. and Li, T., Bell System Tech. J., 40, 1961, p.453.

23. Becker, R.C. and Coleman, P.D., Proc. Symp. on mm waves, New York, 1959, p.191.

24. Jenkins and White, Fundamentals of Optics.

25. Schawlow, A.L. and Townes, C.H., Phys. Rev., 112, 1958, p.1940-1949.

26. Fox, A.G. and Li, T., Bell Syst. Tech. J., 40, March 1961, p.453-488.

27. Javan, A., Bennett, W.R. and Herriott, R., Phys. Rev. Lett., 6, Feb. 1961, p.106-110.

28. Boyd, G.D. and Gordon, J.P., Bell Syst. Tech. J., 40, March 1961, p.489-508.

29. Fox, A.G. and Li, T., Proc. I.R.E., 48, 1960, p.185.

30. Connes, P., J. Phys. Radium, 19, 1958, p.262.

31. Marcuse, D., Proc. I.R.E., 49, 1961, p.1706.

32. Dakin, T.W., Good, W.E. and Coles, D.K., Phys. Rev., 70, 1946, p.560.

33. Van Vleck, J.H. and Weisskopf, V.F., Rev. Mod. Phys., 17, 1945, p.227.

34 Townes, C.H., Phys. Rev., 70, 1946, p.665.

35. Herzberg, G., Infrared and Raman Spectra, D. van Nostrand Co. Inc., New York, 1945, p.377.

36. Nielson, A.H., J. Chem. Phys., 11, 1943, p.160.

37. Nielson, H.H. and Shaffer, W.H., J. Chem. Phys., 11, 1943, p.140.

38. King, G.W., Hainer, R.M. and Cross, P.C., J. Chem. Physics, 11, 1943, p.27.

39. Cleeton, C.E. and Williams, N.H., Phys. Rev., 45, 1934, p.234.

40. Good, W.E. and Coles, D.K., Phys. Rev., 71, 1947, p.383.

41. Simmons, J.W. and Gordy, W., Phys. Rev., 73, 1948, p.713.

Sharbaugh, A.H., Madison, T.C. and Bragg, J.K., Phys. Rev., 76, 1949, p.1529.

42. Townes, C.H. and Schawlow, A.L., Microwave Spectroscopy, McGraw-Hill Co. Inc., New York, 1955.

43. Beringer, E.R., Radiation Laboratory Report, 1944, p.638.

44. Torrey, H.C. and Whitmer, C.A., Crystal Rectifiers, 1948, p.344.

45. Gordon, J.P., Zeiger, H.J. and Townes, C.H., Phys. Rev., 99, 1955, p.1264-1274.

46. Wittke, J.P., Proc. I.R.E., 1957, p.307.

47. Einstein, A., Phys. Zeit, 18, 1917, p.121-128.

48. Bloch, F., Phys. Rev., 70, 1946, p.460-474.

49. Bloembergen, N., Purcell, E.M. and Pound, R.V., Phys. Rev., 73, 1948, p.679.

50. Jacobshon, B.A. and Wangness, R.K., Phys. Rev., 73, 1948, p.942.

51. Hahn, E.L., Phys. Rev., 80, 1950, p.580.

52. Torrey, H.C., Phys. Rev., 76, 1949, p.1059.

53. Hahn, E.L., Phys. Rev., 77, 1950, p.297.

54. Oraevskii, A.N., Soviet Physics Uspekhi, Vol. 10, No. 1, 1967, p.45-51.

55. Kurnit, N.A., Abella, I.D. and Hartman, S.R., Phys. Rev. Lett., 13, 1964, p.567.

56. Abella, I.D., Kurnit, N.A. and Hartman, S.R., Phys. Rev. Lett., 141, 1966, p.391.

57. McCall, S.L. and Hahn, E.L., Phys. Rev. Lett., 18, 1967, p.908.

58. Patel, C.K.N. and Slusher, R.E., Phys. Rev. Lett., 20, 1967, p.1019.

59. Patel, C.K.N. and Slusher, R.E., Phys. Rev. Lett., 20, 1968, p.1087.

60. Lainé, D.C., Physics Letters, 23, 1966, p.557.

61. Kakati, D. and Lainé, D.C., Private Communication.

62. Basov, N.G., Oraevskii, A.N., Strakhovskii, G.M. and Tatarenkov, V.M., Quantum Electronics III, Columbia University Press, New York 1964, p.377.

63. Lainé, D.C. and Srivastava, R.C., Proc. Inst. Radio Electron. Engrs., 26, 1963, p.173.

64. Goldenberg, H.M., Kleppner, D. and Ramsay, N.F., Phys. Rev. Letters, 5, 1960, p.361.

65. Dicke, R.H. and Romer, R.H., Rev. Sci. Inst., 26, 1955, p.915-928.

66. Lainé, D.C., Proc. Phys. Soc., 87, 1966, p.855-857.

67. Norton, L.E., I.R.E. Transactions on Microwave Theory and Techniques, Vol. MTT-5, No. 4, Oct. 1957, p.262-265.

68. Hill, R.M., Kaplan, D.E., Herrmann, G.F. and Ichiki, S.K., Phys. Rev. Lett., 18, 1967, p.105-107.

69. Dicke, R.H., Phys. Rev., 93, 1954, p.99.

70. Condon, E.U. and Shortley, G.H., Theory of Atomic Spectra, Cambridge University Press, Cambridge, 1935, p.45-49.

71. Ibid. p.48.

72. Ibid. p.48.

73. Bloch, F. and Rabi, I.I., Rev. Mod. Phys., 17, 1945, p.237.

74. Bloch, F., Phys. Rev., 70, 1946, p.460.

75. Bloom, S., Journal of Appl. Phys., 27, 1956.

76. Gordon, J.P., Zeiger, H.J. and Townes, C.H., Phys. Rev., 99, 1955, p.1264.

77. Johnson, C.M. and Slager, D.M., Phys. Rev., 87, 1952, p.677.

78. Dakin, T.W., Good, W.E. and Coles, D.K., Phys. Rev., 71, 1947, p.640.

79. Johnson, Trambarulo and Gordy, Phys. Rev., 84, 1951, p.1178.

80. Gordon, J.P.. Zeiger, H.J. and Townes, C.H., Phys. Rev., 95, 1954, p.282.

81. Gordon, J.P., Zeiger, H.J. and Townes, C.H., Phys. Rev., 99, 1955, p.1253.

82. Shimoda, K., Trans. I.R.E., 11, 1962, p.195.

83. Shulten, G., Philips Research Reports, 19, 1964, p.395.

84. Thaddeus, Janvan, Krisher and Lecar, Symposium on Quantum Electronics, New York, 1960, p.48.

85. Gordon, J.P., Zeiger, H.J. and Townes, C.H., Phys. Rev., 95, 1954, 282L.

86. Gordon, J.P., Zeiger, H.J. and Townes, C.H., Phys. Rev., 99, 1955, p.1264.

87. Basov, N.G. and Prokhorov, A.M., Dokaldy, Soviet Physics, 101, 1955, p.47.

88. Basov, N.G. and Prokhorov, A.M., Trans. Faraday Society, 19, 1955, p.96.

89. Basov, N.G. and Prokhorov, A.M., Soviet Physics, JETP, 3, 1956, p.426.

90. Shimoda, K., J. Phys. Soc. Japan, 12, 1957, p.1006.

91. Shimoda, K., Proc. Int. School of Physics, E. Fermi, XVII, "Topics on Radio Frequency Spectroscopy", Academic Press, 1962.

92. Vonbun, F.O., J. App. Phys., 29, 1958, p.632.

93. Hirono, M., J. Radio Res. Lab., 6, 1959, p.515.

94. Shimuzu, T. and Shimoda, K., J. Phys. Soc. Japan, 16, 1961, p.777.

95. Becker, G., Zeit Angew. Phys., 15, 1963, p.13.

96. Becker, G., Proc. 3rd Int. Quantum Electronics Conference, Paris, 1963, p.393.

97. Basov, N.G. and Zuev, V.S., S.P. Instruments and Experimental Techniques, 1, 1961, p.122.

98. Krupnov, A., Izv, Vuz. MVO SSSR Radiofizika, 2, 1959, p.658 (English translation).

99. Kazachok, V.S., S.P. Technical Physics, 10, 1965, p.882.

100. Becker, G., Proc. 3rd Int. Quantum Electronics Conference, Paris, 1963, p.393.

101. Krupnov, A.F., Izv. Vuz. MVO SSSR Radiofizika, 2, 1959, p.658.

102. Becker, F., Paris Conference, Ed. by Grivet, P. and Bloembergen, N., Columbia University Press, New York, 1963, p.393.

103. Shimoda, K., Ibid, p.349.

104. Krupnov, A.F. and Skvortzov, V.A., Soviet Physics, JETP,220, 1965, p.1079.

105. Krupnov, A.F. and Skvortsov, V.A., Soviet Physics, JETP, 18, 1964, p.1426.

106. Krupnov, A.F. and Skvortsov, V.A., Izv. VUZ, Radiofizika, 5, 1962, p.820.

107. Krupnov, A.F.,and Skvortsov, V.A., Izv. VUZ, Radiofizika, 8, 1965, p.200-203.

Additional Bibliography

108. Krupnov, A.F. and Skvortsov, V.A., Radio Eng. Electron Phys., 10, 1965, p.320-322.

109. Krupnov, A.F. and Skvortsov, V.A., Pribory i Tekhnika Experimenta, 1, 1965, p.128-132.

110. Ingram, D.J.E., "Spectroscopy at Radio and Microwave Frequencies", London, Butterworths, 1967.

111. Gordy, W., Smith, W.V. and Trambarulo, R.F., "Microwave Spectroscopy", New York, John Wiley & Sons Inc., 1953.

112. Sugden, T.M. and Kenney, C.N., "Microwave Spectroscopy of Gases", D. Van Nostrand Co. Ltd., London, 1965.

113. Townes, C.H. and Schawlow, A.L., "Microwave Spectroscopy", McGraw-Hill Publishing Co. Ltd., London, 1955.

114. Harvey, A.F., "Microwave Engineering", Academic Press, New York, 1963.

115. Torrey, H.C. and Whitmer, C.A., "Crystal Rectifiers", MIT Radiation Laboratory Series, 15, 1948.

116. Montgomery, C.G., "Technique of Microwave Measurements", MIT Radiation Laboratory Series, 11, 1947.

117. White, G.K., "Experimental Techniques in Low-Temp. Physics", Clarendon Press, Oxford, 1959.

118. Vuylsteke, A.A., "Elements of Maser Theory", Princeton, Van Nostrand, 1960.

119. Singer, J.R., "Masers", Wiley, 1959.

120. Abragam, A., "The Principles of Nuclear Magnetism", Clarendon Press, Oxford, 1961.

121. Martin, D.H., "Spectroscopic Techniques for far infra-red, submillimetre and millimetre waves".

122. Andrew, E.R., "Nuclear Magnetic Resonance", The University Press, Cambridge, 1958.

123. Transactions of the P.N. Lebedev Physics Institute, Vol. XXI, Soviet Maser Research, Consultants Bureau, New York.

124. Proceedings of the Symposium on Millimetre waves, Polytechnic Press of the Polytechnic Institute of Brooklyn, Brooklyn, N.Y., 1959.